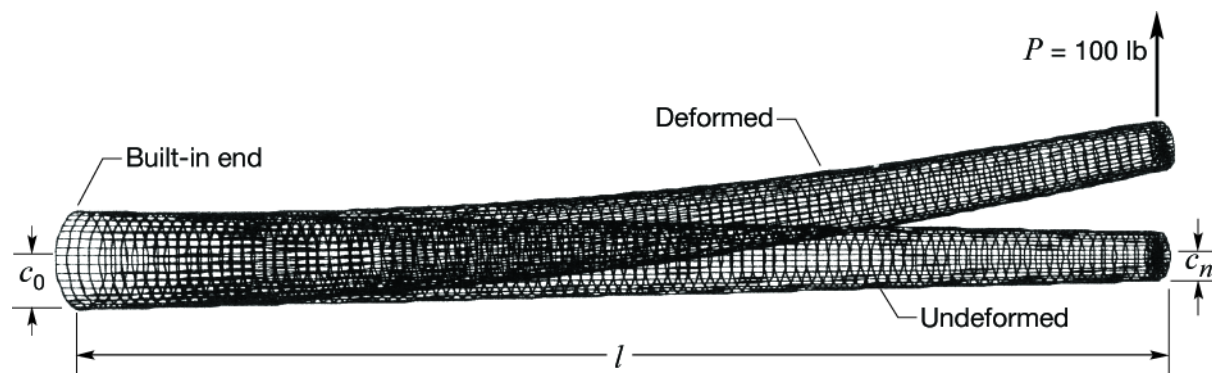


Improved Displacement Transfer Functions for Structure Deformed Shape Predictions Using Discretely Distributed Surface Strains

William L. Ko and Van Tran Fleischer

Dryden Flight Research Center, Edwards, California



$l = 100.5$ in.	Nodes	3673
$t = 0.02296$ in.	Four-node elements	3636
$c_0 = 4$ in.	Three-node elements	36
$c_n = 4, 3, 2, 1, 0.5, 0.25$ in.		

110283

NASA STI Program ... in Profile

Since its founding, NASA has been dedicated to the advancement of aeronautics and space science. The NASA scientific and technical information (STI) program plays a key part in helping NASA maintain this important role.

The NASA STI program operates under the auspices of the Agency Chief Information Officer. It collects, organizes, provides for archiving, and disseminates NASA's STI. The NASA STI program provides access to the NASA Aeronautics and Space Database and its public interface, the NASA Technical Report Server, thus providing one of the largest collections of aeronautical and space science STI in the world. Results are published in both non-NASA channels and by NASA in the NASA STI Report Series, which includes the following report types:

- **TECHNICAL PUBLICATION.** Reports of completed research or a major significant phase of research that present the results of NASA Programs and include extensive data or theoretical analysis. Includes compilations of significant scientific and technical data and information deemed to be of continuing reference value. NASA counterpart of peer-reviewed formal professional papers but has less stringent limitations on manuscript length and extent of graphic presentations.
- **TECHNICAL MEMORANDUM.** Scientific and technical findings that are preliminary or of specialized interest, e.g., quick release reports, working papers, and bibliographies that contain minimal annotation. Does not contain extensive analysis.
- **CONTRACTOR REPORT.** Scientific and technical findings by NASA-sponsored contractors and grantees.

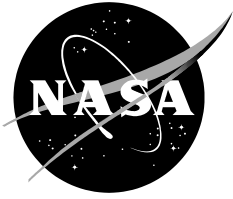
- **CONFERENCE PUBLICATION.** Collected papers from scientific and technical conferences, symposia, seminars, or other meetings sponsored or co-sponsored by NASA.
- **SPECIAL PUBLICATION.** Scientific, technical, or historical information from NASA programs, projects, and missions, often concerned with subjects having substantial public interest.
- **TECHNICAL TRANSLATION.** English-language translations of foreign scientific and technical material pertinent to NASA's mission.

Specialized services also include organizing and publishing research results, distributing specialized research announcements and feeds, providing help desk and personal search support, and enabling data exchange services.

For more information about the NASA STI program, see the following:

- Access the NASA STI program home page at <http://www.sti.nasa.gov>
- E-mail your question via the Internet to help@sti.nasa.gov
- Fax your question to the NASA STI Help Desk at 443-757-5803
- Phone the NASA STI Help Desk at 443-757-5802
- Write to:
NASA STI Help Desk
NASA Center for AeroSpace Information
7115 Standard Drive
Hanover, MD 21076-1320

NASA/TP—2012–216060



Improved Displacement Transfer Functions for Structure Deformed Shape Predictions Using Discretely Distributed Surface Strains

William. L. Ko and Van Tran Fleischer

Dryden Flight Research Center, Edwards, California

National Aeronautics and
Space Administration

*Dryden Flight Research Center
Edwards, CA 93523-0273*

November 2012

PATENT NOTICE

The method for structural deformed shape predictions using discretely distributed surface strains and embodied Displacement Transfer Functions for conversion into deflections described in this technical paper is protected under “*Method for Real-Time Structure Shape-Sensing*”, U.S. Patent No. 7,520,176 issued April 21, 2009. Therefore, those interested in using the method should contact the NASA Innovative Partnership Program Office at NASA Dryden Flight Research Center, Edwards, California, for more information.

NOTICE

Use of trade names or names of manufacturers in this document does not constitute an official endorsement of such products or manufacturers, either expressed or implied, by the National Aeronautics and Space Administration

Available from:

NASA Center for AeroSpace Information
7115 Standard Drive
Hanover, MD 21076-1320
443-757-5802

TABLE OF CONTENTS

ABSTRACT.....	1
NOMENCLATURE	1
INTRODUCTION	2
NONUNIFORM AND UNIFORM BEAMS.....	3
EMBEDDED BEAM CURVATURE EQUATIONS.....	3
DISCRETIZATION OF NONUNIFORM EMBEDDED BEAM.....	4
SUMMARY OF PREVIOUS DISPLACEMENT TRANSFER FUNCTIONS	5
CHARACTERISTICS OF DISPLACEMENT TRANSFER FUNCTIONS.....	6
PREVIOUS PIECEWISE LINEAR REPRESENTATIONS.....	6
BEHAVIOR OF STRAIN CURVES FOR DIFFERENT TAPERED BEAMS.....	7
Tapered Cantilever Tubular Beams	7
Analytical Surface Strains.....	7
Shapes of Strain Curves	8
FORMULATIONS OF IMPROVED DISPLACEMENT TRANSFER FUNCTIONS	9
Piecewise Nonlinear Strain Representations.....	9
Strain Extrapolation	9
Piecewise Nonlinear Strain Curves.....	10
UNIFORM BEAMS	10
Improved Slope Equation.....	10
Improved Deflection Equation.....	11
Improved Displacement Transfer Function	12
NONUNIFORM BEAMS.....	12
Improved Slope Equation.....	12
Improved Deflection Equation.....	13
Improved Displacement Transfer Function	14
LOG-EXPANDED CASE	15
Log-Expanded Slope Equation	15
Log-Expanded Deflection Equation.....	16
Log-Expanded Displacement Transfer Function	17
Log-Expanded Slope Equation for Uniform Beams	17
Log-Expanded Deflection Equation for Uniform Beams	17

DEPTH-EXPANDED CASE.....	18
Depth-Expanded Slope Equation	18
Depth-Expanded Deflection Equation	20
Depth-Expanded Displacement Transfer Function.....	21
NEW STRUCTURE SHAPE-SENSING TECHNOLOGY	21
SHAPE-PREDICTION ACCURACIES.....	22
Tapered Cantilever Tubular Beams	22
Comparisons of Predicted Deflections.....	22
Shape-Prediction Errors	26
Normalized Shape-Prediction Errors	27
DISCUSSION.....	28
CONCLUDING REMARKS	28
FIGURES	30
APPENDIX A: DERIVATIONS OF IMPROVED SLOPE AND DEFLECTION EQUATIONS FOR UNIFORM BEAMS	40
APPENDIX B: DERIVATIONS OF IMPROVED DISPLACEMENT TRANSFER FUNCTION FOR UNIFORM BEAMS	42
APPENDIX C: DERIVATIONS OF IMPROVED SLOPE AND DEFLECTION EQUATIONS FOR NONUNIFORM BEAMS.....	44
APPENDIX D: DERIVATIONS OF IMPROVED DISPLACEMENT TRANSFER FUNCTION FOR NONUNIFORM BEAMS.....	50
APPENDIX E: DERIVATIONS OF LOG-EXPANDED SLOPE AND DEFLECTION EQUATIONS FOR NONUNIFORM BEAMS	54
APPENDIX F: DERIVATIONS OF LOG-EXPANDED DISPLACEMENT TRANSFER FUNCTION FOR NONUNIFORM BEAMS	61
APPENDIX G: DERIVATIONS OF DEPTH-EXPANDED SLOPE AND DEFLECTION EQUATIONS FOR NONUNIFORM BEAMS	64
APPENDIX H: DERIVATIONS OF DEPTH-EXPANDED DISPLACEMENT TRANSFER FUNCTION FOR NONUNIFORM BEAMS	70
APPENDIX I: FLOW CHART FOR STRUCTURE DEFORMED SHAPE VISUALIZATIONS	74
REFERENCES	78

ABSTRACT

In the formulations of earlier Displacement Transfer Functions for structure shape predictions, the surface strain distributions, along a strain-sensing line, were represented with piecewise linear functions. To improve the shape-prediction accuracies, Improved Displacement Transfer Functions were formulated using piecewise nonlinear strain representations. Through discretization of an embedded beam (depth-wise cross section of a structure along a strain-sensing line) into multiple small domains, piecewise nonlinear functions were used to describe the surface strain distributions along the discretized embedded beam. Such piecewise approach enabled the piecewise integrations of the embedded beam curvature equations to yield slope and deflection equations in recursive forms. The resulting Improved Displacement Transfer Functions, written in summation forms, were expressed in terms of beam geometrical parameters and surface strains along the strain-sensing line. By feeding the surface strains into the Improved Displacement Transfer Functions, structural deflections could be calculated at multiple points for mapping out the overall structural deformed shapes for visual display. The shape-prediction accuracies of the Improved Displacement Transfer Functions were then examined in view of finite-element-calculated deflections using different tapered cantilever tubular beams. It was found that by using the piecewise nonlinear strain representations, the shape-prediction accuracies could be greatly improved, especially for highly-tapered cantilever tubular beams.

NOMENCLATURE

A	$\equiv -(3\varepsilon_{i-1} - 4\varepsilon_i + \varepsilon_{i+1})/2\Delta l$, 1/in.
B	$\equiv (\varepsilon_{i-1} - 2\varepsilon_i + \varepsilon_{i+1})/2(\Delta l)^2$, 1/in ²
c	depth factor (vertical distance from neutral surface to outermost fiber of bottom surface of uniform beam), in.
c_i	$\equiv c(x_i)$, depth factor of nonuniform beam at strain-sensing station, x_p , in.
c_n	value of c_i at free end (beam tip), $x = x_n = l$, in.
c_n/c_0	depth ratio, no dimension
$c(x)$	depth factor (vertical distance from neutral surface to bottom surface outermost fiber of nonuniform beam) at axial location, x , in.
c_0	value of c_i at fixed end (beam root), $x = x_0 = 0$, in.
C	$\equiv (c_i - c_{i-1})/\Delta l$, in/in
CG	center of gravity
d_i	chord-wise distance between front and rear strain-sensing stations at $\{x_i, x'_i\}$, in.
D	$\equiv [(c_i/c_{i-1}) - 1]/\Delta l$, 1/in.
DLL	design limit load
i	$= 0, 1, 2, 3, \dots, n$, strain-sensing station identification number
j	dummy index
l	length of beam, in.
n	index for the last span-wise strain-sensing station (or strain-sensing station density)
P	force, lb
RRF	rotated reference frame, aligns with the wing's out-of-plane direction
$R(x)$	radius of curvature of beam elastic curve, in.
SPAR	Structural Performance And Resizing (finite-element computer program)
t	tubular beam wall thickness, in.
x, y	Cartesian coordinates (x in beam axial direction, y in lateral direction), in.
x_i	axial coordinate or symbol of i -th strain-sensing station, in.

- $y(x)$ beam deflection in y-direction at axial location, x , in.
 y_i $\equiv y(x_i)$, beam deflection in y-direction at axial location, $x = x_i$, in.
 y_n^{SPAR} beam-tip deflection calculated from SPAR, in.
 Δl $\equiv (x_i - x_{i-1}) = l/n$, distance between two adjacent strain-sensing stations $\{x_{i-1}, x_i\}$, in.
 Δy_n $\equiv |y_n - y_n^{SPAR}|$, beam-tip shape-prediction error (difference between predicted and SPAR-generated beam-tip deflections), in.
 α $\equiv \tan^{-1}[(c_0 - c_n)/l]$, beam taper angle, deg
 $\varepsilon(x)$ surface bending strain at axial location, x , in/in
 ε_i $\equiv \varepsilon(x_i)$, surface bending strain at strain-sensing station, x_i , in/in
 $\theta(x)$ slope of deformed beam at axial location, x , rad or deg
 θ_i $\equiv \theta(x_i)$, slope of deformed beam at axial location, $x = x_i$, rad or deg
 ξ $\equiv (x - x_{i-1})$, local axial coordinate with origin at x_{i-1} , in.
 ϕ_i cross-sectional twist angle, rad or deg
 (Y) quantities associated with rear strain-sensing line

INTRODUCTION

In the formulations of earlier Displacement Transfer Functions (refs. 1-5) for structure shape predictions using distributed surface strains, the embedded beam (depth-wise cross-section of the structure along a strain-sensing line) was first discretized into multiple small domains of equal length. Through discretization, the axial distributions of both beam depth and surface strain within each small domain could be represented with piecewise linear functions. The discretization approach enabled the piecewise integrations of the beam curvature equation (second-order differential equation) over the small domains in closed forms to yield beam slope and deflection equations in recursive forms. Each set of recursive slope and deflection equations was then combined into a single dual summation-form deflection equation called a Displacement Transfer Function (refs. 1-5). The Displacement Transfer Function was then written in terms of geometrical parameters of discretized embedded beam and surface strains obtained at strain-sensing stations (at domain junctures) evenly spaced along the strain-sensing line. By inputting the surface strains from multiple strain-sensing lines, the associated Displacement Transfer Functions can convert the surface strains into deflections at multiple points, enabling the mapping of overall structural deformed shapes for visual display. Thus, the Displacement Transfer Functions with an accompanying surface strain-sensing system [for example, fiber optic strain sensors (refs. 6-8)], has created a new structure shape-sensing technology, called *Method for Real-Time Structure Shape-Sensing* (U.S. Patent Number 7,520,176) (ref. 9), which could be very useful for in-flight deformed shape monitoring of flexible wings and tails, such as those often employed on unmanned flight vehicles by the ground-based pilot for maintaining safe flights. In addition, the wing shape being monitored in real time could then be input to the aircraft control system for aeroelastic wing shape control.

Similar to the structure deformed shape predictions, the distributed surface strains can also be fed into the special stiffness and Load Transfer Functions described in *Process for Using Surface Strain Measurements to Obtain Operational Loads for Complex Structures* (U.S. Patent No. 7,715,994) (ref. 10), for predicting the operational loads on a flight vehicle.

The previously-developed Displacement Transfer Functions were successfully validated for their accuracies in view of finite-element analysis of different sample structures such as cantilever tubular beams (uniform, tapered, slightly tapered, and step-wisely tapered); two-point supported tapered tubular beams, flat panels, and tapered wing boxes (un-swept and swept) (refs. 1, 2, 4, and 5); and the doubly-tapered wing of the NASA Ikhana Unmanned Science and Research Aircraft System (a modified Predator-B unmanned aerial system, General Atomics Aeronautical Systems Inc., San Diego, California). (ref. 3).

The earlier Displacement Transfer Functions were formulated for straight embedded beams. With the introduction of empirical curvature-effect correction terms, however, those Displacement Transfer Functions could be used for the shape predictions of slender curved structures with different arc-angles up to 360 deg (a complete circle) (ref. 11).

All the earlier Displacement Transfer Functions were formulated using piecewise linear representations of the actual strain distributions. For the shape predictions of tapered beam structures, for which the strain gradients change rapidly (highly nonlinear strain distributions) (ref. 3), the use of piecewise linear strain representations could result in a loss of accuracy. One way to avoid this loss of shape-prediction accuracy is to increase the domain density (that is, use increasing strain-sensing stations) so that the piecewise linear strain representation can maintain a good approximation. An alternative approach is to introduce piecewise nonlinear representations of the actual strain distributions.

This technical paper discusses the mathematical formulations of the Improved Displacement Transfer Functions using the piecewise nonlinear strain representations. A family of tapered cantilever tubular beams with different taper angles was used to study the shape-prediction accuracies of the Improved Displacement Transfer Functions. The shape-prediction accuracies were then analyzed by comparing the predicted values with the analytically-predicted values obtained from the finite-element analyses. The results showed that by using the piecewise nonlinear strain representations in the formulation of the Displacement Transfer Functions, the shape-prediction accuracies were greatly improved, especially for highly-tapered beam structures.

NONUNIFORM AND UNIFORM BEAMS

In the present technical paper, the term “beam” implies the imaginary embedded beam, which is defined as the depth-wise cross-section of the structure along the strain-sensing line. The “nonuniform beam” in the present technical paper is defined as the embedded beam with a varying depth factor, $c(x)$, a vertical distance from the neutral surface to the bottom surface of the nonuniform beam at axial location, x . For a nonuniform tubular beam, $c(x)$ will be the outward radius. The “slightly nonuniform beam” in the present technical paper is defined as the embedded beam with slowly changing depth factor, $c(x)$. The “uniform beam” in the present technical paper is defined as the embedded beam with constant depth factor [that is, $c(x) = c$].

EMBEDDED BEAM CURVATURE EQUATIONS

Figure 1 shows a deformed uniform embedded beam with constant depth factor, c . In a small beam segment bounded by $d\theta$, the small un-deformed curve length, $AB(= ds)$, is on the beam neutral surface, and the deformed curve length, $A'B' \{= AB[1 + \varepsilon(x)] = ds[1 + \varepsilon(x)]\}$, lies on the beam bottom surface under bending strain, $\varepsilon(x)$. From the two similar slender sectors, $O'AB$ and $O'A'B'$, the local radius of

curvature, $R(x)$, of the beam elastic curve, can be related to the bottom surface bending strain, $\varepsilon(x)$, through the beam depth factor, c , as:

$$\frac{O'A'}{O'A} = 1 + \frac{c}{R(x)} = \frac{A'B'}{AB} = 1 + \varepsilon(x) \quad (1)$$

Applying the Lagrangian curvature equation, $1/R(x) = (d^2y/dx^2)/\sqrt{1-(dy/dx)^2}$ (refs. 12 and 13), neglecting the term, $(dy/dx)^2$ (negligible axial displacements), equation (1) can be written in the form of a second-order differential equation as:

$$\frac{d^2y}{dx^2} = \frac{\varepsilon(x)}{c} \quad (2)$$

In equation (2), x is the undeformed axial coordinate, and y is the out-of-plane deflection. Because equation (2) is referred to the un-deformed x -coordinate (Lagrangian formulation), the term, d^2y/dx^2 , in equation (2) is not the simplified form of the classical curvature equation, $1/R(x) = (d^2y/dx^2)/[1+(dy/dx)^2]^{3/2}$, which is referred to the deformed x -coordinate (Eulerian formulation) (refs. 12, 13, and 14).

Notice that curvature equation (2) is purely a geometrical relationship, containing no material or structural properties. In fact, the effect of the material or structural properties is felt by the surface bending strains, $\varepsilon(x)$; the value of $\varepsilon(x)$ is influenced by the material or structural properties.

The curvature equation (2) could also be extended to the nonuniform embedded beam without losing accuracy if the embedded beam depth factor, $c(x)$, changes slowly along the beam axis (ref. 15). Namely,

$$\frac{d^2y}{dx^2} = \frac{\varepsilon(x)}{c(x)} \quad (3)$$

For given beam geometries, the depth factors $\{c, c(x)\}$ are known. If the functional form of the surface strain, $\varepsilon(x)$, is specified, equation (2) or (3) can be integrated once to yield the beam slope equation, and the second integration will yield the beam deflection equation. To integrate the curvature equations (2) or (3), the piecewise integration method can be used. (refs. 1-5).

DISCRETIZATION OF NONUNIFORM EMBEDDED BEAM

The integrations of curvature equation (2) or (3) can be achieved by means of piecewise integrations through beam discretizations (refs. 1, 2, and 5). As shown in figure 2, the embedded beam of length, l , is first discretized evenly into n multiple small domains, $x_{i-1} \leq x \leq x_i$ ($i = 1, 2, 3, \dots, n$), with equal domain length, $\Delta l (= l/n)$. The strain-sensing stations where the bending strains will be measured (or analytically calculated) are located on the beam bottom surface at the domain junctures (including at both ends of the beam), $x = x_0, x_1, x_2, \dots, x_n$ (fig. 2). Through discretization, both beam depth factor and surface bending strain, $\{c(x), \varepsilon(x)\}$, within each small domain, $x_{i-1} \leq x \leq x_i$, could be expressed with

simple linear functions. Such an approach enables the piecewise integrations of curvature equation (2) or (3) in closed forms for each small domain to yield beam slope and deflection equations in recursive forms. These recursive slope and deflection equations can be combined into a dual summation-form deflection equation called the Displacement Transfer Function (refs. 1-5) and expressed in terms of domain length, Δl , beam depth factors, and surface bending strains, $\{c_i, \varepsilon_i\}$, (fig. 2).

SUMMARY OF PREVIOUS DISPLACEMENT TRANSFER FUNCTIONS

All the earlier Displacement Transfer Functions were formulated through piecewise integrations of equation (2) or (3). Four earlier Displacement Transfer Functions formulated for nonuniform, slightly nonuniform, and uniform straight embedded beams, are shown below for comparison of their mathematical functional forms (refs. 1, 2, and 5).

1. Displacement Transfer Function for nonuniform beams ($c_i \neq c_{i-1}$) (derivations in Appendix A of ref. 2):

$$\begin{aligned}
 y_i = & \underbrace{(\Delta l)^2 \sum_{j=1}^i \left\{ \frac{\varepsilon_{j-1} - \varepsilon_j}{2(c_{j-1} - c_j)} - \frac{\varepsilon_{j-1}c_j - \varepsilon_jc_{j-1}}{(c_{j-1} - c_j)^3} \left[c_j \log_e \frac{c_j}{c_{j-1}} + (c_{j-1} - c_j) \right] \right\}}_{\text{Contributions from deflection terms}} \\
 & + \underbrace{(\Delta l)^2 \sum_{j=1}^{i-1} \left\{ (i-j) \left[\frac{\varepsilon_{j-1} - \varepsilon_j}{c_{j-1} - c_j} + \frac{\varepsilon_{j-1}c_j - \varepsilon_jc_{j-1}}{(c_{j-1} - c_j)^2} \log_e \frac{c_j}{c_{j-1}} \right] \right\}}_{\text{Contribution from slope terms}} + \underbrace{y_0 + (i)\Delta l \tan \theta_0}_{=0 \text{ for cantilever beams}} \\
 & \qquad \qquad \qquad (i = 1, 2, 3, \dots, n)
 \end{aligned} \tag{4}$$

2. Displacement Transfer Function for slightly nonuniform beams ($c_i/c_{i-1} \rightarrow 1$) (derivations in Appendix C of ref. 2):

$$\begin{aligned}
 y_i = & \underbrace{\frac{(\Delta l)^2}{6} \sum_{j=1}^i \left\{ \frac{1}{c_{j-1}} \left[\left(3 - \frac{c_j}{c_{j-1}} \right) \varepsilon_{j-1} + \varepsilon_j \right] \right\}}_{\text{Contribution from deflection terms}} + \underbrace{\frac{(\Delta l)^2}{2} \sum_{j=1}^{i-1} \left\{ \frac{(i-j)}{c_{j-1}} \left[\left(2 - \frac{c_j}{c_{j-1}} \right) \varepsilon_{j-1} + \varepsilon_j \right] \right\}}_{\text{Contributions from slope terms}} \\
 & + \underbrace{y_0 + \Delta l \tan \theta_0}_{=0 \text{ for cantilever beams}} \\
 & \qquad \qquad \qquad (i = 1, 2, 3, \dots, n)
 \end{aligned} \tag{5}$$

which was obtained from equation (4) by expanding the logarithmic terms in the neighborhood of $c_i/c_{i-1} \approx 1$.

3. Second-order Displacement Transfer Function for nonuniform beams ($c_i \neq c_{i-1}$) [$1/c(x)$ in equation (3) expanded in series up to the second-order term] (ref. 5):

$$\begin{aligned}
y_i = & \underbrace{\frac{(\Delta l)^2}{60} \sum_{j=1}^i \frac{1}{c_{j-1}} \left\{ \left[27 - 9 \frac{c_j}{c_{j-1}} + 2 \left(\frac{c_j}{c_{j-1}} \right)^2 \right] \varepsilon_{j-1} + \left[18 - 11 \frac{c_j}{c_{j-1}} + 3 \left(\frac{c_j}{c_{j-1}} \right)^2 \right] \varepsilon_j \right\}}_{\text{Contributions from deflection terms}} \\
& + \underbrace{\frac{(\Delta l)^2}{12} \sum_{j=1}^{i-1} \frac{(i-j)}{c_{j-1}} \left\{ \left[9 - 4 \frac{c_j}{c_{j-1}} + \left(\frac{c_j}{c_{j-1}} \right)^2 \right] \varepsilon_{j-1} + \left[13 - 10 \frac{c_j}{c_{j-1}} + 3 \left(\frac{c_j}{c_{j-1}} \right)^2 \right] \varepsilon_j \right\}}_{\text{Contributions from slope terms}} \\
& + \underbrace{y_0 + (i)\Delta l \tan \theta_0}_{=0 \text{ for cantilever beams}}
\end{aligned} \tag{6}$$

$(i = 1, 2, 3, \dots, n)$

4. Displacement Transfer Function for uniform beams ($c_i = c_{i-1} = c$) (derivations in ref. 1; Appendix D of ref. 2; Appendix A of ref. 5):

$$y_i = \frac{(\Delta l)^2}{6c} \left[(3i-1)\varepsilon_0 + 6 \sum_{j=1}^{i-1} (i-j)\varepsilon_j + \varepsilon_i \right] + \underbrace{y_0 + (i)\Delta l \tan \theta_0}_{=0 \text{ for cantilever beams}} ; \quad (i = 1, 2, 3, \dots, n) \tag{7}$$

Equation (7) is the degenerated form of equations (5) and (6) for the uniform beam case, ($c_i = c_{i-1} = c$).

CHARACTERISTICS OF DISPLACEMENT TRANSFER FUNCTIONS

Except for equation (4), equations (5) and (6) could degenerate into equation (7) for the uniform beam case ($c_i = c_{i-1} = c$) without incurring mathematical indeterminacy problems (refs. 1 and 2). Note that in each of the deflection equations (4)–(7), the deflection, y_i , at the current strain-sensing station, x_i , is expressed in terms of domain length, Δl , inboard beam depth factors, ($c_0, c_1, c_2, c_3, \dots, c_i$), and the associated inboard surface strains, ($\varepsilon_0, \varepsilon_1, \varepsilon_2, \varepsilon_3, \dots, \varepsilon_i$), including the values of (c_i, ε_i) at the current strain-sensing station x_i , where deflection, y_i , is calculated. Because equations (4)–(7) contain no material or structural properties, when equations (4)–(7) are used in the deformed shape calculations of complex structures (for example, aircraft wings), there is no need to know the material or structural properties. In fact, the effect of the material or structural properties is felt by the surface strains, ε_i ($i = 1, 2, 3, \dots, n$). This is the key characteristic of the Displacement Transfer Functions (refs. 1–5).

PREVIOUS PIECEWISE LINEAR REPRESENTATIONS

The above four displacement transfer functions, equations (4)–(7), were formulated through discretization of the embedded beam into multiple small domains (fig. 2). The variation of the beam depth factor, $c(x)$, and the surface bending strain, $\varepsilon(x)$, within each small domain, $x_{i-1} \leq x \leq x_i$, between the two adjacent strain-sensing stations, $\{x_{i-1}, x_i\}$, was then expressed with linear functions as:

$$c(x) = c_{i-1} + (c_i - c_{i-1}) \frac{x - x_{i-1}}{\Delta l} ; \quad (x_{i-1} \leq x \leq x_i) \tag{8}$$

$$\varepsilon(x) = \varepsilon_{i-1} + (\varepsilon_i - \varepsilon_{i-1}) \frac{x - x_{i-1}}{\Delta l} \quad ; \quad (x_{i-1} \leq x \leq x_i) \quad (9)$$

Equation (8) can be a good piecewise linear representation of the slowly-varying depth factor, $c(x)$, of the nonuniform beams. The accuracy of equation (9) for piecewise linear representation of varying surface strain, $\varepsilon(x)$, however, needs to be examined when the beam taper angle increases and causes strain distributions to be highly nonlinear.

BEHAVIOR OF STRAIN CURVES FOR DIFFERENT TAPERED BEAMS

This section is to examine the accuracy of piecewise linear strain representation equation (9) using tapered beams with different taper angles, and to show that equation (9) can lose accuracy in representing nonlinear strain distributions for the cases of highly-tapered beams.

Tapered Cantilever Tubular Beams

To study the accuracy degradation of the piecewise linear strain representations equation (9), a family of tapered cantilever tubular beams with different taper angles was chosen. The dimensions and taper angles, α , of the aluminum tapered cantilever tubular beams considered are listed in Table 1.

Table 1. Dimensions of aluminum tapered cantilever tubular beams.

l , in. (length)	t , in. (wall thickness)	c_0 , in. (root depth)	c_n , in. (tip depth)	c_n/c_0 (depth ratio)	$\alpha \{= \tan^{-1}[(c_0 - c_n)/l]\}$, deg (taper angle)
100.5	0.02296	4	4 (uniform)	4/4 (1.0)	0.00
100.5	0.02296	4	3	3/4 (0.75)	0.57
100.5	0.02296	4	2	2/4 (0.5)	1.14
100.5	0.02296	4	1	1/4 (0.25)	1.71
100.5	0.02296	4	0.5	0.5/4 (0.125)	1.99
100.5	0.02296	4	0.25	0.25/4 (0.0625)	2.14

The imaginary embedded beam shown in figure 2 can also represent the embedded beam of a typical tubular beam, which is defined as the span-wise cross section through vertical diameters along the strain-sensing line. For each tapered tubular beam, the depth factor, c_i , of the embedded beam is the known local outer radius. Therefore, only one strain-sensing line on the bottom surface oriented in the span-wise direction is needed for shape predictions (fig. 2).

Figure 3 shows the finite-element model of a typical tapered cantilever tubular beam (depth ratio, $c_n/c_0 = 2/4$) generated from the SPAR (Structure Performance And Resizing) finite-element computer program (ref. 16). The size of the SPAR model (identical for all tapered beams) is also indicated in figure 3. The tapered cantilever tubular beam is subjected to upward load of $P = 100$ lb at the beam tip.

Analytical Surface Strains

In the present technical paper, the surface strains at the strain-sensing stations (fig. 2) were calculated analytically (not actually measured) using the SPAR program. Namely, finite elements were used to simulate actual strain gages. The surface bending strains, ε_i ($i = 0, 1, 2, 3, \dots, n$), at the i -th strain-sensing

stations (fig. 2) were obtained by converting SPAR-generated nodal or element axial stresses into axial strains, $\boldsymbol{\varepsilon}_i$ (bending strains), through stress-strain law.

Also, the surface strain, $\boldsymbol{\varepsilon}_i$, can be obtained from the span-wise nodal displacement differentials of the SPAR elements. It was found, however, that in the beam-tip regions of highly-bent tapered beams, the SPAR element strains became negative because the output nodal displacements were the projected displacements along the original beam axis, and not along the deformed beam axis to reflect true span-wise displacements. Therefore, this displacement method was not used.

Shapes of Strain Curves

The SPAR-generated strain curves were approximated with piecewise linear functions using domain densities of $n = 8$ and $n = 16$.

For $n = 8$

Figure 4 shows the shapes of piecewise linear strain curves (solid lines with solid circular symbols) using domain density, $n = 8$, to approximate the SPAR-generated strain curves (dashed curves with open circular symbols) for different tapered cantilever tubular beams. Note that the SPAR-generated strain data are not exactly zero (theoretically zero) at the free beam tip (especially for the $\boldsymbol{c}_n / \boldsymbol{c}_0 = 0.5/4, 0.25/4$ cases); the reason being that the beam-tip finite element (simulated strain gage) has one end at the beam tip, but the other end is slightly off from the beam tip because of finite length. By reducing the element sizes, the beam-tip strain should approach zero. If an actual strain gage were installed at the beam tip, the strain output could also be nonzero because of finite length of the strain gage.

For moderately-bent strain curves (for example, $\boldsymbol{c}_n / \boldsymbol{c}_0 = 3/4, 2/4, 1/4$) (fig. 4), the piecewise linear strain representations could be reasonably good, but for highly-bent regions of the strain curves (for example, $\boldsymbol{c}_n / \boldsymbol{c}_0 = 0.5/4, 0.25/4$), the piecewise linear strain representations could lose accuracy. Note from figure 4 in the highly-bent regions of the strain curves (for example, $\boldsymbol{c}_n / \boldsymbol{c}_0 = 0.5/4, 0.25/4$), the typical piecewise linear points, calculated from equation (9), lie slightly off from the corresponding SPAR data points.

Keep in mind that for the low depth ratios, (for example, $\boldsymbol{c}_n / \boldsymbol{c}_0 = 0.5/4, 0.25/4$), each beam will bend like a fishing pole in the outboard regions. These unrealistic very low depth ratios were included in the current analysis solely for theoretical interest to examine the shape-prediction accuracies of the Displacement Transfer Functions. For real aircraft wings, the depth ratios are much higher. For example, the Ikhana wing has a depth ratio of $\boldsymbol{c}_n / \boldsymbol{c}_0 = 0.4444$, for which the strain curve is bow-shaped (ref. 3).

For $n = 16$

To improve piecewise linear strain representations using equation (9), the domain density was increased from $n = 8$ to $n = 16$ to cause the piecewise linear strain curves to approach the corresponding SPAR-generated smooth strain curves.

Figure 5 shows that by using domain density $n = 16$, the piecewise linear strain representations greatly improved except for the sharply-bent regions. The peak strain point at strain-sensing station $i = 15$, which was missed at $n = 8$ for the $\boldsymbol{c}_n / \boldsymbol{c}_0 = 0.25/4$ case, is now included. In the sharply-bent region of the strain curve of the $\boldsymbol{c}_n / \boldsymbol{c}_0 = 0.25/4$ case, the typical piecewise linear point calculated from

equation (9) lies below the corresponding SPAR data point; however, further increasing of the domain density, n , could cause the piecewise linear strain curves to approach the corresponding SPAR-generated smooth strain curves.

An alternative approach is to use piecewise nonlinear strain representations (described below) to approximate the nonlinear strain curves and thereby improve the shape-prediction accuracies.

FORMULATIONS OF IMPROVED DISPLACEMENT TRANSFER FUNCTIONS

In the formulation of the Improved Displacement Transfer Functions, the piecewise linear assumption according to equation (9) for strain distribution was replaced with the piecewise nonlinear strain representations described below. Equation (8) was used without modification, however, because equation (8) is a good piecewise linear representation of the slowly-varying depth factor, $\mathbf{c}(\mathbf{x})$, of the nonuniform beams.

Piecewise Nonlinear Strain Representations

In the formulation of the Improved Displacement Transfer Functions, the distribution of surface bending strain, $\boldsymbol{\varepsilon}(\mathbf{x})$, within the dual domain, $\mathbf{x}_{i-1} \leq \mathbf{x} \leq \mathbf{x}_{i+1}$, was described with piecewise nonlinear (second-order) functions in terms of three strain values, $\{\boldsymbol{\varepsilon}_{i-1}, \boldsymbol{\varepsilon}_i, \boldsymbol{\varepsilon}_{i+1}\}$, respectively at three adjacent strain-sensing stations, $\{\mathbf{x}_{i-1}, \mathbf{x}_i, \mathbf{x}_{i+1}\}$, (fig. 6). The resulting piecewise nonlinear strain equation has the following form:

$$\boldsymbol{\varepsilon}(\mathbf{x}) = \boldsymbol{\varepsilon}_{i-1} - \frac{3\boldsymbol{\varepsilon}_{i-1} - 4\boldsymbol{\varepsilon}_i + \boldsymbol{\varepsilon}_{i+1}}{2\Delta l}(\mathbf{x} - \mathbf{x}_{i-1}) + \frac{\boldsymbol{\varepsilon}_{i-1} - 2\boldsymbol{\varepsilon}_i + \boldsymbol{\varepsilon}_{i+1}}{2(\Delta l)^2}(\mathbf{x} - \mathbf{x}_{i-1})^2 \quad (10)$$

$$(i = 0, 1, 2, 3, \dots, n)$$

Equation (10) is the piecewise nonlinear strain equation to replace the piecewise linear strain equation (9) for formulating the Improved Displacement Transfer Functions.

Strain Extrapolation

Note that equation (10) is for the strain-sensing stations $\mathbf{x}_i = \mathbf{x}_0, \mathbf{x}_1, \mathbf{x}_2, \mathbf{x}_3, \dots, \mathbf{x}_n$. At the beam tip strain-sensing station $\mathbf{x}_i = \mathbf{x}_n$, however, an extra strain point, $\boldsymbol{\varepsilon}_{n+1}$, is needed for three-points strain curve approximation. A simple way to estimate $\boldsymbol{\varepsilon}_{n+1}$ is through extrapolation using the three known strains, $\{\boldsymbol{\varepsilon}_{n-2}, \boldsymbol{\varepsilon}_{n-1}, \boldsymbol{\varepsilon}_n\}$, respectively at the three adjacent strain-sensing stations, $\{\mathbf{x}_{n-2}, \mathbf{x}_{n-1}, \mathbf{x}_n\}$, (fig. 7). The three-point extrapolation equation established for calculating $\boldsymbol{\varepsilon}_{n+1}$ has the following form:

$$\boldsymbol{\varepsilon}_{n+1} = \boldsymbol{\varepsilon}_{n-2} - 3\boldsymbol{\varepsilon}_{n-1} + 3\boldsymbol{\varepsilon}_n \quad (11)$$

Equation (11) was obtained from equation (10) by setting $i = n - 1$ and $\mathbf{x} - \mathbf{x}_{i-1} = \mathbf{x}_{n+1} - \mathbf{x}_{n-2} = 3\Delta l$.

Piecewise Nonlinear Strain Curves

Figure 8 compares the piecewise nonlinear strain curves (solid curves with solid circular symbols) based on equation (10) using the domain density $n = 16$, and the corresponding SPAR-generated strain curves (dashed curves with open circular symbols) for different tapered cantilever tubular beams. In the sharply-bent segment of the strain curve of the $c_n/c_0 = 0.25/4$ case (fig. 8), the typical piecewise nonlinear point, calculated from equation (10), has now moved above the corresponding SPAR data point. Except for the $c_n/c_0 = 0.25/4$ case, the piecewise nonlinear strain representations based on equation (10) could provide very good approximations of the bow-shaped SPAR strain curves. As will be seen, by changing from piecewise linear to piecewise nonlinear strain representations (see figs. 5 and 8), shape-prediction accuracies could be greatly improved.

UNIFORM BEAMS

The formulation of the Improved Displacement Transfer Functions will start from the mathematically simpler case of uniform beams, and progress to the mathematically more complex case of nonuniform beams. As mentioned above, the uniform beam considered in the present technical paper is the embedded beam with constant depth. In the formulations of the Displacement Transfer Functions, dimensions of beam width are not needed. Using the piecewise linear depth equation (8), and the piecewise nonlinear strain equation (10), the Improved Displacement Transfer Functions were formulated first for the uniform beams. The slope and deflection equations are to be obtained by piecewise integrations of the curvature equation (2) for the uniform beams.

Improved Slope Equation

The slope, $\tan \theta(x)$ of the uniform beam at axial location x within the small domain, $x_{i-1} \leq x \leq x_i$, bounded by the two adjacent strain-sensing stations, $\{x_{i-1}, x_i\}$, can be obtained by integrating the uniform-beam curvature equation (2) once, and enforcing the continuity of slope at the adjacent inboard strain-sensing station, x_{i-1} . Namely,

$$\tan \theta(x) = \underbrace{\int_{x_{i-1}}^x \frac{d^2 y}{dx^2} dx}_{\text{Slope increment}} + \underbrace{\tan \theta_{i-1}}_{\text{Slope at } x_{i-1}} = \int_{x_{i-1}}^x \underbrace{\frac{\varepsilon(x)}{c}}_{\text{Eq. (2)}} dx + \tan \theta_{i-1} \quad ; \quad (x_{i-1} \leq x \leq x_i) \quad (12)$$

in which $\tan \theta_{i-1}$ is the slope at x_{i-1} . Substituting equation (10) into equation (12) and carrying out the integration (ref. 17), one obtains the slope equation for the small domain, $x_{i-1} \leq x \leq x_i$ (see Appendix A):

$$\tan \theta(x) = \frac{1}{c} \left[\varepsilon_{i-1}(x - x_{i-1}) - \frac{3\varepsilon_{i-1} - 4\varepsilon_i + \varepsilon_{i+1}}{4\Delta l} (x - x_{i-1})^2 + \frac{\varepsilon_{i-1} - 2\varepsilon_i + \varepsilon_{i+1}}{6(\Delta l)^2} (x - x_{i-1})^3 \right] + \tan \theta_{i-1} \quad (13)$$

$(x_{i-1} \leq x \leq x_i)$

At the strain-sensing station, $x = x_i$, we have $x_i - x_{i-1} = \Delta l$, and equation (13) gives the slope, $\tan \theta_i [\equiv \tan \theta(x_i)]$, at the strain-sensing station, x_i , as:

$$\tan \theta_i = \frac{\Delta l}{12c} (5\varepsilon_{i-1} + 8\varepsilon_i - \varepsilon_{i+1}) + \tan \theta_{i-1} \quad ; \quad (i = 1, 2, 3, \dots, n) \quad (14)$$

Equation (14) is the Improved slope equation for the uniform beams in recursive form. Applying the recursive relationship, equation (14) can be written as:

$$\tan \theta_i = \frac{\Delta l}{12c} \sum_{j=1}^i (5\varepsilon_{j-1} + 8\varepsilon_j - \varepsilon_{j+1}) + \tan \theta_0 \quad ; \quad (i = 1, 2, 3, \dots, n) \quad (15)$$

Equation (15) is the Improved slope equation for the uniform beams in summation form.

Improved Deflection Equation

The deflection, $y(x)$, of the uniform cantilever beam within the small domain, $x_{i-1} \leq x \leq x_i$, can be obtained by integrating the slope equation (13) and enforcing the continuity of deflection at the inboard adjacent strain-sensing station, x_{i-1} , as:

$$y(x) = \int_{x_{i-1}}^x \underbrace{\tan \theta(x)}_{\text{eq. (13)}} dx + y_{i-1} \quad ; \quad (x_{i-1} \leq x \leq x_i) \quad (16)$$

in which y_{i-1} is the deflection at the inboard strain-sensing station, x_{i-1} .

In view of equation (13), equation (16) can be integrated (ref. 17) to yield the following deflection equation for the small domain, $x_{i-1} \leq x \leq x_i$, as (see Appendix A):

$$y(x) = \frac{1}{c} \left[\frac{\varepsilon_{i-1}}{2} (x - x_{i-1})^2 - \frac{3\varepsilon_{i-1} - 4\varepsilon_i + \varepsilon_{i+1}}{12\Delta l} (x - x_{i-1})^3 + \frac{\varepsilon_{i-1} - 2\varepsilon_i + \varepsilon_{i+1}}{24(\Delta l)^2} (x - x_{i-1})^4 \right] + (x - x_{i-1}) \tan \theta_{i-1} + y_{i-1} \quad (x_{i-1} \leq x \leq x_i) \quad (17)$$

At the strain-sensing station, $x = x_i$, we have $x_i - x_{i-1} = \Delta l$, and equation (17) gives the deflection, $y_i [\equiv y(x_i)]$, at the strain-sensing station, x_i , as:

$$y_i = \frac{(\Delta l)^2}{24c} (7\varepsilon_{i-1} + 6\varepsilon_i - \varepsilon_{i+1}) + y_{i-1} + \Delta l \tan \theta_{i-1} \quad ; \quad (i = 1, 2, 3, \dots, n) \quad (18)$$

Equation (18) is the Improved deflection equation for the uniform beams in recursive form.

Improved Displacement Transfer Function

In view of equation (15), and applying recursive relationships, equation (18) can be written in dual summation form as (see Appendix B):

$$y_i = \underbrace{\frac{(\Delta)^2}{24c} \sum_{j=1}^i (7\varepsilon_{j-1} + 6\varepsilon_j - \varepsilon_{j+1}) + y_0}_{\text{Contributions of deflection terms}} + \underbrace{\frac{(\Delta)^2}{12c} \sum_{j=1}^{i-1} (i-j)(5\varepsilon_{j-1} + 8\varepsilon_j - \varepsilon_{j+1}) + (i)\Delta \tan \theta_0}_{\text{Contributions of slope terms}} \quad (19)$$

$(i = 1, 2, 3, \dots, n)$

Equation (19) is called the Improved Displacement Transfer Function for the uniform beams because equation (19) transforms the surface strains into deflections. Note that the first summation is contributed from the deflection terms, and the second summation is contributed from the slope terms. Note also that a factor $(i-j)$ appeared in the second summation term due to cumulative summations of identical terms (see Appendix B). Note that the second summation ends at $j = i-1$ (that is, one term shorter than the first summation) (see Appendix B).

NONUNIFORM BEAMS

As defined earlier, the nonuniform beam has a variable depth factor, $c(x)$. Using the piecewise linear depth equation (8), and the piecewise nonlinear strain equation (10), the Improved Displacement Transfer Functions were formulated for the nonuniform beams. The slope and deflection equations are obtained by piecewise integrations of the curvature equation (3) for the nonuniform beams.

Improved Slope Equation

The slope, $\tan \theta(x)$ of the nonuniform beam at axial location x within the small domain, $x_{i-1} \leq x \leq x_i$, bounded by the two adjacent strain-sensing stations, $\{x_{i-1}, x_i\}$, can be obtained by integrating the nonuniform-beam curvature equation (3) once, and enforcing the continuity of slope at the adjacent inboard strain-sensing station, x_{i-1} . Namely,

$$\tan \theta(x) = \underbrace{\int_{x_{i-1}}^x \frac{d^2 y}{dx^2} dx}_{\text{Slope increment}} + \underbrace{\tan \theta_{i-1}}_{\text{Slope at } x_{i-1}} = \int_{x_{i-1}}^x \underbrace{\frac{\varepsilon(x)}{c(x)}}_{\text{Eq. (3)}} dx + \tan \theta_{i-1} \quad ; \quad (x_{i-1} \leq x \leq x_i) \quad (20)$$

in which $\tan \theta_{i-1}$, is the slope at x_{i-1} . Substituting equations (8) and (10) into equation (20), and carrying out integration, one obtains the slope equation for the small domain, $x_{i-1} \leq x \leq x_i$, as (see Appendix C):

$$\begin{aligned}
\tan \theta(x) = & \frac{\Delta l}{2(c_i - c_{i-1})^3} \left[(2c_i - c_{i-1})(c_i \varepsilon_{i-1} - 2c_{i-1} \varepsilon_i) + c_i c_{i-1} \varepsilon_{i+1} \right] \times \\
& \times \left\{ \log_e \left[c_{i-1} + (c_i - c_{i-1}) \frac{x - x_{i-1}}{\Delta l} \right] - \log_e c_{i-1} \right\} \\
& + \frac{1}{2(c_i - c_{i-1})^2} \left[(2c_i - 3c_{i-1}) \varepsilon_{i-1} + 2(2c_i - c_{i-1}) \varepsilon_i - c_i \varepsilon_{i+1} \right] (x - x_{i-1}) \\
& + \frac{\varepsilon_{i-1} - 2\varepsilon_i + \varepsilon_{i+1}}{4(c_i - c_{i-1})} \frac{(x - x_{i-1})^2}{\Delta l} + \tan \theta_{i-1} \\
& \qquad \qquad \qquad (x_{i-1} \leq x \leq x_i)
\end{aligned} \tag{21}$$

At the strain-sensing station, $x = x_i$, we have $x_i - x_{i-1} = \Delta l$, and equation (21) gives the slope, $\tan \theta_i [\equiv \tan \theta(x_i)]$, at the strain-sensing station, x_i , as:

$$\begin{aligned}
\tan \theta_i = & \frac{\Delta l}{2(c_i - c_{i-1})^3} \left[(2c_i - c_{i-1})(c_i \varepsilon_{i-1} - 2c_{i-1} \varepsilon_i) + c_i c_{i-1} \varepsilon_{i+1} \right] \log_e \frac{c_i}{c_{i-1}} \\
& - \frac{\Delta l}{4(c_i - c_{i-1})^2} \left[(5c_i - 3c_{i-1}) \varepsilon_{i-1} - 2(3c_i - c_{i-1}) \varepsilon_i + (c_i + c_{i-1}) \varepsilon_{i+1} \right] + \tan \theta_{i-1} \\
& \qquad \qquad \qquad (i = 1, 2, 3, \dots, n)
\end{aligned} \tag{22}$$

Equation (22) is the Improved slope equation for the nonuniform beams in recursive form. Applying the recursive relationship, equation (22) can be rewritten as:

$$\begin{aligned}
\tan \theta_i = & \frac{\Delta l}{2} \sum_{j=1}^i \left\{ \frac{1}{(c_j - c_{j-1})^3} \left[(2c_j - c_{j-1})(c_j \varepsilon_{j-1} - 2c_{j-1} \varepsilon_j) + c_j c_{j-1} \varepsilon_{j+1} \right] \log_e \frac{c_j}{c_{j-1}} \right. \\
& \left. - \frac{1}{2(c_j - c_{j-1})^2} \left[(5c_j - 3c_{j-1}) \varepsilon_{j-1} - 2(3c_j - c_{j-1}) \varepsilon_j + (c_j + c_{j-1}) \varepsilon_{j+1} \right] \right\} + \tan \theta_0 \\
& \qquad \qquad \qquad (i = 1, 2, 3, \dots, n)
\end{aligned} \tag{23}$$

Equation (23) is the Improved slope equation for the nonuniform beams in summation form.

Improved Deflection Equation

The deflection, $y(x)$, of the nonuniform cantilever beam within the small domain, $x_{i-1} \leq x \leq x_i$, can be obtained by integrating the slope equation (21), and enforcing the continuity of deflection at the inboard adjacent strain-sensing station, x_{i-1} , as:

$$y(x) = \int_{x_{i-1}}^x \underbrace{\tan \theta(x)}_{\text{eq. (21)}} dx + y_{i-1} \quad ; \quad (x_{i-1} \leq x \leq x_i) \tag{24}$$

in which y_{i-1} is the deflection at the inboard strain-sensing station, x_{i-1} .

In view of equation (21), equation (24) can be integrated (ref. 17) to yield the following deflection equation for the nonuniform beam for the small domain, $x_{i-1} \leq x \leq x_i$, as (see Appendix C):

$$\begin{aligned}
y(x) = & \frac{\Delta l}{2(c_i - c_{i-1})^3} \left\{ \left[(2c_i - c_{i-1})(c_i \varepsilon_{i-1} - 2c_{i-1} \varepsilon_i) + c_i c_{i-1} \varepsilon_{i+1} \right] \left[\frac{\Delta l}{c_i - c_{i-1}} \left\langle \left(c_i + (c_i - c_{i-1}) \frac{x - x_{i-1}}{\Delta l} \right) \right. \right. \right. \\
& \times \log_e \left(c_i + (c_i - c_{i-1}) \frac{x - x_{i-1}}{\Delta l} \right) - (c_i - c_{i-1}) \frac{x - x_{i-1}}{\Delta l} - c_{i-1} \log_e c_{i-1} \left. \left. \left. \right\rangle - (x - x_{i-1}) \log_e c_{i-1} \right] \right\} \quad (25) \\
& + \frac{1}{4(c_i - c_{i-1})^2} \left[(2c_i - 3c_{i-1}) \varepsilon_{i-1} + 2(2c_i - c_{i-1}) \varepsilon_i - c_i \varepsilon_{i+1} \right] (x - x_{i-1})^2 \\
& + \frac{\varepsilon_{i-1} - 2\varepsilon_i + \varepsilon_{i+1}}{12(c_i - c_{i-1})} \frac{(x - x_{i-1})^3}{\Delta l} + y_{i-1} + (x - x_{i-1}) \tan \theta_{i-1} \\
& \hspace{15em} (x_{i-1} \leq x \leq x_i)
\end{aligned}$$

At the strain-sensing station, $x = x_i$, we have $x_i - x_{i-1} = \Delta l$, and equation (25) gives the deflection, $y_i [\equiv y(x_i)]$ at the strain-sensing station, x_i , as:

$$\begin{aligned}
y_i = & \frac{(\Delta l)^2}{2(c_i - c_{i-1})^4} \left[(2c_i - c_{i-1})(c_i \varepsilon_{i-1} - 2c_{i-1} \varepsilon_i) + c_i c_{i-1} \varepsilon_{i+1} \right] \left[c_i \log_e \frac{c_i}{c_{i-1}} - (c_i - c_{i-1}) \right] \quad (26) \\
& - \frac{(\Delta l)^2}{12(c_i - c_{i-1})^2} \left[(8c_i - 5c_{i-1}) \varepsilon_{i-1} - 2(5c_i - 2c_{i-1}) \varepsilon_i + (2c_i + c_{i-1}) \varepsilon_{i+1} \right] + y_{i-1} + \Delta l \tan \theta_{i-1} \\
& \hspace{15em} (i = 1, 2, 3, \dots, n)
\end{aligned}$$

Equation (26) is the Improved deflection equation for the nonuniform beam in recursive form.

Improved Displacement Transfer Function

In view of equation (22), and applying recursive relationships, equation (26) can be written in dual summation form as (see Appendix D):

$$\begin{aligned}
y_i = & (\Delta)^2 \sum_{j=1}^i \left\{ \underbrace{\begin{aligned} & \frac{1}{2(c_j - c_{j-1})^4} \left[(2c_j - c_{j-1})(c_j \varepsilon_{j-1} - 2c_{j-1} \varepsilon_j) + c_j c_{j-1} \varepsilon_{j+1} \right] \left[c_j \log_e \frac{c_j}{c_{j-1}} - (c_j - c_{j-1}) \right] \\ & - \frac{1}{12(c_j - c_{j-1})^2} \left[(8c_j - 5c_{j-1}) \varepsilon_{j-1} - 2(5c_j - 2c_{j-1}) \varepsilon_j + (2c_j + c_{j-1}) \varepsilon_{j+1} \right] \end{aligned}}_{\text{Contribution from deflection terms}} \right\} + y_0 \\
& + (\Delta)^2 \sum_{j=1}^{i-1} (i-j) \left\{ \underbrace{\begin{aligned} & \frac{1}{2(c_j - c_{j-1})^3} \left[(2c_j - c_{j-1})(c_j \varepsilon_{j-1} - 2c_{j-1} \varepsilon_j) + c_j c_{j-1} \varepsilon_{j+1} \right] \log_e \frac{c_j}{c_{j-1}} \\ & - \frac{1}{4(c_j - c_{j-1})^2} \left[(5c_j - 3c_{j-1}) \varepsilon_{j-1} - 2(3c_j - c_{j-1}) \varepsilon_j + (c_j + c_{j-1}) \varepsilon_{j+1} \right] \end{aligned}}_{\text{Contributions from slope terms}} \right\} + (i) \Delta \tan \theta_0 \\
& \qquad \qquad \qquad (i = 1, 2, 3, \dots, n) \quad (27)
\end{aligned}$$

Equation (27) is called the Improved Displacement Transfer Function for the nonuniform beam. Notice that the first summation is contributed from the deflection terms, and the second summation is contributed from the slope terms.

LOG-EXPANDED CASE

Note that the slope equations (22) and (23) and the deflection equations (26) and (27) contain logarithmic terms, $\log_e(c_i/c_{i-1})$, in the numerators, and $(c_i - c_{i-1})$ terms in the denominators, causing mathematical indeterminacy (0/0) when the beam depth becomes uniform (that is, $c_i = c_{i-1} = c$). This mathematical indeterminacy problem can be eliminated if the logarithmic terms are expanded in terms of $(c_i - c_{i-1})$ series to cancel the $(c_i - c_{i-1})$ terms in the denominators (refs. 1, 2).

Log-Expanded Slope Equation

For $(c_i/c_{i-1}) \rightarrow 1$, the logarithm term, $\log_e(c_i/c_{i-1})$, in equations (23) and (24) can be expanded in series form up to the third-order term as (ref. 17):

$$\begin{aligned}
\log_e \frac{c_i}{c_{i-1}} &= \left(\frac{c_i}{c_{i-1}} - 1 \right) - \frac{1}{2} \left(\frac{c_i}{c_{i-1}} - 1 \right)^2 + \frac{1}{3} \left(\frac{c_i}{c_{i-1}} - 1 \right)^3 - \dots \\
&= \frac{c_i - c_{i-1}}{6c_{i-1}^3} \left[6c_{i-1}^2 + (c_i - c_{i-1})(2c_i - 5c_{i-1}) - \dots \right] \quad (28)
\end{aligned}$$

Substitution of equation (28) into equations (22) and (23), and after grouping terms, yields the Log-expanded slope equations given below (see Appendix E):

1. In recursive form:

$$\tan \theta_i = \frac{\Delta l}{12c_{i-1}^3} \left\{ \left[5c_{i-1}^2 + 4(c_i - c_{i-1})^2 \right] \varepsilon_{i-1} - 8c_{i-1}(c_i - 2c_{i-1})\varepsilon_i + c_{i-1}(2c_i - 3c_{i-1})\varepsilon_{i+1} \right\} + \tan \theta_{i-1} \quad (29)$$

$(i = 1, 2, 3, \dots, n)$

2. In summation form:

$$\tan \theta_i = \frac{\Delta l}{12} \sum_{j=1}^i \frac{1}{c_{j-1}^3} \left\{ \left[5c_{j-1}^2 + 4(c_j - c_{j-1})^2 \right] \varepsilon_{j-1} - 8c_{j-1}(c_j - 2c_{j-1})\varepsilon_j + c_{j-1}(2c_j - 3c_{j-1})\varepsilon_{j+1} \right\} + \tan \theta_0 \quad (30)$$

$(i = 1, 2, 3, \dots, n)$

Log-Expanded Deflection Equation

For developing the Log-expanded deflection equations for $(c_i/c_{i-1}) \rightarrow 1$, the logarithm term, $\log_e(c_i/c_{i-1})$, in equations (26) and (27) must be expanded in series form up to the fourth-order term as (ref. 17):

$$\begin{aligned} \log_e \frac{c_i}{c_{i-1}} &= \left(\frac{c_i}{c_{i-1}} - 1 \right) - \frac{1}{2} \left(\frac{c_i}{c_{i-1}} - 1 \right)^2 + \frac{1}{3} \left(\frac{c_i}{c_{i-1}} - 1 \right)^3 - \frac{1}{4} \left(\frac{c_i}{c_{i-1}} - 1 \right)^4 + \dots \\ &= \frac{c_i - c_{i-1}}{12c_{i-1}^4} \left[12c_{i-1}^3 - 6c_{i-1}^2(c_i - c_{i-1}) + 4c_{i-1}(c_i - c_{i-1})^2 - 3(c_i - c_{i-1})^3 + \dots \right] \end{aligned} \quad (31)$$

Substitutions of equation (31) into equations (26) and (27), and after grouping terms, yields the resulting Log-expanded deflection equations given as (see Appendix E):

$$y_i = \frac{(\Delta l)^2}{24c_{i-1}^4} \left\{ \begin{aligned} &\left[7c_{i-1}^3 + (c_i - c_{i-1})(8c_{i-1}c_{i-1} - 3c_i^2) - 3(c_i^3 - c_{i-1}^3) \right] \varepsilon_{i-1} \\ &+ 2c_{i-1} \left[(3c_i^2 + (c_i - c_{i-1})(3c_i - 8c_{i-1})) \varepsilon_i - c_{i-1} \left[c_i^2 + 2(c_i - c_{i-1})^2 \right] \varepsilon_{i+1} \right] \end{aligned} \right\} + y_{i-1} + \Delta l \tan \theta_{i-1} \quad (32)$$

$(i = 1, 2, 3, \dots, n)$

Equation (32) is the Log-expanded deflection equation for the nonuniform beam in recursive form.

Log-Expanded Displacement Transfer Function

In view of equation (29), and applying recursive relationships, equation (32) can be written in dual summation form as (see Appendix F):

$$\begin{aligned}
 y_i = & \frac{(\Delta)^2}{24} \sum_{j=1}^i \frac{1}{c_{j-1}^4} \left\{ \underbrace{\left[\left[7c_{j-1}^3 + (c_j - c_{j-1})(8c_j c_{j-1} - 3c_j^2) - 3(c_j^3 - c_{j-1}^3) \right] \varepsilon_{j-1} \right.}_{\text{Contributions from deflection terms}} \right. \\
 & \left. \left. + 2c_{j-1} \left[(3c_j^2 + (c_j - c_{j-1})(3c_j - 8c_{j-1})) \varepsilon_j - c_{j-1} \left[c_j^2 + 2(c_j - c_{j-1})^2 \right] \varepsilon_{j+1} \right] \right\} + y_0 \\
 & + \frac{(\Delta)^2}{12} \sum_{j=1}^{i-1} \frac{(i-j)}{c_{j-1}^3} \left\{ \underbrace{\left[5c_{j-1}^2 + 4(c_j - c_{j-1})^2 \right] \varepsilon_{j-1} - 8c_{j-1} (c_j - 2c_{j-1}) \varepsilon_j}_{\text{Contributions from slope terms}} \right\} + (i)\Delta l \tan \theta_0 \\
 & \hspace{20em} (i=1,2,3,\dots,n)
 \end{aligned} \tag{33}$$

Equation (33) is called the Log-expanded Displacement Transfer Function for nonuniform beams.

Log-Expanded Slope Equation for Uniform Beams

For uniform beams, we have $c_i = c_{i-1} = c$, and the above Log-expanded slope equations (29) and (30) degenerate respectively into the following simplified forms:

1. In recursive form:

$$\tan \theta_i = \frac{\Delta l}{12c} (5\varepsilon_{i-1} + 8\varepsilon_i - \varepsilon_{i+1}) + \tan \theta_{i-1} \quad ; \quad (i=1,2,3,\dots,n) \tag{34}$$

2. In summation form:

$$\tan \theta_i = \frac{\Delta l}{12c} \sum_{j=1}^i (5\varepsilon_{j-1} + 8\varepsilon_j - \varepsilon_{j+1}) + \tan \theta_0 \quad ; \quad (i=1,2,3,\dots,n) \tag{35}$$

Equations (34) and (35) agree respectively with equations (14) and (15) formulated for the uniform beams, and thus confirm the derivation accuracy of the Log-expanded slope equations (29) and (30).

Log-Expanded Deflection Equation for Uniform Beams

For uniform beams, we have $c_i = c_{i-1} = c$, and the above Log-expanded deflection equations (32) and (33) degenerate respectively into the following simplified forms:

1. In recursive form:

$$y_i = \frac{(\Delta)^2}{24c} (7\varepsilon_{i-1} + 6\varepsilon_i - \varepsilon_{i+1}) + y_{i-1} + \Delta l \tan \theta_{i-1} \quad ; \quad (i=1,2,3,\dots,n) \tag{36}$$

2. In summation form:

$$y_i = \underbrace{\frac{(\Delta)^2}{24c} \sum_{j=1}^i (7\varepsilon_{j-1} + 6\varepsilon_j - \varepsilon_{j+1}) + y_0}_{\text{Contributions from deflection terms}} + \underbrace{\frac{(\Delta)^2}{12c} \sum_{j=1}^{i-1} (i-j)(5\varepsilon_{j-1} + 8\varepsilon_j - \varepsilon_{j+1}) + (i)\Delta \tan \theta_0}_{\text{Contributions from slope terms}} \quad (37)$$

$(i = 1, 2, 3, \dots, n)$

Note that equations (36) and (37) agree respectively with equations (18) and (19) formulated for the uniform beams, and thus confirm the derivation accuracy of the Log-expanded deflection equations (32) and (33).

DEPTH-EXPANDED CASE

This section describes the formulation of the Depth-expanded slope and deflection equations for nonuniform beams. The purpose of this formulation is to avoid the logarithmic terms after carrying out direct integration of curvature equation (3). The depth factor of the nonuniform beam is assumed to change slowly along the beam axis.

Depth-Expanded Slope Equation

The slope, $\tan \theta(x)$ of the nonuniform beam at axial location, x , within the small domain, $x_{i-1} \leq x \leq x_i$, between the two adjacent strain-sensing stations, $\{x_{i-1}, x_i\}$, can be obtained by carrying out the integration of the nonuniform beam curvature equation (3). Namely,

$$\tan \theta(x) = \underbrace{\int_{x_{i-1}}^x \frac{d^2 y}{dx^2} dx}_{\text{Slope increment}} + \underbrace{\tan \theta_{i-1}}_{\text{Slope at } x_{i-1}} = \int_{x_{i-1}}^x \underbrace{\frac{\varepsilon(x)}{c(x)}}_{\text{Eq. (3)}} dx + \tan \theta_{i-1} \quad ; \quad (x_{i-1} \leq x \leq x_i) \quad (38)$$

in which $\tan \theta_{i-1}$ is the slope at x_{i-1} .

An alternative way to avoid the logarithmic terms after direct integration of equation (38) is to expand the term, $1/c(x)$ in the integrand of equation (38) in binomial series form because $c(x)$ is a slowly-varying function of x (ref. 17). Namely,

$$\begin{aligned} \frac{1}{c(x)} &= \frac{1}{c_{i-1} + (c_i - c_{i-1}) \frac{x - x_{i-1}}{\Delta}} = \frac{1}{c_{i-1}} \left[1 + \left(\frac{c_i}{c_{i-1}} - 1 \right) \frac{x - x_{i-1}}{\Delta} \right]^{-1} \\ &= \frac{1}{c_{i-1}} \left[1 - \left(\frac{c_i}{c_{i-1}} - 1 \right) \frac{x - x_{i-1}}{\Delta} + \left(\frac{c_i}{c_{i-1}} - 1 \right)^2 \frac{(x - x_{i-1})^2}{(\Delta)^2} - \dots \right] \end{aligned} \quad (39)$$

Note that in equation (39), the variable term $(x - x_{i-1})$ in the denominator was moved to the numerator. This approach avoids the appearance of logarithmic term, $\log_e(c_i/c_{i-1})$, after direct integration of equation (38). Substituting equations (10) and (39) into equation (38) and carrying out

integration, one obtains the Depth-expanded slope equation for the small domain, $x_{i-1} \leq x \leq x_i$, as (see Appendix G):

$$\begin{aligned} \tan \theta(x) = & \frac{1}{c_{i-1}} \left\{ \varepsilon_{i-1}(x - x_{i-1}) - \left[\frac{3\varepsilon_{i-1} - 4\varepsilon_i + \varepsilon_{i+1}}{2} + \varepsilon_{i-1} \left(\frac{c_i}{c_{i-1}} - 1 \right) \right] \frac{(x - x_{i-1})^2}{2\Delta l} \right. \\ & + \left[\frac{\varepsilon_{i-1} - 2\varepsilon_i + \varepsilon_{i+1}}{2} + \frac{3\varepsilon_{i-1} - 4\varepsilon_i + \varepsilon_{i+1}}{2} \left(\frac{c_i}{c_{i-1}} - 1 \right) + \varepsilon_{i-1} \left(\frac{c_i}{c_{i-1}} - 1 \right)^2 \right] \frac{(x - x_{i-1})^3}{3(\Delta l)^2} \\ & \left. - \left[\frac{\varepsilon_{i-1} - 2\varepsilon_i + \varepsilon_{i+1}}{2} \left(\frac{c_i}{c_{i-1}} - 1 \right) + \frac{3\varepsilon_{i-1} - 4\varepsilon_i + \varepsilon_{i+1}}{2} \left(\frac{c_i}{c_{i-1}} - 1 \right)^2 \right] \frac{(x - x_{i-1})^4}{4(\Delta l)^3} \right\} + \tan \theta_{i-1} \end{aligned} \quad (40)$$

$(x_{i-1} \leq x \leq x_i)$

At the strain-sensing station, $x = x_i$, we have $x_i - x_{i-1} = \Delta l$, and equation (40) gives the slope, $\tan \theta_i [\equiv \tan \theta(x_i)]$ at the strain-sensing station, x_i , as:

$$\begin{aligned} \tan \theta_i = & \frac{\Delta l}{24c_{i-1}} \left[2(5\varepsilon_{i-1} + 8\varepsilon_i - \varepsilon_{i+1}) - \left(\frac{c_i}{c_{i-1}} - 1 \right) (3\varepsilon_{i-1} + 10\varepsilon_i - \varepsilon_{i+1}) \right. \\ & \left. - \left(\frac{c_i}{c_{i-1}} - 1 \right)^2 (\varepsilon_{i-1} - 12\varepsilon_i + 3\varepsilon_{i+1}) \right] + \tan \theta_{i-1} \end{aligned} \quad (41)$$

$(i = 1, 2, 3, \dots, n)$

Equation (41) is the Depth-expanded slope equation for the nonuniform beams in recursive form.

For the uniform beams, we have $c_i = c_{i-1} = c$, and equation (41) degenerates into the following simplified forms:

$$\tan \theta_i = \frac{\Delta l}{12c} (5\varepsilon_{i-1} + 8\varepsilon_i - \varepsilon_{i+1}) + \tan \theta_{i-1} \quad ; \quad (i = 1, 2, 3, \dots, n) \quad (42)$$

which agrees with equation (14) formulated for the uniform beams.

Applying the recursive relationship, equation (41) can be rewritten as:

$$\begin{aligned} \tan \theta_i = & \frac{\Delta l}{24} \sum_{j=1}^i \frac{1}{c_{j-1}} \left[2(5\varepsilon_{j-1} + 8\varepsilon_j - \varepsilon_{j+1}) - \left(\frac{c_j}{c_{j-1}} - 1 \right) (3\varepsilon_{j-1} + 10\varepsilon_j - \varepsilon_{j+1}) \right. \\ & \left. - \left(\frac{c_j}{c_{j-1}} - 1 \right)^2 (\varepsilon_{j-1} - 12\varepsilon_j + 3\varepsilon_{j+1}) \right] + \tan \theta_0 \end{aligned} \quad (43)$$

$(i = 1, 2, 3, \dots, n)$

Equation (43) is the Depth-expanded slope equation for the nonuniform beams in summation form, and which can be degenerated into equation (15) for uniform beams ($c_i = c_{i-1} = c$).

Depth-Expanded Deflection Equation

The deflection, $y(x)$, of the nonuniform cantilever beam within the small domain, $x_{i-1} \leq x \leq x_i$, can be obtained by integrating the slope equation (40), and enforcing the continuity of deflection at the inboard adjacent strain-sensing station, x_{i-1} , as:

$$y(x) = \int_{x_{i-1}}^x \underbrace{\tan \theta(x)}_{\text{Eq. (40)}} dx + \underbrace{y_{i-1}}_{\substack{\text{Deflection} \\ \text{at } x_{i-1}}} \quad ; \quad (x_{i-1} \leq x \leq x_i) \quad (44)$$

in which y_{i-1} is the deflection at the inboard strain-sensing station, x_{i-1} . In light of equation (40), equation (44) can be integrated (ref. 17) to yield the following deflection equation for the small domain, $x_{i-1} \leq x \leq x_i$, (see Appendix G):

$$\begin{aligned} y(x) = & \frac{1}{c_{i-1}} \left\{ \varepsilon_{i-1} \frac{(x-x_{i-1})^2}{2} - \left[\frac{3\varepsilon_{i-1} - 4\varepsilon_i + \varepsilon_{i+1}}{2} + \varepsilon_{i-1} \left(\frac{c_i}{c_{i-1}} - 1 \right) \right] \frac{(x-x_{i-1})^3}{6\Delta l} \right. \\ & + \left[\frac{\varepsilon_{i-1} - 2\varepsilon_i + \varepsilon_{i+1}}{2} + \frac{3\varepsilon_{i-1} - 4\varepsilon_i + \varepsilon_{i+1}}{2} \left(\frac{c_i}{c_{i-1}} - 1 \right) + \varepsilon_{i-1} \left(\frac{c_i}{c_{i-1}} - 1 \right)^2 \right] \frac{(x-x_{i-1})^4}{12(\Delta l)^2} \\ & \left. - \left[\frac{\varepsilon_{i-1} - 2\varepsilon_i + \varepsilon_{i+1}}{2} \left(\frac{c_i}{c_{i-1}} - 1 \right) + \frac{3\varepsilon_{i-1} - 4\varepsilon_i + \varepsilon_{i+1}}{2} \left(\frac{c_i}{c_{i-1}} - 1 \right)^2 \right] \frac{(x-x_{i-1})^5}{20(\Delta l)^3} \right\} \\ & + y_{i-1} + (x-x_{i-1}) \tan \theta_{i-1} \end{aligned} \quad (x_{i-1} \leq x \leq x_i) \quad (45)$$

At the strain-sensing station, $x = x_i$, we have $x_i - x_{i-1} = \Delta l$, and equation (45) gives the deflection, $y_i [\equiv y(x_i)]$ at the strain-sensing station, x_i , as:

$$\begin{aligned} y_i = & \frac{(\Delta l)^2}{24c_{i-1}} \left[(7\varepsilon_{i-1} + 6\varepsilon_i - \varepsilon_{i+1}) - \frac{2}{5} \left(\frac{c_i}{c_{i-1}} - 1 \right) (4\varepsilon_{i-1} + 7\varepsilon_i - \varepsilon_{i+1}) \right. \\ & \left. + \frac{1}{5} \left(\frac{c_i}{c_{i-1}} - 1 \right)^2 (\varepsilon_{i-1} + 12\varepsilon_i - 3\varepsilon_{i+1}) \right] + y_{i-1} + \Delta l \tan \theta_{i-1} \end{aligned} \quad (46)$$

$(i = 1, 2, 3, \dots, n)$

Equation (46) is the Depth-expanded deflection equation for the nonuniform beams in recursive form.

For the uniform beams, we have $c_i = c_{i-1} = c$, and equation (46) degenerates into the following simplified form:

$$y_i = \frac{(\Delta)^2}{24c} (7\varepsilon_{i-1} + 6\varepsilon_i - \varepsilon_{i+1}) + y_{i-1} + \Delta/\tan\theta_{i-1} \quad ; \quad (i=1,2,3,\dots,n) \quad (47)$$

Equation (47) agrees with the deflection equation (18) for the uniform beams.

Depth-Expanded Displacement Transfer Function

In view of equation (41), and applying recursive relationships, equation (46) can be written in dual summation form as (see Appendix H):

$$y_i = \underbrace{\frac{(\Delta)^2}{24} \sum_{j=1}^i \frac{1}{c_{j-1}} \left[\begin{aligned} & (7\varepsilon_{j-1} + 6\varepsilon_j - \varepsilon_{j+1}) - \frac{2}{5} \left(\frac{c_j}{c_{j-1}} - 1 \right) (4\varepsilon_{j-1} + 7\varepsilon_j - \varepsilon_{j+1}) \\ & + \frac{1}{5} \left(\frac{c_j}{c_{j-1}} - 1 \right)^2 (\varepsilon_{j-1} + 12\varepsilon_j - 3\varepsilon_{j+1}) \end{aligned} \right]}_{\text{Contributions from deflection terms}} + y_0$$

$$+ \underbrace{\frac{(\Delta)^2}{24} \sum_{j=1}^{i-1} \frac{(i-j)}{c_{j-1}} \left[\begin{aligned} & 2(5\varepsilon_{j-1} + 8\varepsilon_j - \varepsilon_{j+1}) - \left(\frac{c_j}{c_{j-1}} - 1 \right) (3\varepsilon_{j-1} + 10\varepsilon_j - \varepsilon_{j+1}) \\ & - \left(\frac{c_j}{c_{j-1}} - 1 \right)^2 (\varepsilon_{j-1} - 12\varepsilon_j + 3\varepsilon_{j+1}) \end{aligned} \right]}_{\text{Contributions from slope terms}} + (i)\Delta/\tan\theta_0 \quad (48)$$

$(i=1,2,3,\dots,n)$

Equation (48) is the Depth-expanded Displacement Transfer Function for the nonuniform beams, and which can degenerate into equation (19) for the uniform beams ($c_i = c_{i-1} = c$). Again, the first summation in equation (48) is the contributions from the deflection terms, and the second summation is the contributions from the slope terms.

NEW STRUCTURE SHAPE-SENSING TECHNOLOGY

The Displacement Transfer Functions with the accompanying strain-sensing system thus formed a new technology for structure deformed shape predictions. This new technology is called *Method for Real-Time Structure Shape-Sensing* (U.S. Patent Number 7,520,176, ref. 9), which could be very useful for in-flight deformed shape monitoring of flexible wings and tails, such as those often employed on unmanned flight vehicles by the ground-based pilot for maintaining safe flights.

A typical flow chart of the new structure shape-sensing technology using the two-line strain-sensing system is shown in Appendix I. In the flow chart, only the Depth-expanded Displacement Transfer Function (48) was used as the example for each strain-sensing line. Other Displacement Transfer Functions may also be selected, depending on the types of structures (uniform, nonuniform, slightly nonuniform, et cetera) under consideration.

The two-line strain-sensing system can be used for the shape-sensing of the tapered wing box for which the neutral surface is located at the wing box half-depth (fig. I-1). If, however, the neutral surface is not located at exactly half the depth of a structure, such as aircraft wings, a second set of the two-line sensing system must be installed on the upper surface, right on top of the lower sensing system. Using pairs of lower and upper strains, one can determine the actual location of the neutral surface for finding the values of the depth factors, c_i ($i = 0, 1, 2, 3, \dots, n$), needed for the calculations of deflections (see the Ikhana wing shape predictions, ref. 3).

It is important to mention that when using the two-line strain-sensing system for the wing structures, the Displacement Transfer Functions can not only calculate the deflections but also the cross-sectional rotations. Thus, the need to use surface distortion strains can be eliminated.

Appendix I also describes the application of the two-line strain-sensing system to a free-free beam structure such as an airborne aircraft fuselage (free-free nonuniform tubular beam structure) (fig. I-2) for sensing the horizontal and vertical bending strains for inputs to the Displacement Transfer Functions for the calculations of in-flight deformed shapes in horizontal and vertical planes (ref. 2).

SHAPE-PREDICTION ACCURACIES

As mentioned above, the surface strains were analytically calculated from the SPAR program, and were not directly measured. In the shape-prediction accuracy studies, the deflections calculated from the SPAR program were used as reference yardsticks (0% error) to evaluate the accuracies of the corresponding deflections calculated from the new Displacement Transfer Functions. The shape-prediction accuracies of the newly-formulated Displacement Transfer Functions were also compared with those of the earlier Displacement Transfer Functions.

Tapered Cantilever Tubular Beams

The sample structures chosen in the shape-prediction accuracy studies were again a family of aluminum tapered cantilever tubular beams having the dimensions listed in table 1. The same loading condition of upward load, $P = 100$ lb, was applied at each beam tip.

Comparisons of Predicted Deflections

Tables 2(a)-2(f) compare the accuracies of deflections calculated from different Displacement Transfer Functions based on piecewise linear and piecewise nonlinear strain representations for the six tapered cantilever tubular beams listed in table 1. Note from tables 2(a)-2(f) that only two typical Displacement Transfer Functions [the nonlinear Displacement Transfer Function (4); and the second-order Displacement Transfer Function (6)], based on piecewise linear strain representations were added to the accuracy comparisons. In tables 2(a)-2(f), the shaped prediction errors (in percent) are indicated in parentheses.

Table 2(a). Comparisons of deflections (in inches) calculated from SPAR and from different Displacement Transfer Functions; uniform cantilever tubular beam; $c_n/c_0 = 4/4$; $n = 16$.

Theories	y_0	y_2	y_4	y_6	y_8	y_{10}	y_{12}	y_{14}	y_{16} (% error)
SPAR (reference)	0.00000 (0.0000)	0.01787 (0.0000)	0.06340 (0.0000)	0.13368 (0.0000)	0.22450 (0.0000)	0.33181 (0.0000)	0.45174 (0.0000)	0.57933 (0.0000%)	0.71162 (0.0000)
Piecewise linear strain representations									
Nonuniform, eq. (4)*	-----	-----	-----	-----	-----	-----	-----	-----	-----
Second- order, eq. (6)	0.00000 (0.0000)	0.01576 (0.2965)	0.06034 (0.4300)	0.12962 (0.5705)	0.21948 (0.7054)	0.32580 (0.8446)	0.44448 (0.9752)	0.57139 (1.1158)	0.70243 (1.2914)
Piecewise nonlinear strain representations									
Improved, eq. (27)*	-----	-----	-----	-----	-----	-----	-----	-----	-----
Log- expanded, eq. (33)	0.00000 (0.0000)	0.01577 (0.2951)	0.06036 (0.4272)	0.12965 (0.5663)	0.21951 (0.7012)	0.32585 (0.8375)	0.44454 (1.0118)	0.57146 (1.1059)	0.70249 (1.2830)
Depth- expanded, eq. (48)	0.00000 (0.0000)	0.01577 (0.2951)	0.06036 (0.4272)	0.12965 (0.5663)	0.21951 (0.7012)	0.32585 (0.8375)	0.44454 (1.0118)	0.57146 (1.1059)	0.70249 (1.2830)

* No solutions for uniform beams because of mathematical indeterminacy.

Note from Table 2(a) that both equations (4) and (27) produced no solutions for uniform beams because of mathematical indeterminacy problems.

Table 2(b). Comparisons of deflections (in inches) calculated from SPAR and from different Displacement Transfer Functions; tapered cantilever tubular beam; $c_n/c_0 = 3/4$; $n = 16$.

Theories	y_0	y_2	y_4	y_6	y_8	y_{10}	y_{12}	y_{14}	y_{16} (% error)
SPAR (reference)	0.00000 (0.0000)	0.01823 (0.0000)	0.06697 (0.0000)	0.14572 (0.0000)	0.25204 (0.0000)	0.38294 (0.0000)	0.53428 (0.0000)	0.70092 (0.0000)	0.87634 (0.0000)
Piecewise linear strain representations									
Nonuniform, eq. (4)	0.00000 (0.0000)	0.01627 (0.2237)	0.06417 (0.3195)	0.14199 (0.4256)	0.24738 (0.5310)	0.37726 (0.6482)	0.52758 (0.7645)	0.69312 (0.8901)	0.86711 (1.0532)
Second- order, eq. (6)	0.00000 (0.0000)	0.01627 (0.2237)	0.06417 (0.3195)	0.14199 (0.4256)	0.24738 (0.5310)	0.37726 (0.6482)	0.52759 (0.7634)	0.69313 (0.8888)	0.86712 (1.0521)
Piecewise nonlinear strain representations									
Improved, eq. (27)	0.00000 (0.0000)	0.01627 (0.2237)	0.06419 (0.3172)	0.14204 (0.4199)	0.24748 (0.5203)	0.37741 (0.6310)	0.52781 (0.7383)	0.69345 (0.8524)	0.86754 (1.0042)
Log- expanded, eq. (33)*	0.00000 (0.0000)	0.01627 (0.2237)	0.06419 (0.3172)	0.14205 (0.4188)	0.24748 (0.5203)	0.37742 (0.6299)	0.52782 (0.7372)	0.69346 (0.8513)	0.86755 (1.0030)*
Depth- expanded, eq. (48)	0.00000 (0.0000)	0.01627 (0.2237)	0.06419 (0.3172)	0.14204 (0.4199)	0.24748 (0.5203)	0.37741 (0.6310)	0.52781 (0.7383)	0.69345 (0.8524)	0.86754 (1.0042)

* Most accurate prediction (closest to SPAR).

Table 2(c). Comparisons of deflections (in inches) calculated from SPAR and from different displacement transfer functions; tapered cantilever tubular beam; $c_n/c_0 = 2/4$; $n = 16$.

Theories	y_0	y_2	y_4	y_6	y_8	y_{10}	y_{12}	y_{14}	y_{16} (% error)
SPAR (reference)	0.00000 (0.0000)	0.01864 (0.0000)	0.07113 (0.0000)	0.16057 (0.0000)	0.28831 (0.0000)	0.45510 (0.0000)	0.65965 (0.0000)	0.89759 (0.0000)	1.15801 (0.0000)
Piecwise linear strain representations									
Nonuniform, eq. (4)	0.00000 (0.0000)	0.01682 (0.1572)	0.06859 (0.2193)	0.15719 (0.2919)	0.28407 (0.3661)	0.44983 (0.4551)	0.65325 (0.5527)	0.88981 (0.6718)	1.14828 (0.8402)
Second- order, eq. (6)	0.00000 (0.0000)	0.01682 (0.1572)	0.06859 (0.2193)	0.15719 (0.2919)	0.28407 (0.3661)	0.44983 (0.4551)	0.65324 (0.5535)	0.88980 (0.6727)	1.14826 (0.8420)
Piecwise nonlinear strain representations									
Improved, eq. (27)	0.00000 (0.0000)	0.01682 (0.1572)	0.06861 (0.2176)	0.15723 (0.2884)	0.28417 (0.3575)	0.45002 (0.4387)	0.65359 (0.5233)	0.89042 (0.6192)	1.14930 (0.7522)
Log- expanded, eq. (33)*	0.00000 (0.0000)	0.01682 (0.1572)	0.06861 (0.2176)	0.15723 (0.2884)	0.28417 (0.3575)	0.45002 (0.4387)	0.65359 (0.5233)	0.89044 (0.6174)	1.14935 (0.7478)*
Depth- expanded, eq. (48)	0.00000 (0.0000)	0.01682 (0.1572)	0.06861 (0.2176)	0.15723 (0.2884)	0.28417 (0.3575)	0.45001 (0.4395)	0.65358 (0.5242)	0.89041 (0.6200)	1.14929 (0.7530)

* Most accurate prediction (closest to SPAR).

Table 2(d). Comparisons of deflections (in inches) calculated from SPAR and from different displacement transfer functions; tapered cantilever tubular beam; $c_n/c_0 = 1/4$; $n = 16$.

Theories	y_0	y_2	y_4	y_6	y_8	y_{10}	y_{12}	y_{14}	y_{16} (% error)
SPAR (reference)	0.00000 (0.0000)	0.01912 (0.0000)	0.07598 (0.0000)	0.17923 (0.0000)	0.33816 (0.0000)	0.56506 (0.0000)	0.87454 (0.0000)	1.28196 (0.0000)	1.78417 (0.0000)
Piecwise linear strain representations									
Nonuniform, eq. (4)	0.00000 (0.0000)	0.01739 (0.0970)	0.07364 (0.1312)	0.17612 (0.1743)	0.33427 (0.2180)	0.56011 (0.2774)	0.86835 (0.3469)	1.27375 (0.4602)	1.77144 (0.7135)
Second- order, eq. (6)	0.00000 (0.0000)	0.01739 (0.0970)	0.07364 (0.1312)	0.17611 (0.1749)	0.33426 (0.2186)	0.56009 (0.2786)	0.86829 (0.3503)	1.27365 (0.4658)	1.77124 (0.7247)
Piecwise nonlinear strain representations									
Improved, eq. (27)*	0.00000 (0.0000)	0.01738 (0.0976)	0.07362 (0.1323)	0.17609 (0.1760)	0.33424 (0.2197)	0.56010 (0.2780)	0.86850 (0.3385)	1.27462 (0.4114)	1.77473 (0.5291)*
Log- expanded, eq. (33)	0.00000 (0.0000)	0.01738 (0.0975)	0.07362 (0.1323)	0.17608 (0.1766)	0.33422 (0.2208)	0.56007 (0.2797)	0.86845 (0.3413)	1.27452 (0.4170)	1.77468 (0.5319)
Depth- expanded, eq. (48)	0.00000 (0.0000)	0.01738 (0.0975)	0.07362 (0.1323)	0.17608 (0.1766)	0.33422 (0.2208)	0.56008 (0.2791)	0.86845 (0.3413)	1.27453 (0.4164)	1.77458 (0.5375)

* Most accurate prediction (closest to SPAR).

Table 2(e). Comparisons of deflections (in inches) calculated from SPAR and from different Displacement Transfer Functions; tapered cantilever tubular beam; $c_n/c_0 = 0.5/4$; $n = 16$.

Theories	y_0	y_2	y_4	y_6	y_8	y_{10}	y_{12}	y_{14}	y_{16} (% error)
SPAR (reference)	0.00000 (0.0000)	0.01938 (0.0000)	0.07872 (0.0000)	0.19047 (0.0000)	0.37082 (0.0000)	0.64535 (0.0000)	1.05517 (0.0000)	1.67292 (0.0000)	2.59712 (0.0000)
Piecewise linear strain representations									
Nonuniform, eq. (4)	0.00000 (0.0000)	0.01770 (0.0620)	0.07649 (0.0859)	0.18752 (0.1136)	0.36721 (0.1390)	0.64077 (0.1763)	1.04963 (0.2133)	1.66517 (0.2984)	2.57675 (0.7843)
Second- order, eq. (6)	0.00000 (0.0000)	0.01770 (0.0620)	0.07648 (0.0862)	0.18751 (0.1140)	0.36719 (0.1398)	0.64071 (0.1787)	1.04949 (0.2187)	1.66478 (0.3134)	2.57544 (0.8348)
Piecewise nonlinear strain representations									
Improved, eq. (27)*	0.00000 (0.0000)	0.01768 (0.0655)	0.07644 (0.0878)	0.18741 (0.1178)	0.36700 (0.1417)	0.64038 (0.1914)	1.04905 (0.2356)	1.66527 (0.2946)	2.58806 (0.3488)*
Log- expanded, eq. (33)	0.00000 (0.0000)	0.01769 (0.0651)	0.07644 (0.0878)	0.18740 (0.1182)	0.36697 (0.1482)	0.64030 (0.1944)	1.04887 (0.2426)	1.66475 (0.3146)	2.58595 (0.4301)
Depth- expanded, eq. (48)	0.00000 (0.0000)	0.01768 (0.0655)	0.07644 (0.0878)	0.18740 (0.1182)	0.36698 (0.1479)	0.64032 (0.1937)	1.04891 (0.2410)	1.66489 (0.3092)	2.58719 (0.3823)

* Most accurate prediction (closest to SPAR).

Table 2(f). Comparisons of deflections (in inches) calculated from SPAR and from different Displacement Transfer Functions; tapered cantilever tubular beam; $c_n/c_0 = 0.25/4$; $n = 16$.

Theories	y_0	y_2	y_4	y_6	y_8	y_{10}	y_{12}	y_{14}	y_{16} (% error)
SPAR (Reference)	0.00000 (0.0000)	0.01952 (0.0000)	0.08017 (0.0000)	0.19668 (0.0000)	0.38984 (0.0000)	0.69566 (0.0000)	1.18157 (0.0000)	2.00286 (0.0000)	3.58289 (0.0000)
Piecewise linear strain representations									
Nonuniform, Eq. (4)	0.00000 (0.0000)	0.01786 (0.0463)	0.07802 (0.0600)	0.19387 (0.0784)	0.38651 (0.0929)	0.69143 (0.1181)	1.17563 (0.1658)	1.99425 (0.2403)	3.53790 (1.2557)
Second- order, eq. (6)	0.00000 (0.0000)	0.01786 (0.00463)	0.07801 (0.0603)	0.19385 (0.0790)	0.38648 (0.0938)	0.69135 (0.1203)	1.17539 (0.1725)	1.99331 (0.2665)	3.53116 (1.4398)
Piecewise nonlinear strain representations									
Improved, eq. (27)*	0.00000 (0.0000)	0.01784 (0.0469)	0.07795 (0.0620)	0.19369 (0.0835)	0.38615 (0.1030)	0.69068 (0.1390)	1.17400 (0.2113)	1.99125 (0.3240)	3.57152 (0.3173)*
Log- expanded, eq. (33)	0.00000 (0.0000)	0.01784 (0.0469)	0.07794 (0.0622)	0.19368 (0.0837)	0.38609 (0.1047)	0.69057 (0.1421)	1.17372 (0.2191)	1.99044 (0.3466)	3.56071 (0.6191)
Depth- expanded, eq. (48)	0.00000 (0.0000)	0.01784 (0.0469)	0.07794 (0.0622)	0.19368 (0.0837)	0.38611 (0.1041)	0.69058 (0.1418)	1.17373 (0.2188)	1.99026 (0.3517)	3.56740 (0.4323)

* Most accurate prediction (closest to SPAR).

The deflections calculated from equations (4), (6), (27), (33), and (48), and listed in tables 2(a)-2(f) are plotted respectively in figures 9-13 (solid curves with solid circular symbols) for visual comparisons with the corresponding SPAR deflection curves (dashed curves with open circular symbols). Note that by using the piecewise nonlinear strain representations (figs. 11-13) instead of the piecewise linear strain representations (figs. 9 and 10), the shape-prediction accuracies, especially for the smaller depth ratios, $c_n/c_0 = \{0.25/4, 0.5/4\}$, were greatly improved. Pictorially, the deflection curves calculated from

equations (27), (33), and (48), and shown respectively in figures 11-13, fell extremely close to the corresponding SPAR deflection curves because the piecewise nonlinear strain representations were used [see the actual values of the prediction errors indicated within the parentheses in tables 2(a)-2(f)].

Shape-Prediction Errors

In the shape-prediction error studies, the SPAR-generated deflections were used as the reference yardsticks with which to measure the shape-prediction errors. The shape-prediction error studies focused only on the beam tips because of peak deflections. The beam-tip shape-prediction error, Δy_n ($\equiv |y_n - y_n^{SPAR}|$) (in.) for each type of beam is defined as the magnitude of difference between the SPAR-generated beam-tip deflection, y_n^{SPAR} , and the corresponding beam-tip deflection, y_n , calculated from equations (4), (6), (27), (33), and (48). From data listed in Table 2(a)-2(f), the calculated beam-tip shape-prediction errors, Δy_n , are compared in table 3.

Table 3. Comparisons of beam-tip shape-prediction errors, Δy_n (in.) of different Displacement Transfer Functions; tapered cantilever tubular beams with depth ratios $4/4 \geq c_n/c_0 \geq 0.25/4$.

		Beam-tip shape-prediction error, Δy_n , in.				
c_n/c_0	y_n^{SPAR} , in.	Piecewise linear		Piecewise nonlinear		
		Nonuniform, eq. (4)	Second - order, eq. (6)	Improved, eq. (27)	Log- expanded, eq. (33)	Depth-expanded, eq. (48)
4/4	0.71162	----	0.00919	----	0.00913	0.00913
3/4	0.87634	0.00923	0.00922	0.00880	0.00879*	0.00880
2/4	1.15801	0.00973	0.00975	0.00871	0.00866*	0.00872
1/4	1.78417	0.01273	0.01293	0.00944*	0.00949	0.00959
0.5/4	2.59712	0.02037	0.02168	0.00906*	0.01117	0.00993
0.25/4	3.68289	0.04499	0.05173	0.01137*	0.02218	0.01549

* Most accurate.

The beam-tip shape-prediction errors, Δy_n , listed in table 3 are plotted in figure 14 for visual comparisons of the shape-prediction accuracies of the Displacement Transfer Functions (4), (6), (27), (33), and (48). One observes from figure 14 that, for the uniform beam ($c_n/c_0 = 4/4$), changing from piecewise linear to piecewise nonlinear strain representations has no effect in reducing the shape-prediction errors because it is immaterial to use either piecewise linear or piecewise nonlinear function to represent the linear (straight-line) strain curve for the uniform beam (figs. 5 and 8). Note also that the values of the beam-tip shape-prediction errors, Δy_n , are practically insensitive to the change of the depth ratio, c_n/c_0 , and stayed almost unchanged in the region, $4/4 \geq c_n/c_0 \geq 2/4$, but started to increase rapidly as the depth ratio, c_n/c_0 , decreases, and reached the maximum values of 0.04499, 0.05173, 0.01137, 0.02218, and 0.01549 in. at the minimum depth ratio, $c_n/c_0 = 0.25/4$, respectively for equations (4), (6), (27), (33), and (48) (table 3). Because at lower depth ratios, $c_n/c_0 \leq 1/4$, the strain curves are highly nonlinear (fig. 8), and using the piecewise nonlinear strain representations [equations (27), (33), and (48)], instead of using the piecewise linear strain representations [equations (4) and (6)], greatly reduced the beam-tip shape-prediction errors (fig. 14). Note also in figure 14 that all the error curves bent

upward (increasing errors) when the depth ratio decreased toward the minimum depth ratio, $c_n/c_0 = 0.25/4$. This upward bend is most severe for the piecewise linear strain representations [equations (4) and (6)], and to a lesser degree for the piecewise nonlinear strain representations [equations (27), (33), and (48)]. The increasing errors at low depth ratios, $c_n/c_0 = \{0.25/4, 0.5/4\}$, can be attributed to the relatively poor strain representations of the sharply-bent segments of the strain curves (figs. 5 and 8). The beam-tip shape-prediction errors plotted in figure 14, however, are very small and under 0.06 inches. The Improved Displacement Transfer Function (27) has the smallest error (0.01137 in.).

Normalized Shape-Prediction Errors

The beam-tip shape-prediction errors, Δy_n , of different Displacement Transfer Functions can be better compared if each Δy_n is normalized by the corresponding SPAR-generated beam-tip deflection, y_n^{SPAR} , (prediction-error measuring yardsticks). The normalized beam-tip shape-prediction errors, $\Delta y_n / y_n^{SPAR}$, of different Displacement Transfer Functions are compared in table 4.

Table 4. Comparisons of normalized beam-tip shape-prediction errors ($\Delta y_n / y_n^{SPAR} \times 100\%$) of different Displacement Transfer Functions; tapered cantilever tubular beams with depth ratios, $4/4 \geq c_n/c_0 \geq 1/4$.

c_n/c_0	Normalized beam-tip shape-prediction error, $\Delta y_n / y_n^{SPAR} \times 100\%$				
	Piecewise linear		Piecewise nonlinear		
	Nonuniform, eq. (4)	Second-order, eq. (6)	Improved, eq. (27)	Log-expanded, eq. (33)	Depth-expanded, eq. (48)
4/4	----	1.2914	----	1.2830	1.2830
3/4	1.0532	1.0521	1.0042	1.0030*	1.0042
2/4	0.8402	0.8420	0.7522	0.7478*	0.7530
1/4	0.7135	0.7147	0.5291*	0.5319	0.5375
0.5/4	0.7843	0.8248	0.3488*	0.4301	0.3823
0.25/4	1.2557	1.4398	0.3173*	0.6191	0.4323

*Most accurate.

The normalized beam-tip shape-prediction errors, $\Delta y_n / y_n^{SPAR}$ (in percent), listed in table 4 are plotted in figure 15 as functions of depth ratio, c_n/c_0 , for visual comparisons of the shape prediction accuracies of different Displacement Transfer Functions. Note from figure 15 that the values of $\Delta y_n / y_n^{SPAR}$ associated with all types of Displacement Transfer Functions decreased almost linearly with decreasing depth ratio, c_n/c_0 , and then [except for the Improved Displacement Transfer Function (27)] increased rapidly with further decreasing depth ratio, c_n/c_0 (see fig. 14). The reason for the values of $\Delta y_n / y_n^{SPAR}$ decreasing with decreasing c_n/c_0 in the region, $4/4 \geq c_n/c_0 \geq 1/4$, is dividing the almost-unchanging values of Δy_n (see fig. 14) by the associated values of y_n^{SPAR} , which increase with decreasing depth ratio, c_n/c_0 (see column 2 of table 3).

At the low depth ratios, $c_n/c_0 = \{0.5/4, 0.25/4\}$, the Improved Displacement Transfer Function (27) gave the lowest value of $\Delta y_n / y_n^{SPAR}$ among all of the five Displacement Transfer Functions that were considered (fig. 15). At the lowest depth ratio, $c_n/c_0 = 0.25/4$, the beam-tip shape-prediction errors of the Improved, Depth-expanded, and Log-expanded Displacement Transfer Functions (27), (48), and (33) are respectively 25%, 34%, and 49% of the error produced by the Nonuniform Displacement Transfer Function (4) (the most accurate equation, based on piecewise linear strain representations, see table 4). This is equivalent to error reductions of 75%, 66%, and 51%, respectively, by using the Displacement Transfer Functions (27), (48), and (33). Note from figure 15 that in the depth ratio region, $4/4 \geq c_n/c_0 \geq 1/4$, all three of the Displacement Transfer Functions (27), (48), and (33) exhibited nearly equal shape-prediction accuracies. Similarly, in the same depth ratio region, $4/4 \geq c_n/c_0 \geq 1/4$, the error curves of the Displacement Transfer Functions (4) and (6) (based on piecewise linear strain representations), also collapsed into a single curve. Overall, the prediction errors of the five Displacement Transfer Functions are very small: only in the ranges of (0.7135~1.4398)% based on piecewise linear strain representations and (0.3173~1.2830)% based on piecewise nonlinear strain representations.

DISCUSSION

For shape predictions of complex aircraft wings (which are constructed with stiffened panels) using the Displacement Transfer Functions, one must first locate the local cross-sectional neutral axis using pairs of lower and upper surface strains, and then determine the local depth factors, $c_i (i = 1, 2, 3, \dots, n)$ (see Appendix I), which are needed for the deflection calculations. The surface strain values will change with the material or structural properties. The above approach was applied in the shape predictions of an Ikhana wing (ref. 3) and a Global Observer wing (ref. 18), for which the local neutral axes are not at the half-depth of the wing cross sections.

Concurrently with the writing of this technical paper, large-scale ground load tests of the Global Observer (175-ft wingspan) were carried out at the NASA Dryden Flight Loads Laboratory (ref. 18). The measured strain test data were later used in the previously listed Displacement Transfer Function (5), (suitable for the slightly-tapered Global Observer wing) to calculate the wing deflections. The calculated values were then compared with the real-time photogrammetry data as shown in figures 16 and 17 (taken from ref. 18). Note that equation (5) proved to be very accurate, having prediction errors in the range of (0.09-1.72)% at the wingtip, which was at nearly 14 ft of deflection.

CONCLUDING REMARKS

New Improved Displacement Transfer Functions were formulated using the piecewise nonlinear representations of surface strain distributions. Four different Displacement Transfer Functions were formulated for both uniform and nonuniform beams:

- Improved Displacement Transfer Function for uniform beams
- Improved Displacement Transfer Function for nonuniform beams
- Log-expanded Displacement Transfer Function for nonuniform beams
- Depth-expanded Displacement Transfer Function for nonuniform beams.

The key findings resulting from using the new Displacement Transfer Functions to improve the accuracies of structure shape predictions of tapered cantilever tubular beams are:

1. By using the piecewise nonlinear strain representations, beam-tip prediction errors could be greatly reduced by up to 75% for the peak taper angle case.

2. For smaller taper angles, changing the strain representations from piecewise linear to piecewise nonlinear improved the shape-prediction accuracies along the entire beam.
3. For larger taper angles, changing the strain representations from piecewise linear to piecewise nonlinear improved the prediction accuracies only in the beam tip regions where the strain gradients change signs, but did not improve the prediction accuracies in the inboard regions where the strain gradients change very slowly.
4. For larger taper angles, among the three new Displacement Transfer Functions formulated for nonuniform cantilever beams, the Improved Displacement Transfer Function provided the most accurate shape predictions.
5. For smaller taper angles, the shape-prediction accuracies of the Improved, Depth-expanded, and Log-expanded Displacement Transfer Functions are practically the same.
6. For the uniform beams, there is no benefit in the prediction error reductions by changing from linear strain representations to nonlinear strain representations. As the depth ratio decreases (that is, increasing taper angles), however, the benefits of prediction error reductions gradually increased and finally reached the peaks at the minimum depth ratio (the highest taper angle).

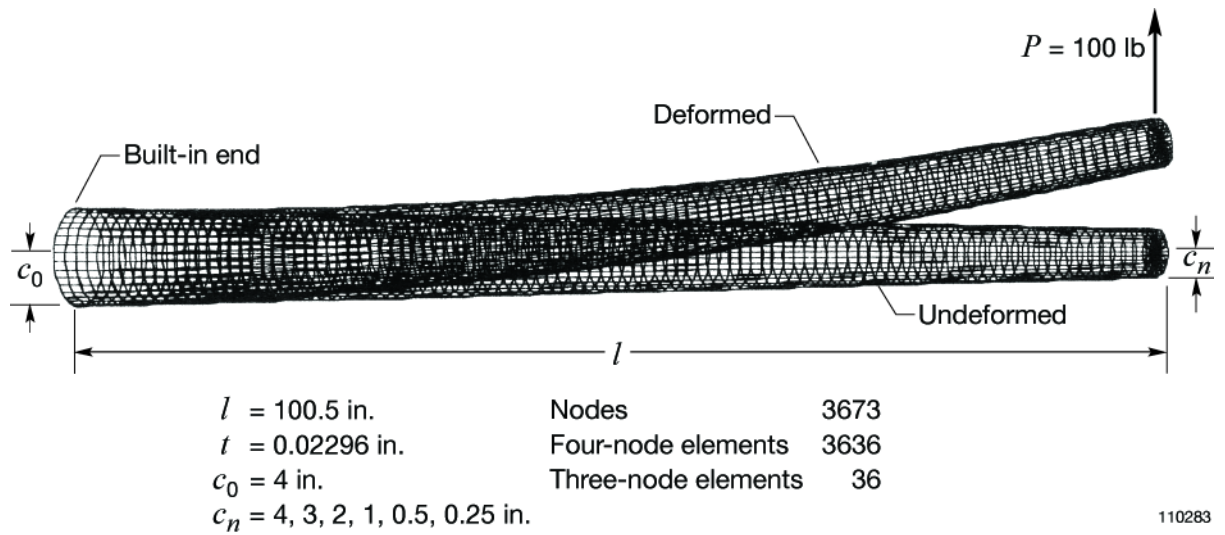


Figure 3. Finite-element model for tapered cantilever tubular beam subjected to tip vertical load $P = 100$ lb.

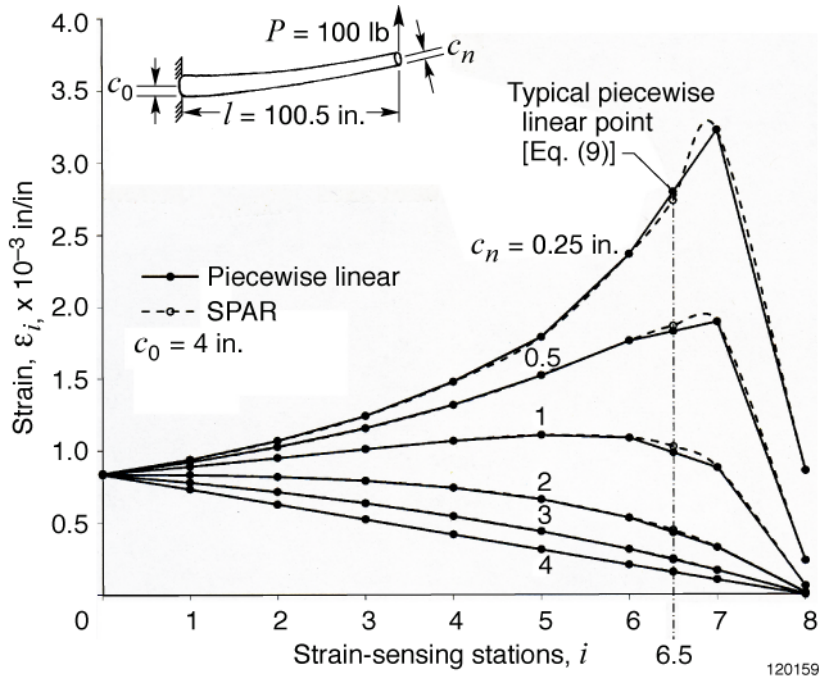


Figure 4. SPAR-generated surface strain data points fitted with piecewise linear strain curves calculated from equation (9) for different tapered cantilever tubular beams discretized with $n = 8$ domains; $P = 100$ lb.

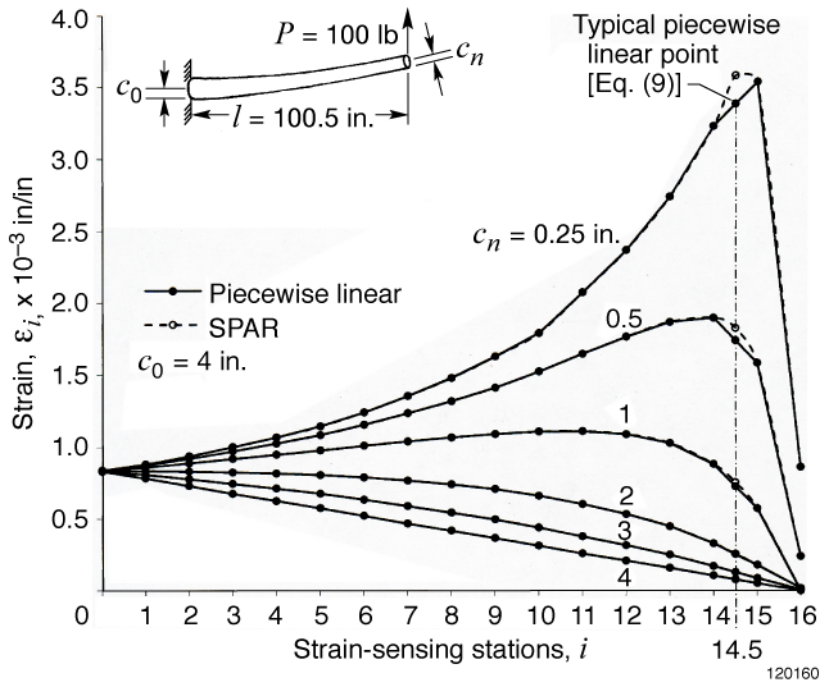


Figure 5. SPAR-generated surface strain data points fitted with piecewise linear strain curves calculated from equation (9) for different tapered cantilever tubular beams discretized with $n = 16$ domains; $P = 100$ lb.

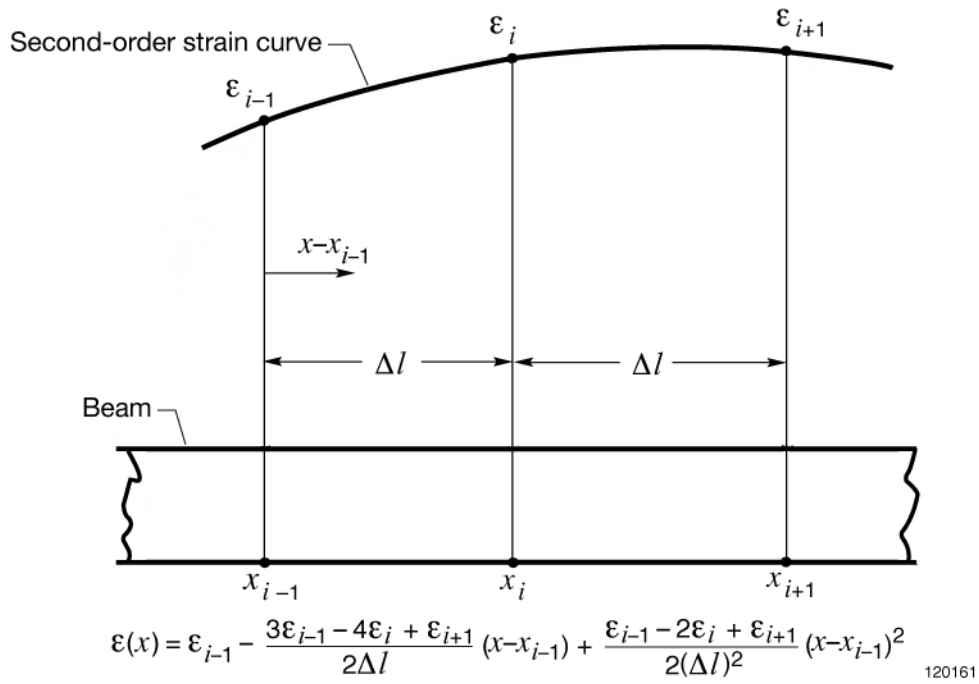


Figure 6. Local second-order curve fitting of three adjacent strain points.

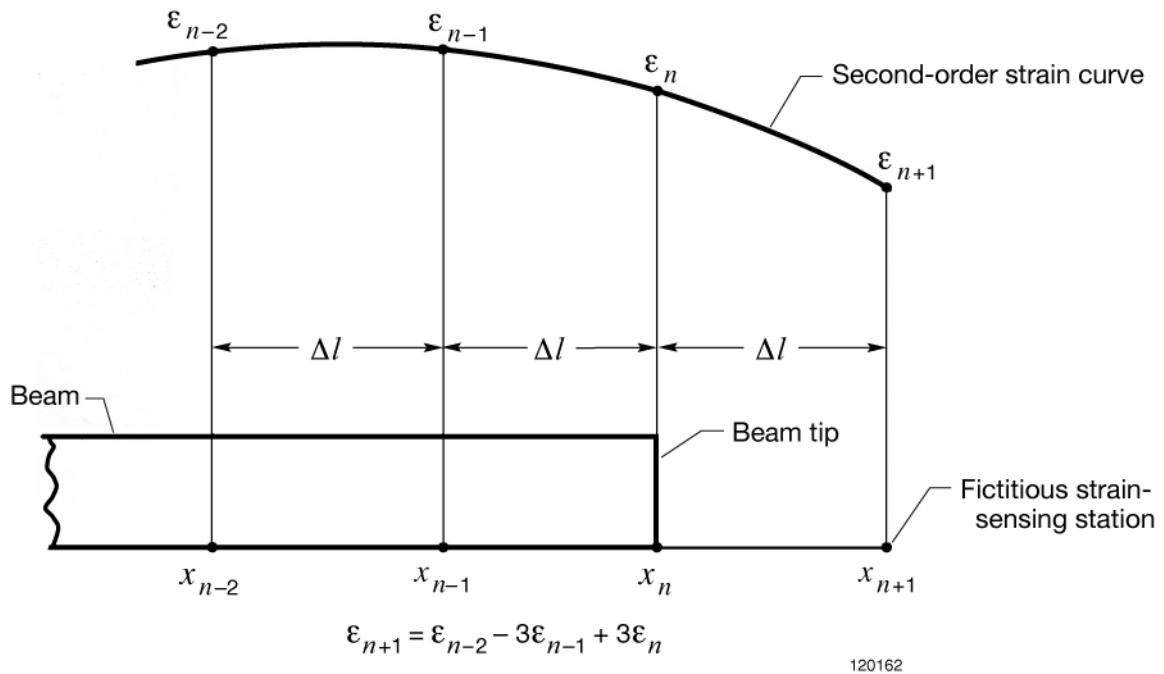


Figure 7. Extrapolation of three adjacent strains $\{\epsilon_{n-2}, \epsilon_{n-1}, \epsilon_n\}$ to obtain fictitious strain, ϵ_{n+1} .

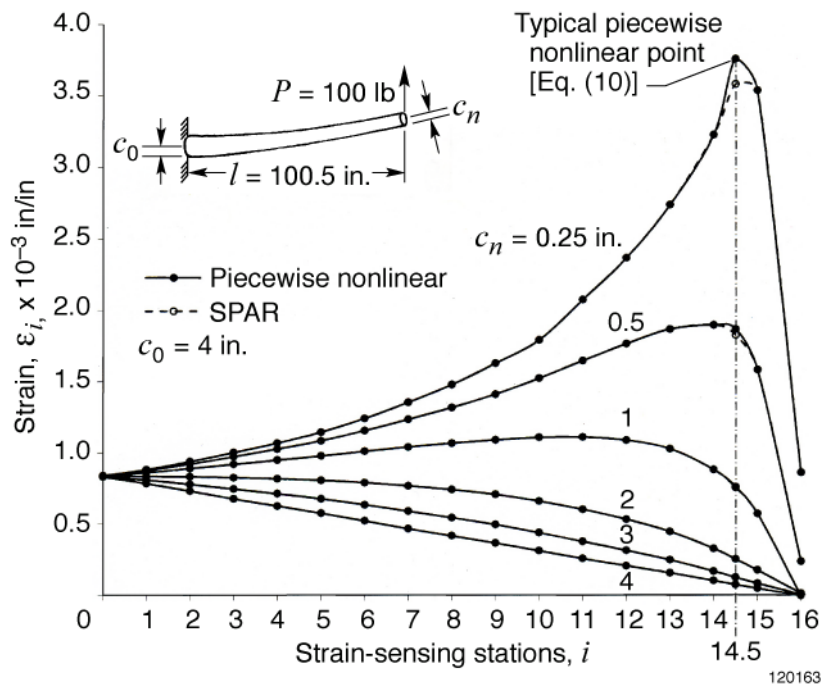


Figure 8. SPAR-generated surface strain data points fitted with piecewise linear strain curves calculated from equation (10) for different tapered cantilever tubular beams discretized with $n = 16$ domains; $P = 100$ lb.

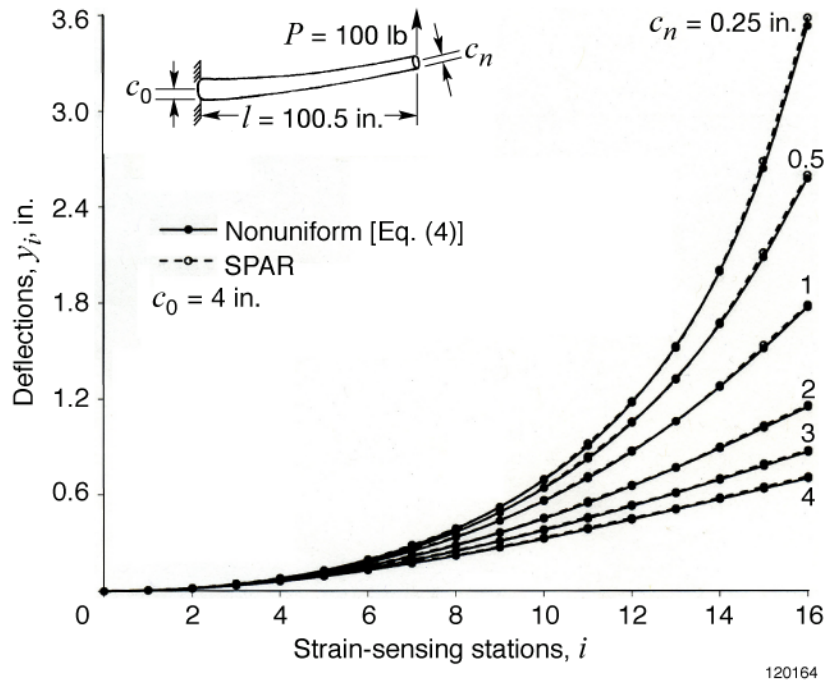


Figure 9. Comparisons of deflections calculated from SPAR program and from Nonuniform Displacement Transfer Function [equation (4)] (based on piecewise linear strain representations) for tapered cantilever tubular beams; $P = 100$ lb.

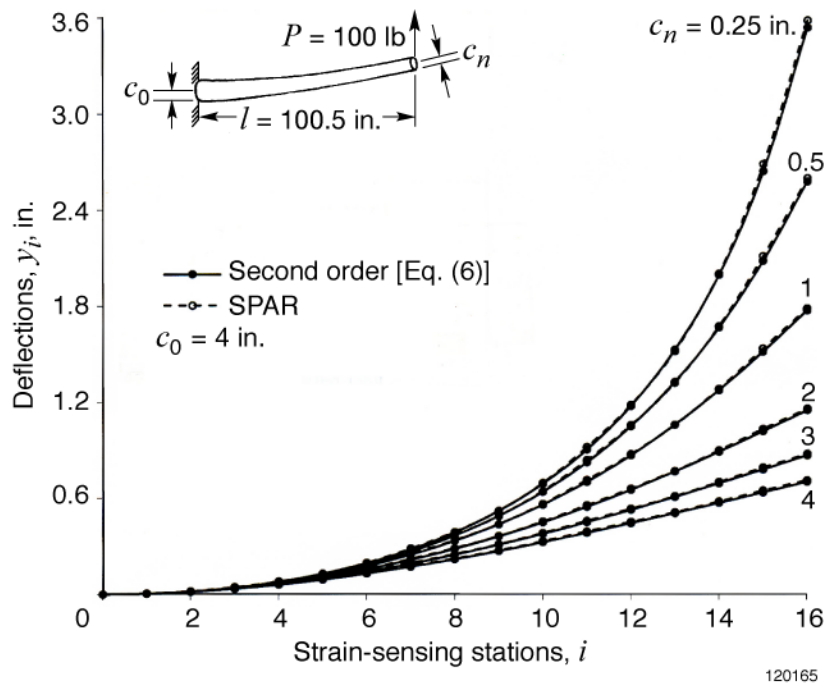


Figure 10. Comparisons of deflections calculated from SPAR program and from Second-order Displacement Transfer Function [equation (6)] (based on piecewise linear strain representations) for tapered cantilever tubular beams; $P = 100$ lb.

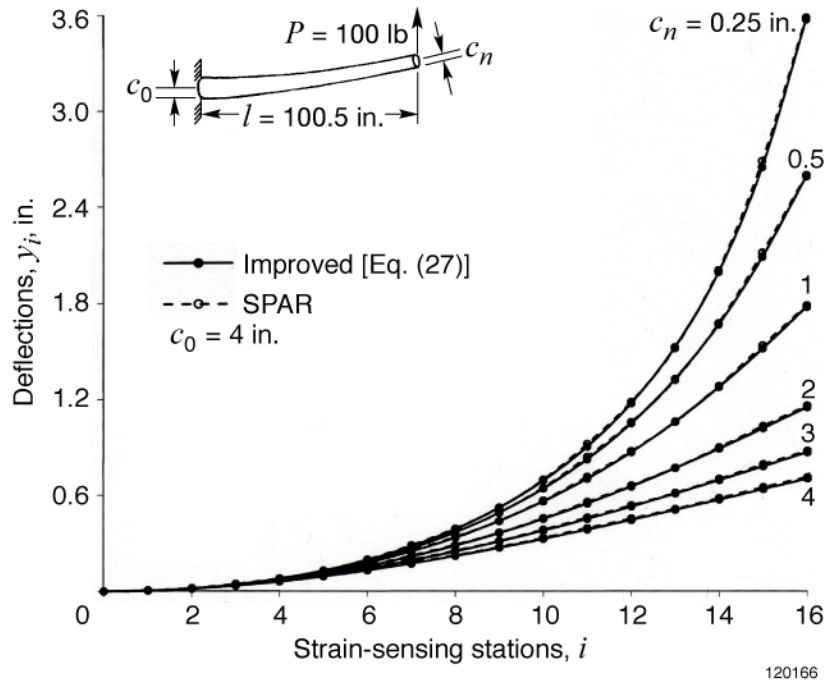


Figure 11. Comparisons of deflections calculated from SPAR program and from Improved Displacement Transfer Function [equation (27)] (based on piecewise nonlinear strain representations) for tapered cantilever tubular beams; $P = 100$ lb.

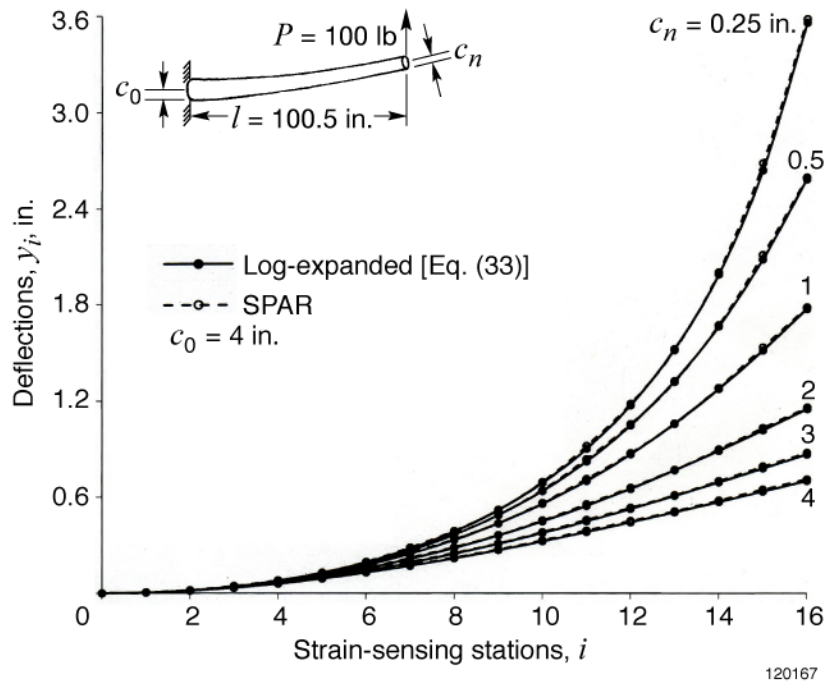


Figure 12. Comparisons of deflections calculated from SPAR program and from Log-expanded Displacement Transfer Function [equation (33)] (based on piecewise nonlinear strain representations) for tapered cantilever tubular beams; $P = 100$ lb.

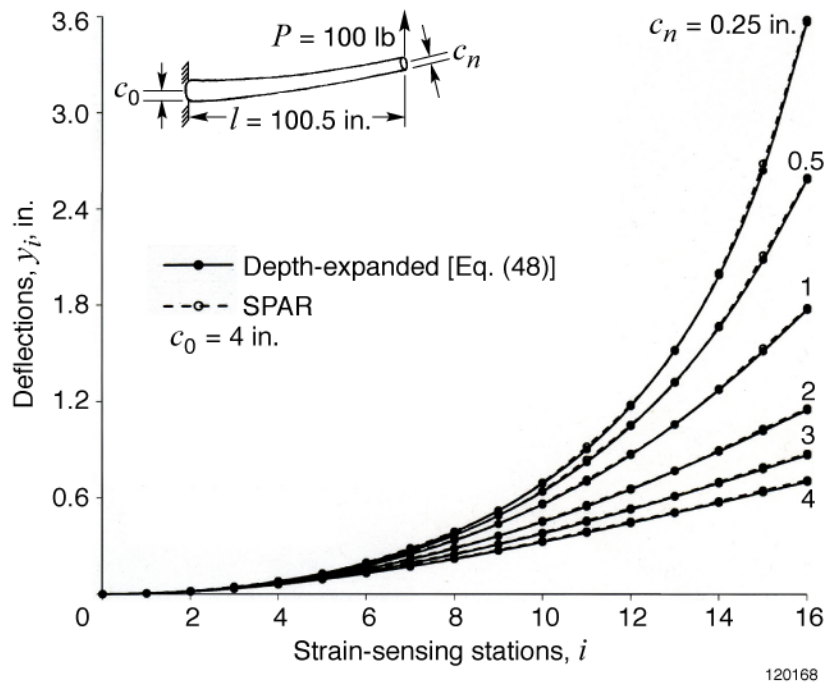


Figure 13. Comparisons of deflections calculated from SPAR program and from Depth-expanded Displacement Transfer Function [equation (48)] (based on piecewise nonlinear strain representations) for tapered cantilever tubular beams; $P = 100$ lb.

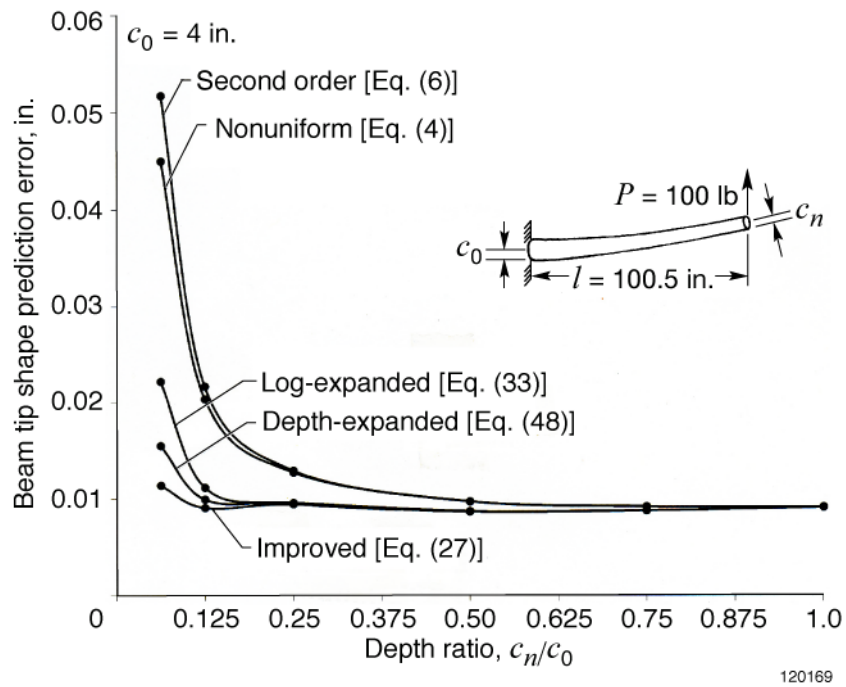


Figure 14. Comparisons of beam-tip deflection prediction errors of different Displacement Transfer Functions based on piecewise linear and piecewise nonlinear strain representations.

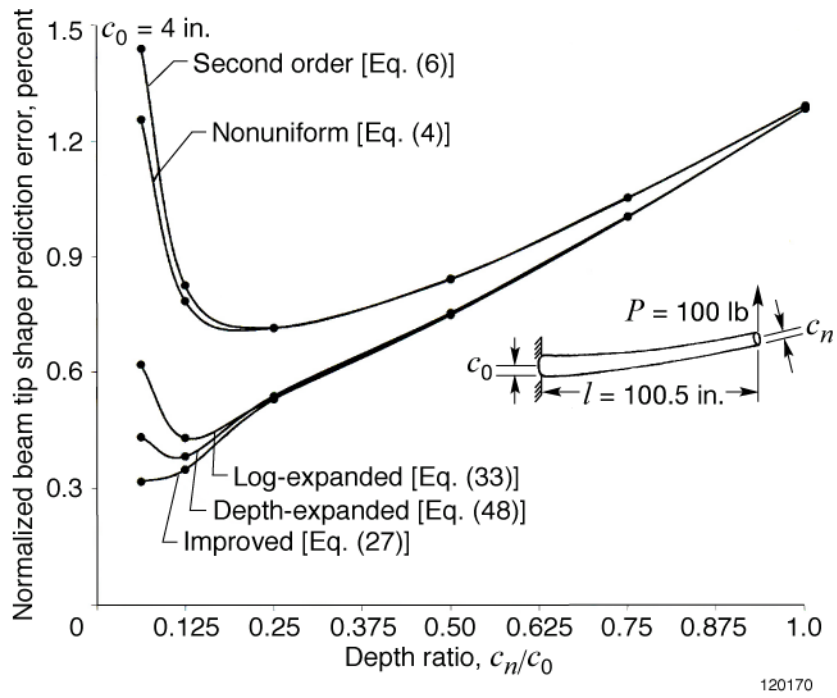


Figure 15. Comparisons of percent beam-tip deflection prediction errors of different Displacement Transfer Functions based on piecewise linear and piecewise nonlinear strain representations.

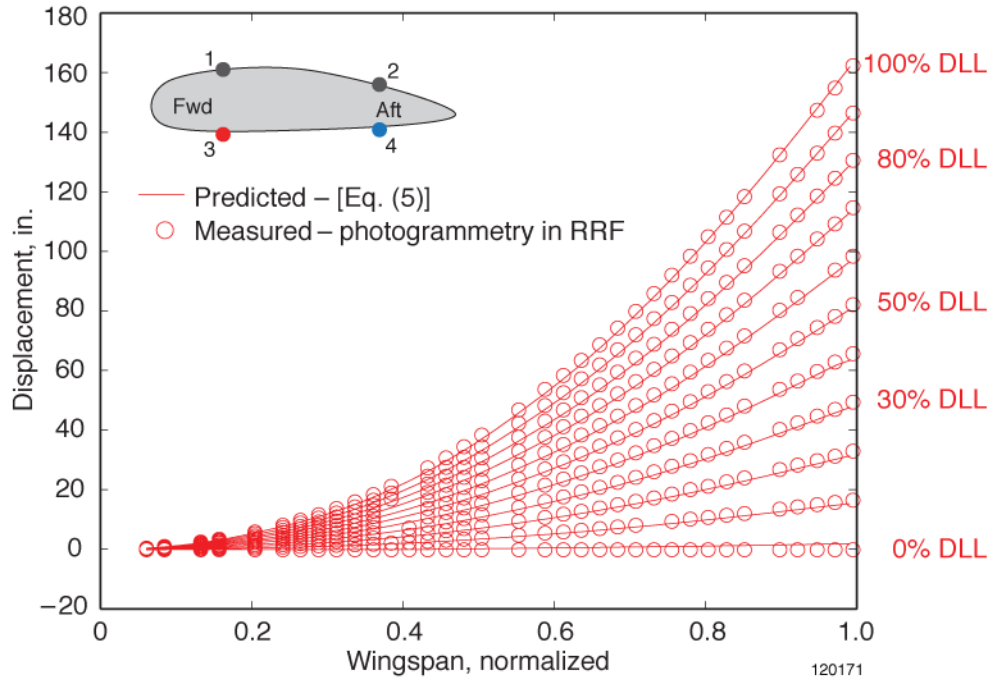


Figure 16. Comparison of predicted and measured wing deflections along No. 3 strain-sensing line for different loading levels (ref. 18).

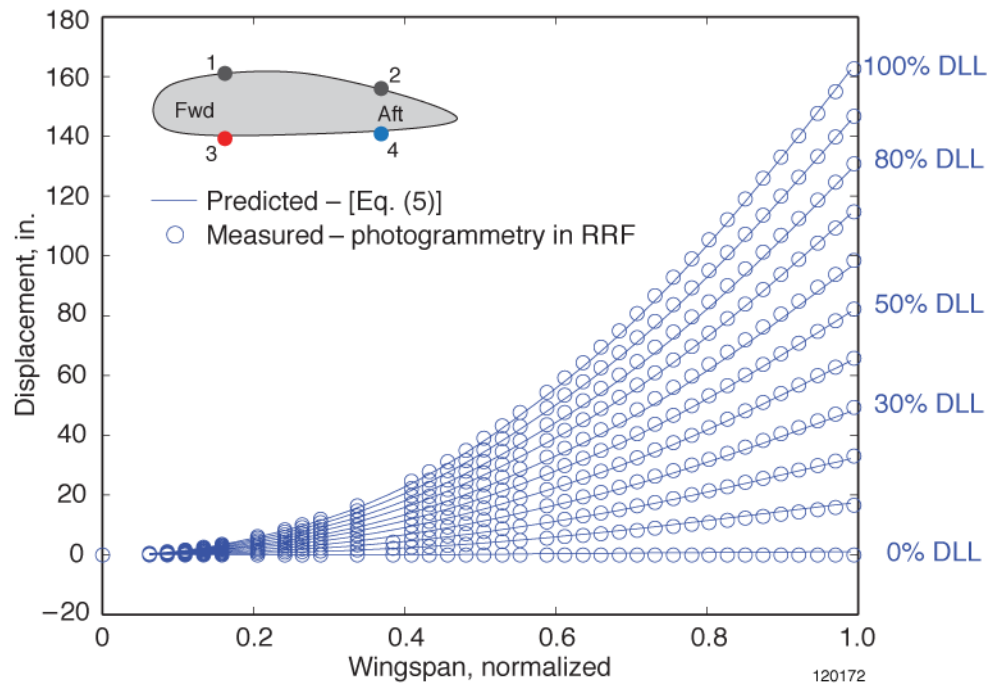


Figure 17. Comparison of predicted and measured wing deflections along No. 4 strain-sensing line for different loading levels (ref. 18).

APPENDIX A

DERIVATIONS OF IMPROVED SLOPE AND DEFLECTION EQUATIONS FOR UNIFORM BEAMS

Appendix A presents the details of integrations of the slope equation (12) and the deflection equation (16) for the uniform beams to obtain the final mathematical forms given respectively by equations (14) and (18).

Slope Equations

The slope, $\tan \theta(x)$ of the uniform beam in the small domain, $x_{i-1} \leq x \leq x_i$, between the two adjacent strain-sensing stations, $\{x_{i-1}, x_i\}$, can be obtained by carrying out the integration of equation (12), which is reproduced below:

$$\tan \theta(x) = \underbrace{\int_{x_{i-1}}^x \frac{d^2 y}{dx^2} dx}_{\text{Slope increment}} + \underbrace{\tan \theta_{i-1}}_{\text{Slope at } x_{i-1}} = \int_{x_{i-1}}^x \underbrace{\frac{\varepsilon(x)}{c}}_{\text{Eq. (2)}} dx + \tan \theta_{i-1} \quad ; \quad (x_{i-1} \leq x \leq x_i) \quad (\text{A-1})$$

The nonlinear distribution of strain, $\varepsilon(x)$, in the domain, $x_{i-1} \leq x \leq x_i$, between the two adjacent strain-sensing stations, $\{x_{i-1}, x_i\}$, described by equation (10), is duplicated below:

$$\varepsilon(x) = \varepsilon_{i-1} - \frac{3\varepsilon_{i-1} - 4\varepsilon_i + \varepsilon_{i+1}}{2\Delta l} (x - x_{i-1}) + \frac{\varepsilon_{i-1} - 2\varepsilon_i + \varepsilon_{i+1}}{2(\Delta l)^2} (x - x_{i-1})^2 \quad (\text{A-2})$$

$(x_{i-1} \leq x \leq x_i)$

In view of equation (A-2), equation (A-1) can be integrated to yield (ref. 17):

$$\begin{aligned} \tan \theta(x) &= \frac{1}{c} \int_{x_{i-1}}^x \left[\varepsilon_{i-1} - \frac{3\varepsilon_{i-1} - 4\varepsilon_i + \varepsilon_{i+1}}{2\Delta l} (x - x_{i-1}) + \frac{\varepsilon_{i-1} - 2\varepsilon_i + \varepsilon_{i+1}}{2(\Delta l)^2} (x - x_{i-1})^2 \right] dx + \tan \theta_{i-1} \\ &= \frac{1}{c} \left[\varepsilon_{i-1} (x - x_{i-1}) - \frac{3\varepsilon_{i-1} - 4\varepsilon_i + \varepsilon_{i+1}}{4\Delta l} (x - x_{i-1})^2 + \frac{\varepsilon_{i-1} - 2\varepsilon_i + \varepsilon_{i+1}}{6(\Delta l)^2} (x - x_{i-1})^3 \right] + \tan \theta_{i-1} \end{aligned} \quad (\text{A-3})$$

$(x_{i-1} \leq x \leq x_i)$

which is equation (13) in the text. At the strain-sensing station x_i , one can write $x_i - x_{i-1} \equiv \Delta l$, and equation (A-3) yields the slope, $\tan \theta_i [\equiv \tan \theta(x_i)]$, at the strain-sensing station, x_i as:

$$\tan \theta_i = \frac{\Delta l}{c} \left[\varepsilon_{i-1} - \frac{3\varepsilon_{i-1} - 4\varepsilon_i + \varepsilon_{i+1}}{4} + \frac{\varepsilon_{i-1} - 2\varepsilon_i + \varepsilon_{i+1}}{6} \right] + \tan \theta_{i-1} \quad ; \quad (i = 1, 2, 3, \dots, n) \quad (\text{A-4})$$

After grouping terms, equation (A-4) takes on the following form:

$$\tan \theta_i = \frac{\Delta l}{12c} (5\varepsilon_{i-1} + 8\varepsilon_i - \varepsilon_{i+1}) + \tan \theta_{i-1} \quad ; \quad (i=1,2,3,\dots,n) \quad (\text{A-5})$$

which is equation (14) in the text, the Improved slope equation for the uniform beams.

Deflection Equations

The deflection, $y(x)$, of the uniform-depth beam in the small domain, $x_{i-1} \leq x \leq x_i$, between the two adjacent strain-sensing stations, $\{x_{i-1}, x_i\}$, can be obtained by integrating the slope equation (A-3) [or equation (13)] with constant of integration determined by enforcing the continuity of deflection at the inboard adjacent strain-sensing station, x_{i-1} , as:

$$y(x) = \int_{x_{i-1}}^x \underbrace{\tan \theta(x)}_{\text{Eq. (A-3)}} dx + \underbrace{y_{i-1}}_{\substack{\text{Deflection} \\ \text{at } x_{i-1}}} \quad ; \quad (x_{i-1} \leq x \leq x_i) \quad (\text{A-6})$$

in which y_{i-1} is the deflection at the strain-sensing station x_{i-1} .

Substituting equation (A-3) into equation (A-6), and carrying out integrations, one obtains (ref. 17):

$$\begin{aligned} y(x) &= \frac{1}{c} \int_{x_{i-1}}^x \left[\varepsilon_{i-1} (x - x_{i-1}) - \frac{3\varepsilon_{i-1} - 4\varepsilon_i + \varepsilon_{i+1}}{4\Delta l} (x - x_{i-1})^2 + \frac{\varepsilon_{i-1} - 2\varepsilon_i + \varepsilon_{i+1}}{6(\Delta l)^2} (x - x_{i-1})^3 \right] dx \\ &\quad + \int_{x_{i-1}}^x \tan \theta_{i-1} dx + y_{i-1} \\ &= \frac{1}{c} \left[\frac{\varepsilon_{i-1}}{2} (x - x_{i-1})^2 - \frac{3\varepsilon_{i-1} - 4\varepsilon_i + \varepsilon_{i+1}}{12\Delta l} (x - x_{i-1})^3 + \frac{\varepsilon_{i-1} - 2\varepsilon_i + \varepsilon_{i+1}}{24(\Delta l)^2} (x - x_{i-1})^4 \right] \\ &\quad + (x - x_{i-1}) \tan \theta_{i-1} + y_{i-1} \end{aligned} \quad (\text{A-7})$$

$(x_{i-1} \leq x \leq x_i)$

which is equation (17) in the text. At the strain-sensing station, x_i , one can write $x_i - x_{i-1} \equiv \Delta l$, and equation (A-7) gives the deflection, $y_i \equiv y(x_i)$ at the strain-sensing station, x_i , as:

$$y_i \equiv y(x_i) = \frac{(\Delta l)^2}{c} \left[\frac{\varepsilon_{i-1}}{2} - \frac{3\varepsilon_{i-1} - 4\varepsilon_i + \varepsilon_{i+1}}{12} + \frac{\varepsilon_{i-1} - 2\varepsilon_i + \varepsilon_{i+1}}{24} \right] + y_{i-1} + (\Delta l) \tan \theta_{i-1} \quad (\text{A-8})$$

$(i=1,2,3,\dots,n)$

After grouping terms, equation (A-8) takes on the form:

$$y_i = \frac{(\Delta l)^2}{24c} (7\varepsilon_{i-1} + 6\varepsilon_i - \varepsilon_{i+1}) + y_{i-1} + \Delta l \tan \theta_{i-1} \quad ; \quad (i=1,2,3,\dots,n) \quad (\text{A-9})$$

which is equation (18) in the text, the Improved deflection equation for the uniform beams.

APPENDIX B

DERIVATIONS OF IMPROVED DISPLACEMENT TRANSFER FUNCTION FOR UNIFORM BEAMS

Appendix B presents the derivation of the final dual summation form of the deflection equation for the uniform cantilever beams. Equations (14) [or equation (A-5)] and (18) [or equation (A-9)] are duplicated below as equations (B-1) and (B-2), respectively, and can be combined into one equation with two summation terms as derived below.

$$\tan \theta_i = \frac{\Delta l}{12c} (5\varepsilon_{i-1} + 8\varepsilon_i - \varepsilon_{i+1}) + \tan \theta_{i-1} \quad ; \quad (i = 1, 2, 3, \dots, n) \quad (\text{B-1})$$

$$y_i = \frac{(\Delta l)^2}{24c} (7\varepsilon_{i-1} + 6\varepsilon_i - \varepsilon_{i+1}) + y_{i-1} + \Delta l \tan \theta_{i-1} \quad ; \quad (i = 1, 2, 3, \dots, n) \quad (\text{B-2})$$

In view of equation (B-1), equation (B-2) may be written for different indices as:

For $i = 1$:

$$y_1 = \frac{(\Delta l)^2}{24c} (7\varepsilon_0 + 6\varepsilon_1 - \varepsilon_2) + y_0 + \Delta l \tan \theta_0 \quad (\text{B-3})$$

For $i = 2$:

$$\begin{aligned} y_2 &= \frac{(\Delta l)^2}{24c} (7\varepsilon_1 + 6\varepsilon_2 - \varepsilon_3) + y_1 + \Delta l \tan \theta_1 \\ &= \frac{(\Delta l)^2}{24c} (7\varepsilon_1 + 6\varepsilon_2 - \varepsilon_3) + \underbrace{\frac{(\Delta l)^2}{24c} (7\varepsilon_0 + 6\varepsilon_1 - \varepsilon_2) + y_0 + \Delta l \tan \theta_0}_{y_1} \\ &\quad + \underbrace{\frac{(\Delta l)^2}{12c} (5\varepsilon_0 + 8\varepsilon_1 - \varepsilon_2) + \Delta l \tan \theta_0}_{\Delta l \tan \theta_1} \end{aligned} \quad (\text{B-4})$$

After grouping terms, equation (B-4) becomes:

$$\begin{aligned} y_2 &= \frac{(\Delta l)^2}{24c} (7\varepsilon_1 + 6\varepsilon_2 - \varepsilon_3) + \frac{(\Delta l)^2}{24c} (7\varepsilon_0 + 6\varepsilon_1 - \varepsilon_2) + (2-1) \frac{(\Delta l)^2}{12c} (5\varepsilon_0 + 8\varepsilon_1 - \varepsilon_2) \\ &\quad + y_0 + 2\Delta l \tan \theta_0 \end{aligned} \quad (\text{B-5})$$

For $i = 3$:

$$\begin{aligned}
y_3 &= \frac{(\Delta)^2}{24c} (7\varepsilon_2 + 6\varepsilon_3 - \varepsilon_4) + y_2 + \Delta \tan \theta_2 \\
&= \frac{(\Delta)^2}{24c} (7\varepsilon_2 + 6\varepsilon_3 - \varepsilon_4) \\
&+ \underbrace{\frac{(\Delta)^2}{24c} (7\varepsilon_1 + 6\varepsilon_2 - \varepsilon_3) + \frac{(\Delta)^2}{24c} (7\varepsilon_0 + 6\varepsilon_1 - \varepsilon_2) + (2-1) \frac{(\Delta)^2}{12c} (5\varepsilon_0 + 8\varepsilon_1 - \varepsilon_2) + y_0 + 2\Delta \tan \theta_0}_{y_2} \\
&+ \underbrace{\frac{(\Delta)^2}{12c} (5\varepsilon_1 + 8\varepsilon_2 - \varepsilon_3) + \frac{(\Delta)^2}{12c} (5\varepsilon_0 + 8\varepsilon_1 - \varepsilon_2) + \Delta \tan \theta_0}_{\Delta \tan \theta_2}
\end{aligned} \tag{B-6}$$

After grouping terms, equation (B-6) becomes:

$$\begin{aligned}
y_3 &= \frac{(\Delta)^2}{24c} (7\varepsilon_2 + 6\varepsilon_3 - \varepsilon_4) + \frac{(\Delta)^2}{24c} (7\varepsilon_1 + 6\varepsilon_2 - \varepsilon_3) + \frac{(\Delta)^2}{24c} (7\varepsilon_0 + 6\varepsilon_1 - \varepsilon_2) \\
&+ (3-2) \frac{(\Delta)^2}{12c} (5\varepsilon_1 + 8\varepsilon_2 - \varepsilon_3) + (3-1) \frac{(\Delta)^2}{12c} (5\varepsilon_0 + 8\varepsilon_1 - \varepsilon_2) + y_0 + 3\Delta \tan \theta_0
\end{aligned} \tag{B-7}$$

Observing the indicial behavior, equation (B-7) can be generalized for index i , and the deflection, y_i , can be expressed in dual summation form as:

$$\begin{aligned}
y_i &= \underbrace{\frac{(\Delta)^2}{24c} \sum_{j=1}^i (7\varepsilon_{j-1} + 6\varepsilon_j - \varepsilon_{j+1}) + y_0}_{\text{Contributions from deflection terms}} + \underbrace{\frac{(\Delta)^2}{12c} \sum_{j=1}^{i-1} (i-j)(5\varepsilon_{j-1} + 8\varepsilon_j - \varepsilon_{j+1}) + (i)\Delta \tan \theta_0}_{\text{Contributions from slope terms}} \\
&\hspace{20em} (i = 1, 2, 3, \dots, n)
\end{aligned} \tag{B-8}$$

which is equation (19) in the text, the Improved Displacement Transfer Function for the uniform beams.

APPENDIX C

DERIVATIONS OF IMPROVED SLOPE AND DEFLECTION EQUATIONS FOR NONUNIFORM BEAMS

Appendix C presents the details of integrations of the slope equation (20) and the deflection equation (24) for the nonuniform beams to obtain the final mathematical forms given respectively by equations (22) and (26).

Improved Slope Equations

The slope, $\tan \theta(x)$ of the nonuniform beam in the small domain, $x_{i-1} \leq x \leq x_i$, between the two adjacent strain-sensing stations, $\{x_{i-1}, x_i\}$, can be obtained by carrying out the integration of equation (20) which is reproduced below as equation (C-1):

$$\tan \theta(x) = \underbrace{\int_{x_{i-1}}^x \frac{d^2 y}{dx^2} dx}_{\text{Slope increment}} + \underbrace{\tan \theta_{i-1}}_{\text{Slope at } x_{i-1}} = \int_{x_{i-1}}^x \underbrace{\frac{\varepsilon(x)}{c(x)}}_{\text{Eq.(3)}} dx + \tan \theta_{i-1} \quad ; \quad (x_{i-1} \leq x \leq x_i) \quad (\text{C-1})$$

The distributions of beam depth factor, $c(x)$ [equation (8)], and bending strain, $\varepsilon(x)$ [equation (10)], in the small domain, $x_{i-1} \leq x \leq x_i$, between the two adjacent strain-sensing stations, $\{x_{i-1}, x_i\}$, are respectively duplicated below as equations (C-2) and (C-3):

$$c(x) = c_{i-1} + (c_i - c_{i-1}) \frac{x - x_{i-1}}{\Delta l} \quad ; \quad (x_{i-1} \leq x \leq x_i) \quad (\text{C-2})$$

$$\varepsilon(x) = \varepsilon_{i-1} - \frac{3\varepsilon_{i-1} - 4\varepsilon_i + \varepsilon_{i+1}}{2\Delta l} (x - x_{i-1}) + \frac{\varepsilon_{i-1} - 2\varepsilon_i + \varepsilon_{i+1}}{2(\Delta l)^2} (x - x_{i-1})^2 \quad ; \quad (x_{i-1} \leq x \leq x_i) \quad (\text{C-3})$$

Substituting equations (C-2) and (C-3) into equation (C-1) yields:

$$\tan \theta(x) = \int_{x_{i-1}}^x \left[\frac{\varepsilon_{i-1} - \frac{3\varepsilon_{i-1} - 4\varepsilon_i + \varepsilon_{i+1}}{2\Delta l} (x - x_{i-1}) + \frac{\varepsilon_{i-1} - 2\varepsilon_i + \varepsilon_{i+1}}{2(\Delta l)^2} (x - x_{i-1})^2}{c_{i-1} + \frac{c_i - c_{i-1}}{2\Delta l} (x - x_{i-1})} \right] dx + \tan \theta_{i-1} \quad (\text{C-4})$$

$(x_{i-1} \leq x \leq x_i)$

Let

$$A \equiv -\frac{3\varepsilon_{i-1} - 4\varepsilon_i + \varepsilon_{i+1}}{2\Delta l} \quad (\text{C-5})$$

$$B \equiv \frac{\varepsilon_{i-1} - 2\varepsilon_i + \varepsilon_{i+1}}{2(\Delta l)^2} \quad (\text{C-6})$$

$$C \equiv \frac{c_i - c_{i-1}}{\Delta l} \quad (\text{C-7})$$

$$\xi \equiv (x - x_{i-1}) \quad (\text{C-8})$$

then equation (C-4) takes on the following simplified form:

$$\tan \theta(x) = \int_0^\xi \frac{\varepsilon_{i-1} + A\xi + B\xi^2}{c_{i-1} + C\xi} d\xi + \tan \theta_{i-1} \quad (\text{C-9})$$

After carrying out integration of equation (C-9), one obtains (ref. 17):

$$\begin{aligned} \tan \theta(\xi) &= \left[\underbrace{\frac{\varepsilon_{i-1}}{C} \log_e(c_{i-1} + C\xi)}_{\text{Integration of 1st term in eq. (C-4)}} + \underbrace{A \frac{\xi}{C} - A \frac{c_{i-1}}{C^2} \log_e(c_{i-1} + C\xi)}_{\text{Integration of 2nd term in eq. (C-4)}} \right. \\ &\quad \left. + \underbrace{\frac{B}{C^3} \left[\frac{1}{2}(c_{i-1} + C\xi)^2 - 2c_{i-1}(c_{i-1} + C\xi) + c_{i-1}^2 \log_e(c_{i-1} + C\xi) \right]}_{\text{Integration of 3rd term in eq. (C-4)}} \right]_{0}^{\xi} + \tan \theta_{i-1} \\ &= \left(\frac{\varepsilon_{i-1}}{C} - A \frac{c_{i-1}}{C^2} + B \frac{c_{i-1}^2}{C^3} \right) \log_e(c_{i-1} + C\xi) + \frac{A}{C} \xi + \frac{1}{2} \frac{B}{C^3} (c_{i-1} + C\xi)^2 - 2 \frac{B}{C^3} c_{i-1} (c_{i-1} + C\xi) \\ &\quad - \left(\frac{\varepsilon_{i-1}}{C} - A \frac{c_{i-1}}{C^2} + B \frac{c_{i-1}^2}{C^3} \right) \log_e c_{i-1} - \frac{1}{2} \frac{B}{C^3} c_{i-1}^2 + 2 \frac{B}{C^3} c_{i-1}^2 + \tan \theta_{i-1} \\ &= \frac{1}{C^3} [C^2 \varepsilon_{i-1} - ACc_{i-1} + Bc_{i-1}^2] [\log_e(c_{i-1} + C\xi) - \log_e c_{i-1}] + \frac{A}{C} \xi \\ &\quad + \frac{1}{2} \frac{B}{C^3} [(c_{i-1} + C\xi)^2 - c_{i-1}^2] - 2 \frac{B}{C^3} c_{i-1} [(c_{i-1} + C\xi) - c_{i-1}] + \tan \theta_{i-1} \\ &= \frac{1}{C^3} [C^2 \varepsilon_{i-1} - ACc_{i-1} + Bc_{i-1}^2] [\log_e(c_{i-1} + C\xi) - \log_e c_{i-1}] + \frac{A}{C} \xi \\ &\quad + \frac{1}{2} \frac{B}{C^2} (2c_{i-1}\xi + C\xi^2) - 2 \frac{B}{C^2} c_{i-1}\xi + \tan \theta_{i-1} \\ &= \frac{1}{C^3} [C^2 \varepsilon_{i-1} - ACc_{i-1} + Bc_{i-1}^2] [\log_e(c_{i-1} + C\xi) - \log_e c_{i-1}] + \frac{A}{C} \xi \\ &\quad + \frac{1}{2} \frac{B}{C^2} [-2c_{i-1}\xi + C\xi^2] + \tan \theta_{i-1} \end{aligned} \quad (\text{C-10})$$

In view of the definitions from equations (C-5), (C-6), (C-7), and (C-8), equation (C-10) takes on the following form:

$$\begin{aligned}
\tan \theta(x) &= \frac{(\Delta)^3}{(c_i - c_{i-1})^3} \left[\varepsilon_{i-1} \frac{(c_i - c_{i-1})^2}{(\Delta)^2} + \frac{(3\varepsilon_{i-1} - 4\varepsilon_i + \varepsilon_{i+1})(c_i - c_{i-1})}{2\Delta} c_{i-1} + \frac{(\varepsilon_{i-1} - 2\varepsilon_i + \varepsilon_{i+1})}{2(\Delta)^2} c_{i-1}^2 \right] \\
&\quad \times \left[\log_e \left(c_{i-1} + \frac{c_i - c_{i-1}}{\Delta} (x - x_{i-1}) \right) - \log_e c_{i-1} \right] - \frac{(3\varepsilon_{i-1} - 4\varepsilon_i + \varepsilon_{i+1})}{2\Delta} \frac{\Delta}{c_i - c_{i-1}} (x - x_{i-1}) \\
&\quad + \frac{1}{2} \frac{(\varepsilon_{i-1} - 2\varepsilon_i + \varepsilon_{i+1})}{2(\Delta)^2} \frac{(\Delta)^2}{(c_i - c_{i-1})^2} \left[-2c_{i-1}(x - x_{i-1}) + \frac{c_i - c_{i-1}}{\Delta} (x - x_{i-1})^2 \right] + \tan \theta_{i-1} \\
&= \frac{\Delta}{(c_i - c_{i-1})^3} \underbrace{\left[\varepsilon_{i-1}(c_i - c_{i-1})^2 + \frac{1}{2}(3\varepsilon_{i-1} - 4\varepsilon_i + \varepsilon_{i+1})(c_i - c_{i-1})c_{i-1} + \frac{1}{2}(\varepsilon_{i-1} - 2\varepsilon_i + \varepsilon_{i+1})c_{i-1}^2 \right]}_{I_1} \\
&\quad \times \left[\log_e \left(c_{i-1} + \frac{c_i - c_{i-1}}{\Delta} (x - x_{i-1}) \right) - \log_e c_{i-1} \right] \\
&\quad - \underbrace{\frac{3\varepsilon_{i-1} - 4\varepsilon_i + \varepsilon_{i+1}}{2(c_i - c_{i-1})} (x - x_{i-1}) + \frac{\varepsilon_{i-1} - 2\varepsilon_i + \varepsilon_{i+1}}{4(c_i - c_{i-1})^2} \left[-2c_{i-1}(x - x_{i-1}) + \frac{c_i - c_{i-1}}{\Delta} (x - x_{i-1})^2 \right]}_{I_2} + \tan \theta_{i-1} \\
&\hspace{15em} (x_{i-1} \leq x \leq x_i) \quad (\text{C-11})
\end{aligned}$$

In equation (C-11), the two terms, $\{I_1, I_2\}$, can be simplified through grouping terms as follows:

$$\begin{aligned}
I_1 &\equiv \varepsilon_{i-1}(c_i - c_{i-1})^2 + \frac{1}{2}(3\varepsilon_{i-1} - 4\varepsilon_i + \varepsilon_{i+1})(c_i - c_{i-1})c_{i-1} + \frac{1}{2}(\varepsilon_{i-1} - 2\varepsilon_i + \varepsilon_{i+1})c_{i-1}^2 \\
&= \left[(c_i - c_{i-1})^2 + \frac{3}{2}(c_i - c_{i-1})c_{i-1} + \frac{1}{2}c_{i-1}^2 \right] \varepsilon_{i-1} - \left[2(c_i - c_{i-1})c_{i-1} + c_{i-1}^2 \right] \varepsilon_i + \frac{1}{2} \left[(c_i - c_{i-1})c_{i-1} + c_{i-1}^2 \right] \varepsilon_{i+1} \\
&= \left(c_i^2 - 2c_i c_{i-1} + c_{i-1}^2 + \frac{3}{2}c_i c_{i-1} - \frac{3}{2}c_{i-1}^2 + \frac{1}{2}c_{i-1}^2 \right) \varepsilon_{i-1} - (2c_i - c_{i-1})c_{i-1} \varepsilon_i + \frac{1}{2}c_i c_{i-1} \varepsilon_{i+1} \\
&= \frac{1}{2} \left[(2c_i - c_{i-1})c_i \varepsilon_{i-1} - 2(2c_i - c_{i-1})c_{i-1} \varepsilon_i + c_i c_{i-1} \varepsilon_{i+1} \right] \quad (\text{C-12})
\end{aligned}$$

$$\begin{aligned}
I_2 &\equiv -\frac{(3\varepsilon_{i-1} - 4\varepsilon_i + \varepsilon_{i+1})}{2(c_i - c_{i-1})} (x - x_{i-1}) + \frac{\varepsilon_{i-1} - 2\varepsilon_i + \varepsilon_{i+1}}{4(c_i - c_{i-1})^2} \left[-2c_{i-1}(x - x_{i-1}) + \frac{(c_i - c_{i-1})}{\Delta} (x - x_{i-1})^2 \right] \\
&= \frac{1}{2(c_i - c_{i-1})^2} \left[(-3\varepsilon_{i-1} + 4\varepsilon_i - \varepsilon_{i+1})(c_i - c_{i-1}) - (\varepsilon_{i-1} - 2\varepsilon_i + \varepsilon_{i+1})c_{i-1} \right] (x - x_{i-1}) \\
&\quad + \frac{\varepsilon_{i-1} - 2\varepsilon_i + \varepsilon_{i+1}}{4(c_i - c_{i-1})} \frac{(x - x_{i-1})^2}{\Delta}
\end{aligned}$$

$$\begin{aligned}
&= \frac{1}{2(c_i - c_{i-1})^2} \left\{ [-3(c_i - c_{i-1}) - c_{i-1}] \varepsilon_{i-1} + [4(c_i - c_{i-1}) + 2c_{i-1}] \varepsilon_i + [-(c_i - c_{i-1}) - c_{i-1}] \varepsilon_{i+1} \right\} (x - x_{i-1}) \\
&+ \frac{\varepsilon_{i-1} - 2\varepsilon_i + \varepsilon_{i+1}}{4(c_i - c_{i-1})} \frac{(x - x_{i-1})^2}{\Delta l} \\
&= \frac{1}{2(c_i - c_{i-1})^2} \left[(2c_{i-1} - 3c_i) \varepsilon_{i-1} + 2(2c_i - c_{i-1}) \varepsilon_i - c_i \varepsilon_{i+1} \right] (x - x_{i-1}) + \frac{\varepsilon_{i-1} - 2\varepsilon_i + \varepsilon_{i+1}}{4(c_i - c_{i-1})} \frac{(x - x_{i-1})^2}{\Delta l}
\end{aligned} \tag{C-13}$$

Substitutions of equations (C-12) and (C-13) into equation (C-11) yields:

$$\begin{aligned}
\tan \theta(x) &= \frac{\Delta l}{2(c_i - c_{i-1})^3} \left[(2c_i - c_{i-1})(c_i \varepsilon_{i-1} - 2c_{i-1} \varepsilon_i) + c_i c_{i-1} \varepsilon_{i+1} \right] \\
&\quad \times \left[\log_e \left(c_{i-1} + \frac{c_i - c_{i-1}}{\Delta l} (x - x_{i-1}) \right) - \log_e c_{i-1} \right] \\
&+ \frac{1}{2(c_i - c_{i-1})^2} \left[(2c_{i-1} - 3c_i) \varepsilon_{i-1} + 2(2c_i - c_{i-1}) \varepsilon_i - c_i \varepsilon_{i+1} \right] (x - x_{i-1}) \\
&+ \frac{\varepsilon_{i-1} - 2\varepsilon_i + \varepsilon_{i+1}}{4(c_i - c_{i-1})} \frac{(x - x_{i-1})^2}{\Delta l} + \tan \theta_{i-1}
\end{aligned} \tag{C-14}$$

$(x_{i-1} \leq x \leq x_i)$

At the strain-sensing station, x_i , one can write $(x_i - x_{i-1}) \equiv \Delta l$, and equation (C-14) gives the slope, $\tan \theta_i [\equiv \tan \theta(x_i)]$, at the strain-sensing station, x_i , as

$$\begin{aligned}
\tan \theta_i &= \frac{\Delta l}{2(c_i - c_{i-1})^3} \left[(2c_i - c_{i-1})(c_i \varepsilon_{i-1} - 2c_{i-1} \varepsilon_i) + c_i c_{i-1} \varepsilon_{i+1} \right] \log_e \frac{c_i}{c_{i-1}} \\
&+ \underbrace{\frac{\Delta l}{2(c_i - c_{i-1})^2} \left[(2c_{i-1} - 3c_i) \varepsilon_{i-1} + 2(2c_i - c_{i-1}) \varepsilon_i - c_i \varepsilon_{i+1} \right]}_{I_3} + \frac{\varepsilon_{i-1} - 2\varepsilon_i + \varepsilon_{i+1}}{4(c_i - c_{i-1})} + \tan \theta_{i-1}
\end{aligned} \tag{C-15}$$

$(i = 1, 2, 3, \dots, n)$

The term I_3 in equation (C-15) can be simplified as follows:

$$I_3 \equiv \frac{\Delta l}{2(c_i - c_{i-1})^2} \left[(2c_{i-1} - 3c_i) \varepsilon_{i-1} + 2(2c_i - c_{i-1}) \varepsilon_i - c_i \varepsilon_{i+1} \right] + \frac{\varepsilon_{i-1} - 2\varepsilon_i + \varepsilon_{i+1}}{4(c_i - c_{i-1})} \Delta l$$

$$\begin{aligned}
&= \frac{\Delta l}{2(c_i - c_{i-1})^2} \left\{ \left[2c_{i-1} - 3c_i + \frac{1}{2}(c_i - c_{i-1}) \right] \varepsilon_{i-1} + \left[2(2c_i - c_{i-1}) - (c_i - c_{i-1}) \right] \varepsilon_i \right. \\
&\quad \left. - \left[c_i - \frac{1}{2}(c_i - c_{i-1}) \right] \varepsilon_{i+1} \right\} \\
&= -\frac{\Delta l}{4(c_i - c_{i-1})^2} \left[(5c_i - 3c_{i-1})\varepsilon_{i-1} - 2(3c_i - c_{i-1})\varepsilon_i + (c_i + c_{i-1})\varepsilon_{i+1} \right] \tag{C-16}
\end{aligned}$$

In view of equation (C-16), equation (C-15) takes on the final form as:

$$\begin{aligned}
\tan \theta_i &= \frac{\Delta l}{2(c_i - c_{i-1})^3} \left[(2c_i - c_{i-1})(c_i \varepsilon_{i-1} - 2c_{i-1} \varepsilon_i) + c_i c_{i-1} \varepsilon_{i+1} \right] \log_e \frac{c_i}{c_{i-1}} \\
&\quad - \frac{\Delta l}{4(c_i - c_{i-1})^2} \left[(5c_i - 3c_{i-1})\varepsilon_{i-1} - 2(3c_i - c_{i-1})\varepsilon_i + (c_i + c_{i-1})\varepsilon_{i+1} \right] + \tan \theta_{i-1} \\
&\hspace{20em} (i = 1, 2, 3, \dots, n) \tag{C-17}
\end{aligned}$$

which is equation (22) in the text, the Improved slope equation for the nonuniform beams.

Improved Deflection Equations

The deflection, $y(x)$, of the uniform beam in the small domain, $x_{i-1} \leq x \leq x_i$, between the two adjacent strain-sensing stations, $\{x_{i-1}, x_i\}$, can be obtained by integrating the slope equation (C-14) with the constant of integration determined by enforcing the continuity of deflection at the inboard adjacent strain-sensing station, x_{i-1} , as

$$y(x) = \int_{x_{i-1}}^x \underbrace{\tan \theta(x)}_{\text{Eq. (C-14)}} dx + \underbrace{y_{i-1}}_{\substack{\text{Deflection} \\ \text{at } x_{i-1}}} \quad ; \quad (x_{i-1} \leq x \leq x_i) \tag{C-18}$$

Substituting equation (C-14) into equation (C-18), and carrying out the integrations (ref. 17), one obtains:

$$\begin{aligned}
y(x) = & \frac{\Delta l}{2(c_i - c_{i-1})^3} \left\{ [(2c_i - c_{i-1})(c_i \varepsilon_{i-1} - 2c_{i-1} \varepsilon_i) + c_i c_{i-1} \varepsilon_{i+1}] \right. \\
& \times \left[\frac{\Delta l}{c_i - c_{i-1}} \left(\left(c_{i-1} + \frac{c_i - c_{i-1}}{\Delta l} (x - x_i) \right) \log_e \left(c_{i-1} + \frac{c_i - c_{i-1}}{\Delta l} (x - x_i) \right) \right. \right. \\
& \left. \left. - \frac{c_i - c_{i-1}}{\Delta l} (x - x_i) - c_{i-1} \log_e c_{i-1} \right) - (x - x_{i-1}) \log_e c_{i-1} \right] \left. \right\} \\
& + \frac{1}{4(c_i - c_{i-1})^2} [(2c_{i-1} - 3c_i) \varepsilon_{i-1} + 2(2c_i - c_{i-1}) \varepsilon_i - c_i \varepsilon_{i+1}] (x - x_i)^2 \\
& + \frac{\varepsilon_{i-1} - 2\varepsilon_i + \varepsilon_{i+1}}{12(c_i - c_{i-1})} \frac{(x - x_i)^3}{\Delta l} + (x - x_i) \tan \theta_{i-1} + y_{i-1}
\end{aligned} \tag{C-19}$$

$(x_{i-1} \leq x \leq x_i)$

At the strain-sensing station, x_i , one can write $x_i - x_{i-1} \equiv \Delta l$, and equation (C-19) gives the deflection, $y_i [\equiv y(x_i)]$, at the strain-sensing station, x_i , as follows:

$$\begin{aligned}
y_i = & \frac{(\Delta l)^2}{2(c_i - c_{i-1})^4} \left\{ [(2c_i - c_{i-1})(c_i \varepsilon_{i-1} - 2c_{i-1} \varepsilon_i) + c_i c_{i-1} \varepsilon_{i+1}] \right. \\
& \times [c_i \log_e c_i - (c_i - c_{i-1}) - c_{i-1} \log_e c_{i-1} - (c_i - c_{i-1}) \log_e c_{i-1}] \left. \right\} \\
& + \frac{(\Delta l)^2}{4(c_i - c_{i-1})^2} \left[(2c_{i-1} - 3c_i) \varepsilon_{i-1} + 2(2c_i - c_{i-1}) \varepsilon_i - c_i \varepsilon_{i+1} + \frac{1}{3} (\varepsilon_{i-1} - 2\varepsilon_i + \varepsilon_{i+1}) (c_i - c_{i-1}) \right] \\
& + y_{i-1} + \Delta l \tan \theta_{i-1} \\
= & \frac{(\Delta l)^2}{2(c_i - c_{i-1})^4} [(2c_i - c_{i-1})(c_i \varepsilon_{i-1} - 2c_{i-1} \varepsilon_i) + c_i c_{i-1} \varepsilon_{i+1}] [c_i (\log_e c_i - \log_e c_{i-1}) - (c_i - c_{i-1})] \\
& + \frac{(\Delta l)^2}{4(c_i - c_{i-1})^2} \left[\left(2c_{i-1} - 3c_i + \frac{c_i}{3} - \frac{c_{i-1}}{3} \right) \varepsilon_{i-1} + \left(4c_i - 2c_{i-1} - \frac{2}{3} c_i + \frac{2}{3} c_{i-1} \right) \varepsilon_i + \left(-c_i + \frac{c_i}{3} - \frac{c_{i-1}}{3} \right) \varepsilon_{i+1} \right] \\
& + y_{i-1} + \Delta l \tan \theta_{i-1}
\end{aligned} \tag{C-20}$$

$(i = 1, 2, 3, \dots, n)$

After grouping terms, equation (C-20) becomes:

$$\begin{aligned}
y_i = & \frac{(\Delta l)^2}{2(c_i - c_{i-1})^4} [(2c_i - c_{i-1})(c_i \varepsilon_{i-1} - 2c_{i-1} \varepsilon_i) + c_i c_{i-1} \varepsilon_{i+1}] \left[c_i \log_e \frac{c_i}{c_{i-1}} - (c_i - c_{i-1}) \right] \\
& - \frac{(\Delta l)^2}{12(c_i - c_{i-1})^2} [(8c_i - 5c_{i-1}) \varepsilon_{i-1} - 2(5c_i - 2c_{i-1}) \varepsilon_i + (2c_i + c_{i-1}) \varepsilon_{i+1}] + y_{i-1} + \Delta l \tan \theta_{i-1}
\end{aligned} \tag{C-21}$$

$(i = 1, 2, 3, \dots, n)$

which is equation (26) in the text, the Improved deflection equation for the nonuniform beams.

APPENDIX D

DERIVATIONS OF IMPROVED DISPLACEMENT TRANSFER FUNCTION FOR NONUNIFORM BEAMS

Appendix D presents the derivations of the Improved slope and deflection equations (22) [or equation (C-17)] and (26) [or equation (C-21)] [duplicated below as equations (D-1) and (D-2), respectively] that will be combined into one equation in dual summation form.

$$\begin{aligned} \tan \theta_i &= \frac{\Delta}{2(c_i - c_{i-1})^3} \left[(2c_i - c_{i-1})(c_i \varepsilon_{i-1} - 2c_{i-1} \varepsilon_i) + c_i c_{i-1} \varepsilon_{i+1} \right] \log_e \frac{c_i}{c_{i-1}} \\ &\quad - \frac{\Delta}{4(c_i - c_{i-1})^2} \left[(5c_i - 3c_{i-1}) \varepsilon_{i-1} - 2(3c_i - c_{i-1}) \varepsilon_i + (c_i + c_{i-1}) \varepsilon_{i+1} \right] + \tan \theta_{i-1} \end{aligned} \quad (D-1)$$

$(i = 1, 2, 3, \dots, n)$

$$\begin{aligned} y_i &= \frac{(\Delta)^2}{2(c_i - c_{i-1})^4} \left[(2c_i - c_{i-1})(c_i \varepsilon_{i-1} - 2c_{i-1} \varepsilon_i) + c_i c_{i-1} \varepsilon_{i+1} \right] \left[c_i \log_e \frac{c_i}{c_{i-1}} - (c_i - c_{i-1}) \right] \\ &\quad - \frac{(\Delta)^2}{12(c_i - c_{i-1})^2} \left[(8c_i - 5c_{i-1}) \varepsilon_{i-1} - 2(5c_i - 2c_{i-1}) \varepsilon_i + (2c_i + c_{i-1}) \varepsilon_{i+1} \right] + y_{i-1} + \Delta \tan \theta_{i-1} \end{aligned} \quad (D-2)$$

$(i = 1, 2, 3, \dots, n)$

In view of equation (D-1), equation (D-2) may be written for each index, i , as:

For $i = 1$:

$$\begin{aligned} y_1 &= \frac{(\Delta)^2}{2(c_1 - c_0)^4} \left[(2c_1 - c_0)c_1 \varepsilon_0 - 2(2c_1 - c_0)c_0 \varepsilon_1 + c_1 c_0 \varepsilon_2 \right] \left[c_1 \log_e \frac{c_1}{c_0} - (c_1 - c_0) \right] \\ &\quad - \frac{(\Delta)^2}{12(c_1 - c_0)^2} \left[(8c_1 - 5c_0) \varepsilon_0 - 2(5c_1 - 2c_0) \varepsilon_1 + (2c_1 + c_0) \varepsilon_2 \right] + y_0 + \Delta \tan \theta_0 \end{aligned} \quad (D-3)$$

For $i = 2$:

$$\begin{aligned} y_2 &= \frac{(\Delta)^2}{2(c_2 - c_1)^4} \left[(2c_2 - c_1)c_2 \varepsilon_1 - 2(2c_2 - c_1)c_1 \varepsilon_2 + c_2 c_1 \varepsilon_3 \right] \left[c_2 \log_e \frac{c_2}{c_1} - (c_2 - c_1) \right] \\ &\quad - \frac{(\Delta)^2}{12(c_2 - c_1)^2} \left[(8c_2 - 5c_1) \varepsilon_1 - 2(5c_2 - 2c_1) \varepsilon_2 + (2c_2 + c_1) \varepsilon_3 \right] + y_1 + \Delta \tan \theta_1 \\ &= \frac{(\Delta)^2}{2(c_2 - c_1)^4} \left[(2c_2 - c_1)c_2 \varepsilon_1 - 2(2c_2 - c_1)c_1 \varepsilon_2 + c_2 c_1 \varepsilon_3 \right] \left[c_2 \log_e \frac{c_2}{c_1} - (c_2 - c_1) \right] \\ &\quad - \frac{(\Delta)^2}{12(c_2 - c_1)^2} \left[(8c_2 - 5c_1) \varepsilon_1 - 2(5c_2 - 2c_1) \varepsilon_2 + (2c_2 + c_1) \varepsilon_3 \right] \end{aligned}$$

$$\begin{aligned}
& + \underbrace{\left\{ \begin{aligned} & \frac{(\Delta)^2}{2(c_1 - c_0)^4} \left[(2c_1 - c_0)c_1\varepsilon_0 - 2(2c_1 - c_0)c_0\varepsilon_1 + c_1c_0\varepsilon_2 \right] \left[c_1 \log_e \frac{c_1}{c_0} - (c_1 - c_0) \right] \\ & - \frac{(\Delta)^2}{12(c_1 - c_0)^2} \left[(8c_1 - 5c_0)\varepsilon_0 - 2(5c_1 - 2c_0)\varepsilon_1 + (2c_1 + c_0)\varepsilon_2 \right] + y_0 + \Delta \tan \theta_0 \end{aligned} \right\}}_{y_1} \\
& + \underbrace{\left\{ \begin{aligned} & \frac{(\Delta)^2}{2(c_1 - c_0)^3} \left[(2c_1 - c_0)c_1\varepsilon_0 - 2(2c_1 - c_0)c_0\varepsilon_1 + c_1c_0\varepsilon_2 \right] \log_e \frac{c_1}{c_0} \\ & - \frac{(\Delta)^2}{4(c_1 - c_0)^2} \left[(5c_1 - 3c_0)\varepsilon_0 - 2(3c_1 - c_0)\varepsilon_1 + (c_1 + c_0)\varepsilon_2 \right] + \Delta \tan \theta_0 \end{aligned} \right\}}_{\Delta \tan \theta_1} \quad (D-4)
\end{aligned}$$

After grouping terms, equation (D-4) becomes:

$$\begin{aligned}
y_2 = & \left\{ \begin{aligned} & \frac{(\Delta)^2}{2(c_2 - c_1)^4} \left[(2c_2 - c_1)c_2\varepsilon_1 - 2(2c_2 - c_1)c_1\varepsilon_2 + c_2c_1\varepsilon_3 \right] \left[c_2 \log_e \frac{c_2}{c_1} - (c_2 - c_1) \right] \\ & - \frac{(\Delta)^2}{12(c_2 - c_1)^2} \left[(8c_2 - 5c_1)\varepsilon_1 - 2(5c_2 - 2c_1)\varepsilon_2 + (2c_2 + c_1)\varepsilon_3 \right] \end{aligned} \right\} \\
& + \left\{ \begin{aligned} & \frac{(\Delta)^2}{2(c_1 - c_0)^4} \left[(2c_1 - c_0)c_1\varepsilon_0 - 2(2c_1 - c_0)c_0\varepsilon_1 + c_1c_0\varepsilon_2 \right] \left[c_1 \log_e \frac{c_1}{c_0} - (c_1 - c_0) \right] \\ & - \frac{(\Delta)^2}{12(c_1 - c_0)^2} \left[(8c_1 - 5c_0)\varepsilon_0 - 2(5c_1 - 2c_0)\varepsilon_1 + (2c_1 + c_0)\varepsilon_2 \right] + y_0 \end{aligned} \right\} \\
& + (2-1) \left\{ \begin{aligned} & \frac{(\Delta)^2}{2(c_1 - c_0)^3} \left[(2c_1 - c_0)c_1\varepsilon_0 - 2(2c_1 - c_0)c_0\varepsilon_1 + c_1c_0\varepsilon_2 \right] \log_e \frac{c_1}{c_0} \\ & - \frac{(\Delta)^2}{4(c_1 - c_0)^2} \left[(5c_1 - 3c_0)\varepsilon_0 - 2(3c_1 - c_0)\varepsilon_1 + (c_1 + c_0)\varepsilon_2 \right] \end{aligned} \right\} + (2)\Delta \tan \theta_0 \quad (D-5)
\end{aligned}$$

For $i = 3$:

$$\begin{aligned}
y_3 = & \frac{(\Delta)^2}{2(c_3 - c_2)^4} \left[(2c_3 - c_2)c_3\varepsilon_2 - 2(2c_3 - c_2)c_2\varepsilon_3 + c_3c_2\varepsilon_4 \right] \left[c_3 \log_e \frac{c_3}{c_2} - (c_3 - c_2) \right] \\
& - \frac{(\Delta)^2}{12(c_3 - c_2)^2} \left[(8c_3 - 5c_2)\varepsilon_2 - 2(5c_3 - 2c_2)\varepsilon_3 + (2c_3 + c_2)\varepsilon_4 \right] + y_2 + \Delta \tan \theta_2 \\
= & \left\{ \begin{aligned} & \frac{(\Delta)^2}{2(c_3 - c_2)^4} \left[(2c_3 - c_2)c_3\varepsilon_2 - 2(2c_3 - c_2)c_2\varepsilon_3 + c_3c_2\varepsilon_4 \right] \left[c_3 \log_e \frac{c_3}{c_2} - (c_3 - c_2) \right] \\ & - \frac{(\Delta)^2}{12(c_3 - c_2)^2} \left[(8c_3 - 5c_2)\varepsilon_2 - 2(5c_3 - 2c_2)\varepsilon_3 + (2c_3 + c_2)\varepsilon_4 \right] \end{aligned} \right\}
\end{aligned}$$

$$\begin{aligned}
& \left. \begin{aligned}
& \frac{(\Delta l)^2}{2(c_2 - c_1)^4} \left[(2c_2 - c_1)c_2\varepsilon_1 - 2(2c_2 - c_1)c_1\varepsilon_2 + c_2c_1\varepsilon_3 \right] \left[c_2 \log_e \frac{c_2}{c_1} - (c_2 - c_1) \right] \\
& - \frac{(\Delta l)^2}{12(c_2 - c_1)^2} \left[(8c_2 - 5c_1)\varepsilon_1 - 2(5c_2 - 2c_1)\varepsilon_2 + (2c_2 + c_1)\varepsilon_3 \right] \\
& + \frac{(\Delta l)^2}{2(c_1 - c_0)^4} \left[(2c_1 - c_0)c_1\varepsilon_0 - 2(2c_1 - c_0)c_0\varepsilon_1 + c_1c_0\varepsilon_2 \right] \left[c_1 \log_e \frac{c_1}{c_0} - (c_1 - c_0) \right] \\
& - \frac{(\Delta l)^2}{12(c_1 - c_0)^2} \left[(8c_1 - 5c_0)\varepsilon_0 - 2(5c_1 - 2c_0)\varepsilon_1 + (2c_1 + c_0)\varepsilon_2 \right] + y_0 \\
& + (2-1) \left\{ \begin{aligned}
& \frac{(\Delta l)^2}{2(c_1 - c_0)^3} \left[(2c_1 - c_0)c_1\varepsilon_0 - 2(2c_1 - c_0)c_0\varepsilon_1 + c_1c_0\varepsilon_2 \right] \log_e \frac{c_1}{c_0} \\
& - \frac{(\Delta l)^2}{4(c_1 - c_0)^2} \left[(5c_1 - 3c_0)\varepsilon_0 - 2(3c_1 - c_0)\varepsilon_1 + (c_1 + c_0)\varepsilon_2 \right] \\
& + (2)\Delta l \tan \theta_0
\end{aligned} \right\} \\
\end{aligned} \right\} \underbrace{\hspace{10em}}_{y_2} \\
& + \left. \begin{aligned}
& \frac{(\Delta l)^2}{2(c_2 - c_1)^3} \left[(2c_2 - c_1)c_2\varepsilon_1 - 2(2c_2 - c_1)c_1\varepsilon_2 + c_2c_1\varepsilon_3 \right] \log_e \frac{c_2}{c_1} \\
& - \frac{(\Delta l)^2}{4(c_2 - c_1)^2} \left[(5c_2 - 3c_1)\varepsilon_1 - 2(3c_2 - c_1)\varepsilon_2 + (c_2 + c_1)\varepsilon_3 \right] + \\
& + \frac{(\Delta l)^2}{2(c_1 - c_0)^3} \left[(2c_1 - c_0)c_1\varepsilon_0 - 2(2c_1 - c_0)c_0\varepsilon_1 + c_1c_0\varepsilon_2 \right] \log_e \frac{c_1}{c_0} \\
& - \frac{(\Delta l)^2}{4(c_1 - c_0)^2} \left[(5c_1 - 3c_0)\varepsilon_0 - 2(3c_1 - c_0)\varepsilon_1 + (c_1 + c_0)\varepsilon_2 \right] + \Delta l \tan \theta_0
\end{aligned} \right\} \underbrace{\hspace{10em}}_{\Delta l \tan \theta_2} \tag{D-6}
\end{aligned}$$

After grouping terms, equation (D-6) becomes:

$$\begin{aligned}
y_3 = & \left\{ \begin{aligned}
& \frac{(\Delta l)^2}{2(c_3 - c_2)^4} \left[(2c_3 - c_2)c_3\varepsilon_2 - 2(2c_3 - c_2)c_2\varepsilon_3 + c_3c_2\varepsilon_4 \right] \left[c_3 \log_e \frac{c_3}{c_2} - (c_3 - c_2) \right] \\
& - \frac{(\Delta l)^2}{12(c_3 - c_2)^2} \left[(8c_3 - 5c_2)\varepsilon_2 - 2(5c_3 - 2c_2)\varepsilon_3 + (2c_3 + c_2)\varepsilon_4 \right]
\end{aligned} \right\} \\
& + \left\{ \begin{aligned}
& \frac{(\Delta l)^2}{2(c_2 - c_1)^4} \left[(2c_2 - c_1)c_2\varepsilon_1 - 2(2c_2 - c_1)c_1\varepsilon_2 + c_2c_1\varepsilon_3 \right] \left[c_2 \log_e \frac{c_2}{c_1} - (c_2 - c_1) \right] \\
& - \frac{(\Delta l)^2}{12(c_2 - c_1)^2} \left[(8c_2 - 5c_1)\varepsilon_1 - 2(5c_2 - 2c_1)\varepsilon_2 + (2c_2 + c_1)\varepsilon_3 \right]
\end{aligned} \right\}
\end{aligned}$$

$$\begin{aligned}
& + \left\{ \frac{(\Delta)^2}{2(c_1 - c_0)^4} \left[(2c_1 - c_0)c_1\varepsilon_0 - 2(2c_1 - c_0)c_0\varepsilon_1 + c_1c_0\varepsilon_2 \right] \left[c_1 \log_e \frac{c_1}{c_0} - (c_1 - c_0) \right] \right\} + y_0 \\
& - \left\{ \frac{(\Delta)^2}{12(c_1 - c_0)^2} \left[(8c_1 - 5c_0)\varepsilon_0 - 2(5c_1 - 2c_0)\varepsilon_1 + (2c_1 + c_0)\varepsilon_2 \right] \right\} \\
& + (3-2) \left\{ \frac{(\Delta)^2}{2(c_2 - c_1)^3} \left[(2c_2 - c_1)c_2\varepsilon_1 - 2(2c_2 - c_1)c_1\varepsilon_2 + c_2c_1\varepsilon_3 \right] \log_e \frac{c_2}{c_1} \right\} \\
& - \left\{ \frac{(\Delta)^2}{4(c_2 - c_1)^2} \left[(5c_2 - 3c_1)\varepsilon_1 - 2(3c_2 - c_1)\varepsilon_2 + (c_2 + c_1)\varepsilon_3 \right] \right\} \\
& + (3-1) \left\{ \frac{(\Delta)^2}{2(c_1 - c_0)^3} \left[(2c_1 - c_0)c_1\varepsilon_0 - 2(2c_1 - c_0)c_0\varepsilon_1 + c_1c_0\varepsilon_2 \right] \log_e \frac{c_1}{c_0} \right\} + 3\Delta \tan \theta_0 \quad (D-7) \\
& - \left\{ \frac{(\Delta)^2}{4(c_1 - c_0)^2} \left[(5c_1 - 3c_0)\varepsilon_0 - 2(3c_1 - c_0)\varepsilon_1 + (c_1 + c_0)\varepsilon_2 \right] \right\}
\end{aligned}$$

.....
Observing the indicial behavior, equation (D-7) can be generalized for index i , and the deflection, y_i , can be expressed in dual summation form as:

$$\begin{aligned}
y_i = & \sum_{j=1}^i \left\{ \frac{(\Delta)^2}{2(c_j - c_{j-1})^4} \left[(2c_j - c_{j-1})(c_j\varepsilon_{j-1} - 2c_{j-1}\varepsilon_j) + c_jc_{j-1}\varepsilon_{j+1} \right] \left[c_j \log_e \frac{c_j}{c_{j-1}} - (c_j - c_{j-1}) \right] \right\} + y_0 \\
& - \left\{ \frac{(\Delta)^2}{12(c_j - c_{j-1})^2} \left[(8c_j - 5c_{j-1})\varepsilon_{j-1} - 2(5c_j - 2c_{j-1})\varepsilon_j + (2c_j + c_{j-1})\varepsilon_{j+1} \right] \right\} \\
& \underbrace{\hspace{15em}}_{\text{Contribution from deflection terms}} \\
& + \sum_{j=1}^{i-1} (i-j) \left\{ \frac{(\Delta)^2}{2(c_j - c_{j-1})^3} \left[(2c_j - c_{j-1})(c_j\varepsilon_{j-1} - 2c_{j-1}\varepsilon_j) + c_jc_{j-1}\varepsilon_{j+1} \right] \log_e \frac{c_j}{c_{j-1}} \right\} \\
& - \left\{ \frac{(\Delta)^2}{4(c_j - c_{j-1})^2} \left[(5c_j - 3c_{j-1})\varepsilon_{j-1} - 2(3c_j - c_{j-1})\varepsilon_j + (c_j + c_{j-1})\varepsilon_{j+1} \right] \right\} \\
& \underbrace{\hspace{15em}}_{\text{Contributions from slope terms}} + (i)\Delta \tan \theta_0 \\
& (i=1,2,3,\dots,n) \quad (D-8)
\end{aligned}$$

which is equation (27) in the text, the Improved Displacement Transfer Function for the nonuniform beams.

APPENDIX E

DERIVATIONS OF LOG-EXPANDED SLOPE AND DEFLECTION EQUATIONS FOR NONUNIFORM BEAMS

Appendix E presents the mathematical derivations of the Log-expanded slope equation (29) and the Log-expanded deflection equation (32). The depth factor, $\mathbf{c}(\mathbf{x})$, was considered to be a slowly-changing function of x .

Log-Expanded Slope Equations

For slowly-changing $\mathbf{c}(\mathbf{x})$ [that is, $(c_i - c_{i-1}) \ll 1$], the logarithm term, $\log_e(c_i / c_{i-1})$, in the slope equation (22) may be expanded in series form up to the third-order term as (ref. 17):

$$\begin{aligned}
 \log_e \frac{c_i}{c_{i-1}} &= \left(\frac{c_i}{c_{i-1}} - 1 \right) - \frac{1}{2} \left(\frac{c_i}{c_{i-1}} - 1 \right)^2 + \frac{1}{3} \left(\frac{c_i}{c_{i-1}} - 1 \right)^3 - \dots \\
 &= \frac{c_i - c_{i-1}}{c_{i-1}} \left[1 - \frac{c_i - c_{i-1}}{2c_{i-1}} + \frac{(c_i - c_{i-1})^2}{3c_{i-1}^2} - \dots \right] \\
 &= \frac{c_i - c_{i-1}}{6c_{i-1}^3} \left[6c_{i-1}^2 - 3c_{i-1}(c_i - c_{i-1}) + 2(c_i - c_{i-1})^2 - \dots \right] \\
 &= \frac{c_i - c_{i-1}}{6c_{i-1}^3} \left[6c_{i-1}^2 - (c_i - c_{i-1})(3c_{i-1} - 2(c_i - c_{i-1})) - \dots \right] \\
 &= \frac{c_i - c_{i-1}}{6c_{i-1}^3} \left[6c_{i-1}^2 + (c_i - c_{i-1})(2c_i - 5c_{i-1}) - \dots \right] \tag{E-1}
 \end{aligned}$$

In view of equation (E-1), the Improved slope equation (22) [or equation (C-17)] can be expressed as:

$$\begin{aligned}
 \tan \theta_i &= \frac{\Delta l}{2(c_i - c_{i-1})^3} \left\{ \left[(2c_i - c_{i-1})(c_i \varepsilon_{i-1} - 2c_{i-1} \varepsilon_i) + c_i c_{i-1} \varepsilon_{i+1} \right] \log_e \frac{c_i}{c_{i-1}} \right. \\
 &\quad \left. - \frac{c_i - c_{i-1}}{2} \left[(5c_i - 3c_{i-1}) \varepsilon_{i-1} - 2(3c_i - c_{i-1}) \varepsilon_i + (c_i + c_{i-1}) \varepsilon_{i+1} \right] \right\} + \tan \theta_{i-1} \\
 &= \frac{\Delta l}{2(c_i - c_{i-1})^3} \left\{ \left[(2c_i - c_{i-1})(c_i \varepsilon_{i-1} - 2c_{i-1} \varepsilon_i) + c_i c_{i-1} \varepsilon_{i+1} \right] \frac{c_i - c_{i-1}}{6c_{i-1}^3} \left[6c_{i-1}^2 + (c_i - c_{i-1})(2c_i - 5c_{i-1}) \right] \right. \\
 &\quad \left. - \frac{c_i - c_{i-1}}{2} \left[(5c_i - 3c_{i-1}) \varepsilon_{i-1} - 2(3c_i - c_{i-1}) \varepsilon_i + (c_i + c_{i-1}) \varepsilon_{i+1} \right] \right\} \\
 &\quad + \tan \theta_{i-1} \\
 &= \frac{\Delta l}{12c_{i-1}^3 (c_i - c_{i-1})^2} \left\{ \left[(2c_i - c_{i-1})(c_i \varepsilon_{i-1} - 2c_{i-1} \varepsilon_i) + c_i c_{i-1} \varepsilon_{i+1} \right] \left[6c_{i-1}^2 + (c_i - c_{i-1})(2c_i - 5c_{i-1}) \right] \right. \\
 &\quad \left. - 3c_{i-1}^3 \left[(5c_i - 3c_{i-1}) \varepsilon_{i-1} - 2(3c_i - c_{i-1}) \varepsilon_i + (c_i + c_{i-1}) \varepsilon_{i+1} \right] \right\} + \tan \theta_{i-1}
 \end{aligned}$$

$$\begin{aligned}
&= \frac{\Delta l}{12c_{i-1}^3(c_i - c_{i-1})^2} \left\{ \begin{aligned} &\left[\begin{aligned} &6c_{i-1}^2(2c_i - c_{i-1})c_i + c_i(c_i - c_{i-1})(2c_i - 5c_{i-1})(2c_i - c_{i-1}) \\ &-3c_{i-1}^3(5c_i - 3c_{i-1}) \end{aligned} \right] \varepsilon_{i-1} \\ &+ \left[\begin{aligned} &-12c_{i-1}^3(2c_i - c_{i-1}) - 2c_{i-1}(c_i - c_{i-1})(2c_i - 5c_{i-1})(2c_i - c_{i-1}) \\ &+ 6c_{i-1}^3(3c_i - c_{i-1}) \end{aligned} \right] \varepsilon_i \\ &+ \left[\begin{aligned} &6c_i c_{i-1}^3 + c_i c_{i-1}(c_i - c_{i-1})(2c_i - 5c_{i-1}) \\ &-3c_{i-1}^3(c_i + c_{i-1}) \end{aligned} \right] \varepsilon_{i+1} \end{aligned} \right\} + \tan \theta_{i-1} \\
&= \frac{\Delta l}{12c_{i-1}^3(c_i - c_{i-1})^2} \left\{ \begin{aligned} &\left[\begin{aligned} &6c_{i-1}^2 c_i^2 + 6c_{i-1}^2 c_i(c_i - c_{i-1}) + (c_i - c_{i-1})(4c_i^3 - 12c_i^2 c_{i-1} + 5c_i c_{i-1}^2) \\ &-9c_{i-1}^3(c_i - c_{i-1}) - 6c_{i-1}^3 c_i \end{aligned} \right] \varepsilon_{i-1} \\ &+ \left[\begin{aligned} &-12c_{i-1}^3 c_i - 12c_{i-1}^3(c_i - c_{i-1}) - (c_i - c_{i-1})(8c_i^2 c_{i-1} - 24c_i c_{i-1}^2 + 10c_{i-1}^3) \\ &+ 12c_{i-1}^3 c_i + 6c_{i-1}^3(c_i - c_{i-1}) \end{aligned} \right] \varepsilon_i \\ &+ \left[\begin{aligned} &(c_i - c_{i-1})(2c_i - 5c_{i-1})c_i c_{i-1} \\ &+ 3c_{i-1}^3(c_i - c_{i-1}) \end{aligned} \right] \varepsilon_{i+1} \end{aligned} \right\} + \tan \theta_{i-1} \\
&= \frac{\Delta l}{12c_{i-1}^3(c_i - c_{i-1})^2} \left\{ \begin{aligned} &\left[\begin{aligned} &6c_{i-1}^2 c_i(c_i - c_{i-1}) + 6c_{i-1}^2 c_i(c_i - c_{i-1}) + (c_i - c_{i-1})(4c_i^3 - 12c_i^2 c_{i-1} + 5c_i c_{i-1}^2) \\ &-9c_{i-1}^3(c_i - c_{i-1}) \end{aligned} \right] \varepsilon_{i-1} \\ &+ \left[\begin{aligned} &-12c_{i-1}^3(c_i - c_{i-1}) - (c_i - c_{i-1})(8c_i^2 c_{i-1} - 24c_i c_{i-1}^2 + 10c_{i-1}^3) + 6c_{i-1}^3(c_i - c_{i-1}) \\ &+ \left[(c_i - c_{i-1})(2c_i - 5c_{i-1})c_i c_{i-1} + 3c_{i-1}^3(c_i - c_{i-1}) \right] \varepsilon_{i+1} \end{aligned} \right] \varepsilon_i \end{aligned} \right\} + \tan \theta_{i-1} \\
&= \frac{\Delta l}{12c_{i-1}^3(c_i - c_{i-1})} \left\{ \begin{aligned} &\left[\begin{aligned} &12c_{i-1}^2 c_i + 4c_i^3 - 12c_i^2 c_{i-1} + 5c_i c_{i-1}^2 - 9c_{i-1}^3 \end{aligned} \right] \varepsilon_{i-1} \\ &+ \left[\begin{aligned} &-6c_{i-1}^3 - 8c_i^2 c_{i-1} + 24c_i c_{i-1}^2 - 10c_{i-1}^3 \end{aligned} \right] \varepsilon_i \\ &+ \left[\begin{aligned} &(2c_i - 5c_{i-1})c_i c_{i-1} + 3c_{i-1}^3 \end{aligned} \right] \varepsilon_{i+1} \end{aligned} \right\} + \tan \theta_{i-1} \\
&= \frac{\Delta l}{12c_{i-1}^3(c_i - c_{i-1})} \left\{ \begin{aligned} &\left[\begin{aligned} &-12c_i c_{i-1}(c_i - c_{i-1}) + 5c_{i-1}^2(c_i - c_{i-1}) + 4(c_i^3 - c_{i-1}^3) \end{aligned} \right] \varepsilon_{i-1} \\ &+ \left[\begin{aligned} &-8c_i c_{i-1}(c_i - c_{i-1}) + 16c_{i-1}^2(c_i - c_{i-1}) \end{aligned} \right] \varepsilon_i \\ &+ \left[\begin{aligned} &2(c_i - c_{i-1})c_i c_{i-1} - 3(c_i - c_{i-1})c_{i-1}^2 \end{aligned} \right] \varepsilon_{i+1} \end{aligned} \right\} + \tan \theta_{i-1} \\
&= \frac{\Delta l}{12c_{i-1}^3} \left\{ \left[\begin{aligned} &-12c_i c_{i-1} + 5c_{i-1}^2 + 4(c_i^2 + c_i c_{i-1} + c_{i-1}^2) \end{aligned} \right] \varepsilon_{i-1} - (8c_i c_{i-1} - 16c_{i-1}^2) \varepsilon_i + (2c_i c_{i-1} - 3c_{i-1}^2) \varepsilon_{i+1} \right\} \\
&\quad + \tan \theta_{i-1} \tag{E-2} \\
&\hspace{20em} (i=1,2,3,\dots,n)
\end{aligned}$$

After the final grouping of terms, equation (E-2) becomes:

$$\tan \theta_i = \frac{\Delta l}{12c_{i-1}^3} \left\{ \left[5c_{i-1}^2 + 4(c_i - c_{i-1})^2 \right] \varepsilon_{i-1} - 8c_{i-1}(c_i - 2c_{i-1})\varepsilon_i + c_{i-1}(2c_i - 3c_{i-1})\varepsilon_{i+1} \right\} + \tan \theta_{i-1} \quad (\text{E-3})$$

($i = 1, 2, 3, \dots, n$)

which is equation (29) in the text, the Log-expanded slope equation for the nonuniform beams.

For the uniform beam case ($c_i = c_{i-1} = c$), equation (E-3) degenerates into:

$$\tan \theta_i = \frac{\Delta l}{12c} (5\varepsilon_{i-1} + 8\varepsilon_i - \varepsilon_{i+1}) + \tan \theta_{i-1} \quad ; \quad (i = 1, 2, 3, \dots, n) \quad (\text{E-4})$$

which is identical to equation (14) in the text.

Log-Expanded Deflection Equations

For the case of the Log-expanded deflection equation, the logarithm term, $\log_e(c_i / c_{i-1})$, had to be expanded up to the fourth-order term as (ref. 17):

$$\begin{aligned} \log_e \frac{c_i}{c_{i-1}} &= \left(\frac{c_i}{c_{i-1}} - 1 \right) - \frac{1}{2} \left(\frac{c_i}{c_{i-1}} - 1 \right)^2 + \frac{1}{3} \left(\frac{c_i}{c_{i-1}} - 1 \right)^3 - \frac{1}{4} \left(\frac{c_i}{c_{i-1}} - 1 \right)^4 + \dots \\ &= \frac{c_i - c_{i-1}}{12c_{i-1}^4} \left[12c_{i-1}^3 - 6c_{i-1}^2(c_i - c_{i-1}) + 4c_{i-1}(c_i - c_{i-1})^2 - 3((c_i - c_{i-1})^3 + \dots) \right] \end{aligned} \quad (\text{E-5})$$

The term, $\left[c_i \log_e(c_i / c_{i-1}) - (c_i - c_{i-1}) \right]$, can then be written as:

$$\begin{aligned} c_i \log_e \frac{c_i}{c_{i-1}} - (c_i - c_{i-1}) &= \frac{c_i(c_i - c_{i-1})}{12c_{i-1}^4} \left[12c_{i-1}^3 - 6c_{i-1}^2(c_i - c_{i-1}) + 4c_{i-1}(c_i - c_{i-1})^2 - 3((c_i - c_{i-1})^3 + \dots) \right] - (c_i - c_{i-1}) \\ &= \frac{c_i(c_i - c_{i-1})}{12c_{i-1}^4} \left[12c_{i-1}^3 - 6c_{i-1}^2(c_i - c_{i-1}) + 4c_{i-1}(c_i - c_{i-1})^2 - 3((c_i - c_{i-1})^3 - \frac{12c_{i-1}^4}{c_i}) \right] \\ &= \frac{c_i(c_i - c_{i-1})}{12c_{i-1}^4} \left[\frac{12c_{i-1}^3}{c_i}(c_i - c_{i-1}) - 6c_{i-1}^2(c_i - c_{i-1}) + 4c_{i-1}(c_i - c_{i-1})^2 - 3((c_i - c_{i-1})^3) \right] \\ &= \frac{(c_i - c_{i-1})^2}{12c_{i-1}^4} \left[12c_{i-1}^3 - 6c_i c_{i-1}^2 + 4c_i c_{i-1}(c_i - c_{i-1}) - 3c_i(c_i - c_{i-1})^2 \right] \end{aligned} \quad (\text{E-6})$$

In view of equation (E-6), equation (26) [or equation (C-21)] in the text can be rewritten as:

$$\begin{aligned}
y_i &= \frac{(\Delta)^2}{2(c_i - c_{i-1})^4} \left[(2c_i - c_{i-1})(c_i \varepsilon_{i-1} - 2c_{i-1} \varepsilon_i) + c_i c_{i-1} \varepsilon_{i+1} \right] \left[c_i \log_e \frac{c_i}{c_{i-1}} - (c_i - c_{i-1}) \right] \\
&\quad - \frac{(\Delta)^2}{12(c_i - c_{i-1})^2} \left[(8c_i - 5c_{i-1}) \varepsilon_{i-1} - 2(5c_i - 2c_{i-1}) \varepsilon_i + (2c_i + c_{i-1}) \varepsilon_{i+1} \right] + y_{i-1} + \Delta \tan \theta_{i-1} \\
&= \frac{(\Delta)^2}{2(c_i - c_{i-1})^4} \left[\langle c_i^2 + (c_i - c_{i-1})c_i \rangle \varepsilon_{i-1} - \langle 2c_i c_{i-1} + 2(c_i - c_{i-1})c_{i-1} \rangle \varepsilon_i + c_i c_{i-1} \varepsilon_{i+1} \right] \\
&\quad \times \frac{(c_i - c_{i-1})^2}{12c_{i-1}^4} \left[12c_{i-1}^3 - 6c_i c_{i-1}^2 + 4c_i c_{i-1} (c_i - c_{i-1}) - 3c_i (c_i - c_{i-1})^2 \right] \\
&\quad - \frac{(\Delta)^2}{12(c_i - c_{i-1})^2} \left[(8c_i - 5c_{i-1}) \varepsilon_{i-1} - 2(5c_i - 2c_{i-1}) \varepsilon_i + (2c_i + c_{i-1}) \varepsilon_{i+1} \right] + y_{i-1} + \Delta \tan \theta_{i-1} \\
&= \frac{(\Delta)^2}{24c_{i-1}^4 (c_i - c_{i-1})^2} \left\{ \begin{aligned} &\left[\langle c_i^2 + (c_i - c_{i-1})c_i \rangle \varepsilon_{i-1} - \langle 2c_i c_{i-1} + 2(c_i - c_{i-1})c_{i-1} \rangle \varepsilon_i + c_i c_{i-1} \varepsilon_{i+1} \right] \\ &\quad \times \left[12c_{i-1}^3 - 6c_i c_{i-1}^2 + 4c_i c_{i-1} (c_i - c_{i-1}) - 3c_i (c_i - c_{i-1})^2 \right] \\ &\quad - 2c_{i-1}^4 \left[(8c_i - 5c_{i-1}) \varepsilon_{i-1} - 2(5c_i - 2c_{i-1}) \varepsilon_i + (2c_i + c_{i-1}) \varepsilon_{i+1} \right] \end{aligned} \right\} \\
&\quad + y_{i-1} + \Delta \tan \theta_{i-1} \\
&= \frac{(\Delta)^2}{24c_{i-1}^4 (c_i - c_{i-1})^2} \left\{ \begin{aligned} &\left[\underbrace{\langle c_i^2 + (c_i - c_{i-1})c_i \rangle \langle 12c_{i-1}^3 - 6c_i c_{i-1}^2 + 4c_i c_{i-1} (c_i - c_{i-1}) - 3c_i (c_i - c_{i-1})^2 \rangle}_{f(\varepsilon_{i-1})} \right]_{\varepsilon_{i-1}} \\ &\quad - 2c_{i-1}^4 (8c_i - 5c_{i-1}) \end{aligned} \right\} \\
&\quad + \frac{(\Delta)^2}{24c_{i-1}^4 (c_i - c_{i-1})^2} \left\{ \begin{aligned} &\left[\underbrace{\langle 2c_i c_{i-1} + 2(c_i - c_{i-1})c_{i-1} \rangle \langle 12c_{i-1}^3 - 6c_i c_{i-1}^2 + 4c_i c_{i-1} (c_i - c_{i-1}) - 3c_i (c_i - c_{i-1})^2 \rangle}_{f(\varepsilon_i)} \right]_{\varepsilon_i} \\ &\quad + 4c_{i-1}^4 (5c_i - 2c_{i-1}) \end{aligned} \right\} \\
&\quad + \frac{(\Delta)^2}{24c_{i-1}^4 (c_i - c_{i-1})^2} \left\{ \begin{aligned} &\left[\underbrace{c_i c_{i-1} \varepsilon_{i+1} \langle 12c_{i-1}^3 - 6c_i c_{i-1}^2 + 4c_i c_{i-1} (c_i - c_{i-1}) - 3c_i (c_i - c_{i-1})^2 \rangle}_{f(\varepsilon_{i+1})} \right]_{\varepsilon_{i+1}} \\ &\quad - 2c_{i-1}^4 (2c_i + c_{i-1}) \end{aligned} \right\} \\
&\quad + y_{i-1} + \Delta \tan \theta_{i-1} \quad (i = 1, 2, 3, \dots, n) \tag{E-7}
\end{aligned}$$

The calculations of the terms, $f(\varepsilon_{i-1})$, $f(\varepsilon_i)$, $f(\varepsilon_{i+1})$ in equation (E-7) are shown below:

For the $f(\varepsilon_{i-1})$ term:

$$f(\varepsilon_{i-1}) \equiv \left[\langle c_i^2 + (c_i - c_{i-1})c_i \rangle \langle 12c_{i-1}^3 - 6c_i c_{i-1}^2 + 4c_i c_{i-1} (c_i - c_{i-1}) - 3c_i (c_i - c_{i-1})^2 \rangle \right]_{\varepsilon_{i-1}} - 2c_{i-1}^4 (8c_i - 5c_{i-1})$$

$$\begin{aligned}
&= \left[\begin{array}{l} 12c_i^2c_{i-1}^3 - 6c_i^3c_{i-1}^2 + 4c_i^3c_{i-1}(c_i - c_{i-1}) - 3c_i^3(c_i - c_{i-1})^2 \\ +12c_i^2c_{i-1}^3(c_i - c_{i-1}) - 6c_i^2c_{i-1}^2(c_i - c_{i-1}) + 4c_i^2c_{i-1}(c_i - c_{i-1})^2 - 3c_i^2(c_i - c_{i-1})^3 \\ -16c_i^4c_{i-1} + 10c_i^5 \end{array} \right] \varepsilon_{i-1} \\
&= \left[\begin{array}{l} -6c_i^2c_{i-1}^2(c_i - c_{i-1}) + 4c_i^3c_{i-1}(c_i - c_{i-1}) - 3c_i^3(c_i - c_{i-1})^2 \\ +12c_i^2c_{i-1}^3(c_i - c_{i-1}) - 6c_i^2c_{i-1}^2(c_i - c_{i-1}) + 4c_i^2c_{i-1}(c_i - c_{i-1})^2 - 3c_i^2(c_i - c_{i-1})^3 \\ +6c_i^3c_{i-1}^3(c_i - c_{i-1}) - 10c_i^4(c_i - c_{i-1}) \end{array} \right] \varepsilon_{i-1} \\
&= (c_i - c_{i-1}) \left[\begin{array}{l} -6c_i^2c_{i-1}^2 + 4c_i^3c_{i-1} - 3c_i^3(c_i - c_{i-1}) \\ +12c_i^2c_{i-1}^3 - 6c_i^2c_{i-1}^2 + 4c_i^2c_{i-1}(c_i - c_{i-1}) - 3c_i^2(c_i - c_{i-1})^2 \\ +6c_i^3c_{i-1}^3 - 10c_i^4 \end{array} \right] \varepsilon_{i-1} \\
&= (c_i - c_{i-1}) \left[\begin{array}{l} -12c_i^2c_{i-1}^2(c_i - c_{i-1}) + 4c_i^3c_{i-1} - 3c_i^3(c_i - c_{i-1}) \\ +4c_i^2c_{i-1}(c_i - c_{i-1}) - 3c_i^2(c_i - c_{i-1})^2 \\ -4c_i^3c_{i-1}^3 + 10c_i^3c_{i-1} - 10c_i^4 \end{array} \right] \varepsilon_{i-1} \\
&= (c_i - c_{i-1}) \left[\begin{array}{l} -12c_i^2c_{i-1}^2(c_i - c_{i-1}) + 4c_i^3c_{i-1}(c_i^2 - c_{i-1}^2) - 3c_i^3(c_i - c_{i-1}) \\ +4c_i^2c_{i-1}(c_i - c_{i-1}) - 3c_i^2(c_i - c_{i-1})^2 \\ +10c_i^3(c_i - c_{i-1}) \end{array} \right] \varepsilon_{i-1} \\
&= (c_i - c_{i-1})^2 \left[-12c_i^2c_{i-1}^2 + 4c_i^3c_{i-1}(c_i + c_{i-1}) - 3c_i^3 + 4c_i^2c_{i-1} - 3c_i^2(c_i - c_{i-1}) + 10c_i^3 \right] \varepsilon_{i-1} \\
&= (c_i - c_{i-1})^2 \left[7c_{i-1}^3 + 8c_i^2c_{i-1}(c_i - c_{i-1}) - 3c_i^2(c_i - c_{i-1}) - 3(c_i^3 - c_{i-1}^3) \right] \varepsilon_{i-1} \tag{E-8}
\end{aligned}$$

After grouping terms, one obtains the final form of $f(\varepsilon_{i-1})$ as:

$$f(\varepsilon_{i-1}) = (c_i - c_{i-1})^2 \left[7c_{i-1}^3 + (c_i - c_{i-1})(8c_i^2c_{i-1} - 3c_i^2) - 3(c_i^3 - c_{i-1}^3) \right] \varepsilon_{i-1} \tag{E-9}$$

For the $f(\varepsilon_i)$ term:

$$\begin{aligned}
f(\varepsilon_i) &\equiv \left[\begin{array}{l} -\langle 2c_i c_{i-1} + 2(c_i - c_{i-1})c_i \rangle \langle 12c_{i-1}^3 - 6c_i^2c_{i-1}^2 + 4c_i^2c_{i-1}(c_i - c_{i-1}) - 3c_i(c_i - c_{i-1})^2 \rangle \\ -2c_{i-1}^4 \langle 2(5c_i - 2c_{i-1}) \rangle \end{array} \right] \varepsilon_i \\
&= \left[\begin{array}{l} -24c_i^4c_{i-1}^4 - 24c_i^4(c_i - c_{i-1}) + 12c_i^2c_i^3 + 12c_i^2c_i^3(c_i - c_{i-1}) \\ -8c_i^2c_{i-1}^2(c_i - c_{i-1}) - 8c_i^2c_{i-1}^2(c_i - c_{i-1})^2 \\ +6c_i^2c_{i-1}(c_i - c_{i-1})^2 + 6c_i^2c_{i-1}(c_i - c_{i-1})^3 + 20c_i^4c_{i-1}^4 - 8c_i^5 \end{array} \right] \varepsilon_i \\
&= \left\{ \begin{array}{l} -4c_i^4c_{i-1}^4 + 12c_i^2c_i^3 - 8c_i^5 \\ (c_i - c_{i-1}) \left[\begin{array}{l} -24c_i^4 + 12c_i^2c_i^3 - 8c_i^2c_{i-1}^2 - 8c_i^2c_{i-1}^2(c_i - c_{i-1}) \\ +6c_i^2c_{i-1}(c_i - c_{i-1}) + 6c_i^2c_{i-1}(c_i - c_{i-1})^2 \end{array} \right] \end{array} \right\} \varepsilon_i
\end{aligned}$$

$$\begin{aligned}
&= \left\{ \begin{aligned} &4c_i c_{i-1}^3 (c_i - c_{i-1}) + 8c_{i-1}^3 (c_i^2 - c_{i-1}^2) \\ &(c_i - c_{i-1}) \left[\begin{aligned} &-24c_i^4 + 12c_i c_i^3 - 8c_i^2 c_{i-1}^2 - 8c_i c_{i-1}^2 (c_i - c_{i-1}) \\ &+ 6c_i^2 c_{i-1} (c_i - c_{i-1}) + 6c_i c_{i-1} (c_i - c_{i-1})^2 \end{aligned} \right] \end{aligned} \right\} \varepsilon_i \\
&= (c_i - c_{i-1}) \left[\begin{aligned} &4c_i c_{i-1}^3 + 8c_{i-1}^3 (c_i + c_{i-1}) - 24c_i^4 + 12c_i c_i^3 - 8c_i^2 c_{i-1}^2 \\ &- 8c_i c_{i-1}^2 (c_i - c_{i-1}) + 6c_i^2 c_{i-1} (c_i - c_{i-1}) + 6c_i c_{i-1} (c_i - c_{i-1})^2 \end{aligned} \right] \varepsilon_i \\
&= (c_i - c_{i-1}) \left[\begin{aligned} &16c_i c_{i-1}^3 - 16c_i^4 + 8c_i c_{i-1}^3 - 8c_i^2 c_{i-1}^2 \\ &- 8c_i c_{i-1}^2 (c_i - c_{i-1}) + 6c_i^2 c_{i-1} (c_i - c_{i-1}) + 6c_i c_{i-1} (c_i - c_{i-1})^2 \end{aligned} \right] \varepsilon_i \\
&= (c_i - c_{i-1}) \left[\begin{aligned} &16c_{i-1}^3 (c_i - c_{i-1}) - 8c_i c_{i-1}^2 (c_i - c_{i-1}) \\ &- 8c_i c_{i-1}^2 (c_i - c_{i-1}) + 6c_i^2 c_{i-1} (c_i - c_{i-1}) + 6c_i c_{i-1} (c_i - c_{i-1})^2 \end{aligned} \right] \varepsilon_i \\
&= (c_i - c_{i-1})^2 [16c_{i-1}^3 - 16c_i c_{i-1}^2 + 6c_i^2 c_{i-1} + 6c_i c_{i-1} (c_i - c_{i-1})] \varepsilon_i \\
&= (c_i - c_{i-1})^2 (16c_{i-1}^3 - 22c_i c_{i-1}^2 + 12c_i^2 c_{i-1}) \varepsilon_i \\
&= 2c_{i-1} (c_i - c_{i-1})^2 (6c_i^2 - 11c_i c_{i-1} + 8c_{i-1}^2) \varepsilon_i \tag{E-10}
\end{aligned}$$

After grouping terms, one obtains the following final form of $f(\varepsilon_i)$ as:

$$f(\varepsilon_i) = 2c_{i-1} (c_i - c_{i-1})^2 [3c_i^2 + (c_i - c_{i-1})(3c_i - 8c_{i-1})] \varepsilon_i \tag{E-11}$$

For the $f(\varepsilon_{i+1})$ term:

$$\begin{aligned}
f(\varepsilon_{i+1}) &\equiv \left[\begin{aligned} &c_i c_{i-1} \langle 12c_{i-1}^3 - 6c_i c_{i-1}^2 + 4c_i c_{i-1} (c_i - c_{i-1}) - 3c_i (c_i - c_{i-1})^2 \rangle \\ &- 2c_{i-1}^4 (2c_i + c_{i-1}) \end{aligned} \right] \varepsilon_{i+1} \\
&= \left[\begin{aligned} &12c_i c_{i-1}^4 - 6c_i^2 c_{i-1}^3 + 4c_i^2 c_{i-1}^2 (c_i - c_{i-1}) - 3c_i^2 c_{i-1} (c_i - c_{i-1})^2 \\ &- 4c_i c_{i-1}^4 - 2c_{i-1}^5 \end{aligned} \right] \varepsilon_{i+1} \\
&= \left\{ \begin{aligned} &8c_i c_{i-1}^4 - 6c_i^2 c_{i-1}^3 - 2c_{i-1}^5 \\ &+ (c_i - c_{i-1}) [4c_i^2 c_{i-1}^2 - 3c_i^2 c_{i-1} (c_i - c_{i-1})] \end{aligned} \right\} \varepsilon_{i+1} \\
&= \left\{ \begin{aligned} &-6c_i c_{i-1}^3 (c_i - c_{i-1}) + 2c_{i-1}^4 (c_i - c_{i-1}) \\ &+ (c_i - c_{i-1}) [4c_i^2 c_{i-1}^2 - 3c_i^2 c_{i-1} (c_i - c_{i-1})] \end{aligned} \right\} \varepsilon_{i+1} \\
&= (c_i - c_{i-1}) \left\{ -6c_i c_{i-1}^3 + 2c_{i-1}^4 + 4c_i^2 c_{i-1}^2 - 3c_i^2 c_{i-1} (c_i - c_{i-1}) \right\} \varepsilon_{i+1} \\
&= (c_i - c_{i-1}) [-2c_{i-1}^3 (c_i - c_{i-1}) + 4c_i c_{i-1}^2 (c_i - c_{i-1}) - 3c_i^2 c_{i-1} (c_i - c_{i-1})] \varepsilon_{i+1} \\
&= (c_i - c_{i-1})^2 (-2c_{i-1}^3 + 4c_i c_{i-1}^2 - 3c_i^2 c_{i-1}) \varepsilon_{i+1} \tag{E-12}
\end{aligned}$$

After grouping terms, equation (E-12) becomes:

$$f(\varepsilon_{i+1}) = -c_{i-1} (c_i - c_{i-1})^2 [c_i^2 + 2(c_i - c_{i-1})^2] \varepsilon_{i+1} \tag{E-13}$$

In view of equations (E-9), (E-11), and (E13), the displacement equation (E-7) becomes:

$$\begin{aligned}
 y_i &= \frac{(\Delta)^2}{24c_{i-1}^4(c_i - c_{i-1})^2} [f(\varepsilon_{i-1}) + f(\varepsilon_{i-1}) + f(\varepsilon_{i-1})] + y_{i-1} + \Delta \tan \theta_{i-1} \\
 &= \frac{(\Delta)^2}{24c_{i-1}^4(c_i - c_{i-1})^2} \left\{ \begin{aligned} &(c_i - c_{i-1})^2 [7c_{i-1}^3 + (c_i - c_{i-1})(8c_i c_{i-1} - 3c_i^2) - 3(c_i^3 - c_{i-1}^3)] \varepsilon_{i-1} \\ &+ 2c_{i-1}(c_i - c_{i-1})^2 [(3c_i^2 + (c_i - c_{i-1})(3c_i - 8c_{i-1})) \varepsilon_i \\ &- c_{i-1}(c_i - c_{i-1})^2 [c_i^2 + 2(c_i - c_{i-1})^2] \varepsilon_{i+1} \end{aligned} \right\} \\
 &\quad + y_{i-1} + \Delta \tan \theta_{i-1} \quad (i = 1, 2, 3, \dots, n)
 \end{aligned} \tag{E-14}$$

After eliminating the factor $(c_i - c_{i-1})^2$ in the denominator, there results:

$$\begin{aligned}
 y_i &= \frac{(\Delta)^2}{24c_{i-1}^4} \left\{ \begin{aligned} &[7c_{i-1}^3 + (c_i - c_{i-1})(8c_i c_{i-1} - 3c_i^2) - 3(c_i^3 - c_{i-1}^3)] \varepsilon_{i-1} \\ &+ 2c_{i-1} [(3c_i^2 + (c_i - c_{i-1})(3c_i - 8c_{i-1})) \varepsilon_i - c_{i-1} [c_i^2 + 2(c_i - c_{i-1})^2] \varepsilon_{i+1}] \end{aligned} \right\} \\
 &\quad + y_{i-1} + \Delta \tan \theta_{i-1} \quad (i = 1, 2, 3, \dots, n)
 \end{aligned} \tag{E-15}$$

which is equation (32) in the text, the Log-expanded deflection equation for the nonuniform beams.

APPENDIX F

DERIVATIONS OF LOG-EXPANDED DISPLACEMENT TRANSFER FUNCTION FOR NONUNIFORM BEAMS

Appendix F presents the derivation of the final Log-expanded Displacement Transfer Function written in dual summation form. The Log-expanded slope equation (29) [or equation (E-3)] and the Log-expanded deflection equation (32) [or equation (E-15)] are duplicated below as equations (F-1) and (F-2), respectively:

$$\tan \theta_i = \frac{\Delta l}{12c_{i-1}^3} \left\{ \left[5c_{i-1}^2 + 4(c_i - c_{i-1})^2 \right] \varepsilon_{i-1} - 8c_{i-1}(c_i - 2c_{i-1})\varepsilon_i + c_{i-1}(2c_i - 3c_{i-1})\varepsilon_{i+1} \right\} + \tan \theta_{i-1} \quad (\text{F-1})$$

$(i = 1, 2, 3, \dots, n)$

$$y_i = \frac{(\Delta l)^2}{24c_{i-1}^4} \left\{ \left[7c_{i-1}^3 + (c_i - c_{i-1})(8c_i c_{i-1} - 3c_i^2) - 3(c_i^3 - c_{i-1}^3) \right] \varepsilon_{i-1} \right. \\ \left. + 2c_{i-1} \left[(3c_i^2 + (c_i - c_{i-1})(3c_i - 8c_{i-1})) \right] \varepsilon_i - c_{i-1} \left[c_i^2 + 2(c_i - c_{i-1})^2 \right] \varepsilon_{i+1} \right\} \\ + y_{i-1} + \Delta l \tan \theta_{i-1} \quad (\text{F-2})$$

$(i = 1, 2, 3, \dots, n)$

In view of equation (F-1), equation (F-2) can be written out explicitly for different values of the index, i , as follows.

For $i = 1$:

$$y_1 = \frac{(\Delta l)^2}{24c_0^4} \left\{ \left[7c_0^3 + (c_1 - c_0)(8c_1 c_0 - 3c_1^2) - 3(c_1^3 - c_0^3) \right] \varepsilon_0 \right. \\ \left. + 2c_0 \left[(3c_1^2 + (c_1 - c_0)(3c_1 - 8c_0)) \right] \varepsilon_1 - c_0 \left[c_1^2 + 2(c_1 - c_0)^2 \right] \varepsilon_2 \right\} \\ + y_0 + \Delta l \tan \theta_0 \quad (\text{F-3})$$

For $i = 2$:

$$y_2 = \frac{(\Delta l)^2}{24c_1^4} \left\{ \left[7c_1^3 + (c_2 - c_1)(8c_2 c_1 - 3c_2^2) - 3(c_2^3 - c_1^3) \right] \varepsilon_1 \right. \\ \left. + 2c_1 \left[(3c_2^2 + (c_2 - c_1)(3c_2 - 8c_1)) \right] \varepsilon_2 - c_1 \left[c_2^2 + 2(c_2 - c_1)^2 \right] \varepsilon_3 \right\} \\ + y_1 + \Delta l \tan \theta_1 \quad (\text{F-4})$$

Substitutions of equations (F-1) (for $i = 1$) and (F-3) into equation (F-4) yield:

$$y_2 = \frac{(\Delta l)^2}{24c_1^4} \left\{ \left[7c_1^3 + (c_2 - c_1)(8c_2 c_1 - 3c_2^2) - 3(c_2^3 - c_1^3) \right] \varepsilon_1 \right. \\ \left. + 2c_1 \left[(3c_2^2 + (c_2 - c_1)(3c_2 - 8c_1)) \right] \varepsilon_2 - c_1 \left[c_2^2 + 2(c_2 - c_1)^2 \right] \varepsilon_3 \right\}$$

$$\begin{aligned}
& + \frac{(\Delta l)^2}{24c_0^4} \left\{ \left[7c_0^3 + (c_1 - c_0)(8c_1c_0 - 3c_1^2) - 3(c_1^3 - c_0^3) \right] \varepsilon_0 \right. \\
& \left. + 2c_0 \left[(3c_1^2 + (c_1 - c_0)(3c_1 - 8c_0)) \varepsilon_1 - c_0 \left[c_1^2 + 2(c_1 - c_0)^2 \right] \varepsilon_2 \right] \right\} + y_0 + \Delta l \tan \theta_0 \\
& \underbrace{\hspace{15em}}_{y_1} \\
& + \frac{(\Delta l)^2}{12c_0^3} \left\{ \left[5c_0^2 + 4(c_1 - c_0)^2 \right] \varepsilon_0 - 8c_0(c_1 - 2c_0)\varepsilon_1 + c_0(2c_1 - 3c_0)\varepsilon_2 \right\} + \Delta l \tan \theta_0 \\
& \underbrace{\hspace{15em}}_{\Delta l \tan \theta_1} \tag{F-5}
\end{aligned}$$

After grouping terms, equation (F-5) becomes:

$$\begin{aligned}
y_2 = & \frac{(\Delta l)^2}{24c_1^4} \left\{ \left[7c_1^3 + (c_2 - c_1)(8c_2c_1 - 3c_2^2) - 3(c_2^3 - c_1^3) \right] \varepsilon_1 \right. \\
& \left. + 2c_1 \left[(3c_2^2 + (c_2 - c_1)(3c_2 - 8c_1)) \varepsilon_2 - c_1 \left[c_2^2 + 2(c_2 - c_1)^2 \right] \varepsilon_3 \right] \right\} \\
& + \frac{(\Delta l)^2}{24c_0^4} \left\{ \left[7c_0^3 + (c_1 - c_0)(8c_1c_0 - 3c_1^2) - 3(c_1^3 - c_0^3) \right] \varepsilon_0 \right. \\
& \left. + 2c_0 \left[(3c_1^2 + (c_1 - c_0)(3c_1 - 8c_0)) \varepsilon_1 - c_0 \left[c_1^2 + 2(c_1 - c_0)^2 \right] \varepsilon_2 \right] \right\} + y_0 \\
& + (2-1) \frac{(\Delta l)^2}{12c_0^3} \left\{ \left[5c_0^2 + 4(c_1 - c_0)^2 \right] \varepsilon_0 - 8c_0(c_1 - 2c_0)\varepsilon_1 + c_0(2c_1 - 3c_0)\varepsilon_2 \right\} + (2)\Delta l \tan \theta_0 \tag{F-6}
\end{aligned}$$

For $i = 3$:

$$\begin{aligned}
y_3 = & \frac{(\Delta l)^2}{24c_2^4} \left\{ \left[7c_2^3 + (c_3 - c_2)(8c_3c_2 - 3c_3^2) - 3(c_3^3 - c_2^3) \right] \varepsilon_2 \right. \\
& \left. + 2c_2 \left[(3c_3^2 + (c_3 - c_2)(3c_3 - 8c_2)) \varepsilon_3 - c_2 \left[c_3^2 + 2(c_3 - c_2)^2 \right] \varepsilon_4 \right] \right\} \\
& + y_2 + \Delta l \tan \theta_2 \tag{F-7}
\end{aligned}$$

Substitutions of equations (F-1) (for $i = 2$) and (F-6) into equation (F-7) yield:

$$\begin{aligned}
y_3 = & \frac{(\Delta l)^2}{24c_2^4} \left\{ \left[7c_2^3 + (c_3 - c_2)(8c_3c_2 - 3c_3^2) - 3(c_3^3 - c_2^3) \right] \varepsilon_2 \right. \\
& \left. + 2c_2 \left[(3c_3^2 + (c_3 - c_2)(3c_3 - 8c_2)) \varepsilon_3 - c_2 \left[c_3^2 + 2(c_3 - c_2)^2 \right] \varepsilon_4 \right] \right\} \\
& \left\{ + \frac{(\Delta l)^2}{24c_1^4} \left\{ \left[7c_1^3 + (c_2 - c_1)(8c_2c_1 - 3c_2^2) - 3(c_2^3 - c_1^3) \right] \varepsilon_1 \right. \right. \\
& \left. \left. + 2c_1 \left[(3c_2^2 + (c_2 - c_1)(3c_2 - 8c_1)) \varepsilon_2 - c_1 \left[c_2^2 + 2(c_2 - c_1)^2 \right] \varepsilon_3 \right] \right\} \right. \\
& \left. + \frac{(\Delta l)^2}{24c_0^4} \left\{ \left[7c_0^3 + (c_1 - c_0)(8c_1c_0 - 3c_1^2) - 3(c_1^3 - c_0^3) \right] \varepsilon_0 \right. \right. \\
& \left. \left. + 2c_0 \left[(3c_1^2 + (c_1 - c_0)(3c_1 - 8c_0)) \varepsilon_1 - c_0 \left[c_1^2 + 2(c_1 - c_0)^2 \right] \varepsilon_2 \right] \right\} + y_0 \right. \\
& \left. + (2-1) \frac{(\Delta l)^2}{12c_0^3} \left\{ \left[5c_0^2 + 4(c_1 - c_0)^2 \right] \varepsilon_0 - 8c_0(c_1 - 2c_0)\varepsilon_1 + c_0(2c_1 - 3c_0)\varepsilon_2 \right\} + (2)\Delta l \tan \theta_0 \right\} \\
& \underbrace{\hspace{15em}}_{y_2}
\end{aligned}$$

$$\underbrace{\left\{ \begin{aligned} & + \frac{(\Delta)^2}{12c_1^3} \left\{ [5c_1^2 + 4(c_2 - c_1)^2] \varepsilon_1 - 8c_1(c_2 - 2c_1)\varepsilon_2 + c_1(2c_2 - 3c_1)\varepsilon_3 \right\} \\ & + \frac{(\Delta)^2}{12c_0^3} \left\{ [5c_0^2 + 4(c_1 - c_0)^2] \varepsilon_0 - 8c_0(c_1 - 2c_0)\varepsilon_1 + c_0(2c_1 - 3c_0)\varepsilon_2 \right\} + \Delta l \tan \theta_0 \end{aligned} \right\}}_{\Delta l \tan \theta_2} \quad (\text{F-8})$$

After grouping terms, equation (F-8) becomes:

$$\begin{aligned} y_3 = & \frac{(\Delta)^2}{24c_2^4} \left\{ \begin{aligned} & [7c_2^3 + (c_3 - c_2)(8c_3c_2 - 3c_3^2) - 3(c_3^3 - c_2^3)] \varepsilon_2 \\ & + 2c_2 [(3c_3^2 + (c_3 - c_2)(3c_3 - 8c_2)) \varepsilon_3 - c_2 [c_3^2 + 2(c_3 - c_2)^2] \varepsilon_4 \end{aligned} \right\} \\ & + \frac{(\Delta)^2}{24c_1^4} \left\{ \begin{aligned} & [7c_1^3 + (c_2 - c_1)(8c_2c_1 - 3c_2^2) - 3(c_2^3 - c_1^3)] \varepsilon_1 \\ & + 2c_1 [(3c_2^2 + (c_2 - c_1)(3c_2 - 8c_1)) \varepsilon_2 - c_1 [c_2^2 + 2(c_2 - c_1)^2] \varepsilon_3 \end{aligned} \right\} \\ & + \frac{(\Delta)^2}{24c_0^4} \left\{ \begin{aligned} & [7c_0^3 + (c_1 - c_0)(8c_1c_0 - 3c_1^2) - 3(c_1^3 - c_0^3)] \varepsilon_0 \\ & + 2c_0 [(3c_1^2 + (c_1 - c_0)(3c_1 - 8c_0)) \varepsilon_1 - c_0 [c_1^2 + 2(c_1 - c_0)^2] \varepsilon_2 \end{aligned} \right\} + y_0 \end{aligned} \quad (\text{F-9})$$

$$+ (3-2) \frac{(\Delta)^2}{12c_1^3} \left\{ [5c_1^2 + 4(c_2 - c_1)^2] \varepsilon_1 - 8c_1(c_2 - 2c_1)\varepsilon_2 + c_1(2c_2 - 3c_1)\varepsilon_3 \right\}$$

$$+ (3-1) \frac{(\Delta)^2}{12c_0^3} \left\{ [5c_0^2 + 4(c_1 - c_0)^2] \varepsilon_0 - 8c_0(c_1 - 2c_0)\varepsilon_1 + c_0(2c_1 - 3c_0)\varepsilon_2 \right\} + (3)\Delta l \tan \theta_0$$

.....

Observing the indicial behavior, equation (F-9) can be generalized for index i , and the deflection, y_i , can be expressed in dual summation form as:

$$\begin{aligned} y_i = & \frac{(\Delta)^2}{24} \sum_{j=1}^i \frac{1}{c_{j-1}^4} \left\{ \underbrace{\begin{aligned} & [7c_{j-1}^3 + (c_j - c_{j-1})(8c_jc_{j-1} - 3c_j^2) - 3(c_j^3 - c_{j-1}^3)] \varepsilon_{j-1} \\ & + 2c_{j-1} [(3c_j^2 + (c_j - c_{j-1})(3c_j - 8c_{j-1})) \varepsilon_j - c_{j-1} [c_j^2 + 2(c_j - c_{j-1})^2] \varepsilon_{j+1} \end{aligned}}_{\text{Contributions from deflection terms}} \right\} + y_0 \\ & + \frac{(\Delta)^2}{12} \sum_{j=1}^{i-1} \frac{(i-j)}{c_{j-1}^3} \left\{ \underbrace{\begin{aligned} & [5c_{j-1}^2 + 4(c_j - c_{j-1})^2] \varepsilon_{j-1} - 8c_{j-1}(c_j - 2c_{j-1})\varepsilon_j \\ & + c_{j-1}(2c_j - 3c_{j-1})\varepsilon_{j+1} \end{aligned}}_{\text{Contributions from slope terms}} \right\} + (i)\Delta l \tan \theta_0 \end{aligned} \quad (i=1,2,3,\dots,n) \quad (\text{F-10})$$

which is equation (33) in the text, the Log-expanded Displacement Transfer Function for the nonuniform beams.

APPENDIX G

DERIVATIONS OF DEPTH-EXPANDED SLOPE AND DEFLECTION EQUATIONS FOR NONUNIFORM BEAMS

Appendix G presents the details of the derivations of the Depth-expanded slope equation (41) and the Depth-expanded deflection equation (46) for nonuniform beams. The reciprocal of the depth factor, $1/c(x)$, was first expanded in series form before carrying out the integrations of the curvature equation (3) in the text.

Depth-Expanded Slope Equation

The slope, $\tan \theta(x)$ of the nonuniform beam in the region, $x_{i-1} \leq x \leq x_i$, between the two adjacent strain-sensing stations, $\{x_{i-1}, x_i\}$, can be obtained by integrating the nonuniform-beam curvature equation (3) with the constant of integration determined by enforcing the continuity of slope at the inboard adjacent strain-sensing station, x_{i-1} , as

$$\tan \theta(x) = \underbrace{\int_{x_{i-1}}^x \frac{d^2 y}{dx^2} dx}_{\text{Slope increment}} + \underbrace{\tan \theta_{i-1}}_{\text{Slope at } x_{i-1}} = \int_{x_{i-1}}^x \underbrace{\frac{\varepsilon(x)}{c(x)}}_{\text{Eq. (3)}} dx + \tan \theta_{i-1} \quad ; \quad (x_{i-1} \leq x \leq x_i) \quad (\text{G-1})$$

The distributions of beam depth factor, $c(x)$, and bending strain, $\varepsilon(x)$, in the domain, $x_{i-1} \leq x \leq x_i$, between the two adjacent strain-sensing stations, $\{x_{i-1}, x_i\}$, described by equation (10) are rewritten respectively below:

$$c(x) = c_{i-1} + (c_i - c_{i-1}) \frac{x - x_{i-1}}{\Delta l} \quad ; \quad (x_{i-1} \leq x \leq x_i) \quad (\text{G-2})$$

$$\varepsilon(x) = \varepsilon_{i-1} - \frac{1}{2\Delta l} (3\varepsilon_{i-1} - 4\varepsilon_i + \varepsilon_{i+1})(x - x_{i-1}) + \frac{1}{2(\Delta l)^2} (\varepsilon_{i-1} - 2\varepsilon_i + \varepsilon_{i+1})(x - x_{i-1})^2 \quad (x_{i-1} \leq x \leq x_i) \quad (\text{G-3})$$

Substituting equations (G-2) and (G-3) into equation (G-1) yields:

$$\tan \theta(x) = \int_{x_{i-1}}^x \left[\frac{\varepsilon_{i-1} - (3\varepsilon_{i-1} - 4\varepsilon_i + \varepsilon_{i+1}) \frac{x - x_{i-1}}{2\Delta l} + (\varepsilon_{i-1} - 2\varepsilon_i + \varepsilon_{i+1}) \frac{(x - x_{i-1})^2}{2(\Delta l)^2}}{c_{i-1} + (c_i - c_{i-1}) \frac{x - x_{i-1}}{2\Delta l}} \right] dx + \tan \theta_{i-1} \quad (x_{i-1} \leq x \leq x_i) \quad (\text{G-4})$$

Because the slope term, $(c_i - c_{i-1})/\Delta l$, of the depth factor, $c(x)$, in equation (G-2) is small, its reciprocal, $1/c(x)$, can be expanded in binomial series form as (ref. 17):

$$\begin{aligned} \frac{1}{c(x)} &= \frac{1}{c_{i-1} + (c_i - c_{i-1}) \frac{x - x_{i-1}}{\Delta}} = \frac{1}{c_{i-1}} \left[1 + \left(\frac{c_i}{c_{i-1}} - 1 \right) \frac{x - x_{i-1}}{\Delta} \right]^{-1} \\ &= \frac{1}{c_{i-1}} \left[1 - \left(\frac{c_i}{c_{i-1}} - 1 \right) \frac{x - x_{i-1}}{\Delta} + \left(\frac{c_i}{c_{i-1}} - 1 \right)^2 \frac{(x - x_{i-1})^2}{(\Delta)^2} - \dots \right] \end{aligned} \quad (G-5)$$

$(x_{i-1} \leq x \leq x_i)$

Let

$$A \equiv -\frac{3\varepsilon_{i-1} - 4\varepsilon_i + \varepsilon_{i+1}}{2\Delta} \quad (G-6)$$

$$B \equiv \frac{\varepsilon_{i-1} - 2\varepsilon_i + \varepsilon_{i+1}}{2(\Delta)^2} \quad (G-7)$$

$$D \equiv \left(\frac{c_i}{c_{i-1}} - 1 \right) \frac{1}{\Delta} \quad (G-8)$$

$$\xi \equiv (x - x_{i-1}) \quad (G-9)$$

then, equation (G-4) takes on the following simplified form:

$$\begin{aligned} \tan \theta(\xi) &= \frac{1}{c_{i-1}} \int_0^\xi (\varepsilon_{i-1} + A\xi + B\xi^2)(1 - D\xi + D^2\xi^2 - \dots) d\xi + \tan \theta_{i-1} \\ &= \frac{1}{c_{i-1}} \int_0^\xi [\varepsilon_{i-1} - \varepsilon_{i-1}D\xi + \varepsilon_{i-1}D^2\xi^2 + A\xi - AD\xi^2 + AD^2\xi^3 + B\xi^2 - BD\xi^3 + \dots] d\xi + \tan \theta_{i-1} \\ &= \frac{1}{c_{i-1}} \int_0^\xi [\varepsilon_{i-1} - (A - \varepsilon_{i-1}D)\xi + (-AD + B + \varepsilon_{i-1}D^2)\xi^2 - (BD - AD^2)\xi^3 + \dots] d\xi + \tan \theta_{i-1} \end{aligned} \quad (0 \leq \xi \leq \Delta) \quad (G-10)$$

After carrying out the integration of equation (G-10), one obtains (ref. 17):

$$\tan \theta(\xi) = \frac{1}{c_{i-1}} \left[\varepsilon_{i-1}\xi - (A - \varepsilon_{i-1}D)\frac{\xi^2}{2} + (-AD + B + \varepsilon_{i-1}D^2)\frac{\xi^3}{3} - (BD - AD^2)\frac{\xi^4}{4} + \dots \right] + \tan \theta_{i-1} \quad (0 \leq \xi \leq \Delta) \quad (G-11)$$

In view of the definitions from equations (G-6), (G-7), (G-8), and (G-9), equation (G-11) takes on the following form:

$$\begin{aligned}
\tan \theta(\xi) = & \frac{1}{c_{i-1}} \left\{ \varepsilon_{i-1} \xi - \left[\frac{(3\varepsilon_{i-1} - 4\varepsilon_i + \varepsilon_{i+1})}{2\Delta l} + \varepsilon_{i-1} \left(\frac{c_i}{c_{i-1}} - 1 \right) \frac{1}{\Delta l} \right] \frac{\xi^2}{2} \right. \\
& + \left[\frac{(3\varepsilon_{i-1} - 4\varepsilon_i + \varepsilon_{i+1})}{2\Delta l} \left(\frac{c_i}{c_{i-1}} - 1 \right) \frac{1}{\Delta l} + \frac{(\varepsilon_{i-1} - 2\varepsilon_i + \varepsilon_{i+1})}{2(\Delta l)^2} + \varepsilon_{i-1} \left(\frac{c_i}{c_{i-1}} - 1 \right)^2 \frac{1}{(\Delta l)^2} \right] \frac{\xi^3}{3} \\
& \left. - \left[\frac{(\varepsilon_{i-1} - 2\varepsilon_i + \varepsilon_{i+1})}{2(\Delta l)^2} \left(\frac{c_i}{c_{i-1}} - 1 \right) \frac{1}{\Delta l} + \frac{(3\varepsilon_{i-1} - 4\varepsilon_i + \varepsilon_{i+1})}{2\Delta l} \left(\frac{c_i}{c_{i-1}} - 1 \right)^2 \frac{1}{(\Delta l)^2} \right] \frac{\xi^4}{4} \right\} + \tan \theta_{i-1} \\
& \qquad \qquad \qquad (0 \leq \xi \leq \Delta l) \quad (\text{G-12})
\end{aligned}$$

At the strain-sensing station x_i , one can write $\xi = (x_i - x_{i-1}) = \Delta l$, and equation (G-12) gives the slope, $\tan \theta_i [\equiv \tan \theta(x_i)]$, at the strain-sensing station, x_i as:

$$\begin{aligned}
\tan \theta_i = & \frac{\Delta l}{c_{i-1}} \left\{ \varepsilon_{i-1} - \frac{1}{2} \left[\frac{(3\varepsilon_{i-1} - 4\varepsilon_i + \varepsilon_{i+1})}{2\Delta l} + \varepsilon_{i-1} \left(\frac{c_i}{c_{i-1}} - 1 \right) \right] \right. \\
& + \frac{1}{3} \left[\frac{(3\varepsilon_{i-1} - 4\varepsilon_i + \varepsilon_{i+1})}{2} \left(\frac{c_i}{c_{i-1}} - 1 \right) + \frac{(\varepsilon_{i-1} - 2\varepsilon_i + \varepsilon_{i+1})}{2} + \varepsilon_{i-1} \left(\frac{c_i}{c_{i-1}} - 1 \right)^2 \right] \\
& \left. - \frac{1}{4} \left[\frac{(\varepsilon_{i-1} - 2\varepsilon_i + \varepsilon_{i+1})}{2} \left(\frac{c_i}{c_{i-1}} - 1 \right) + \frac{(3\varepsilon_{i-1} - 4\varepsilon_i + \varepsilon_{i+1})}{2\Delta l} \left(\frac{c_i}{c_{i-1}} - 1 \right)^2 \right] \right\} + \tan \theta_{i-1} \\
= & \frac{\Delta l}{12c_{i-1}} \left\{ 12\varepsilon_{i-1} - 6 \left[\frac{(3\varepsilon_{i-1} - 4\varepsilon_i + \varepsilon_{i+1})}{2} + \varepsilon_{i-1} \left(\frac{c_i}{c_{i-1}} - 1 \right) \right] \right. \\
& + 4 \left[\frac{(3\varepsilon_{i-1} - 4\varepsilon_i + \varepsilon_{i+1})}{2} \left(\frac{c_i}{c_{i-1}} - 1 \right) + \frac{(\varepsilon_{i-1} - 2\varepsilon_i + \varepsilon_{i+1})}{2} + \varepsilon_{i-1} \left(\frac{c_i}{c_{i-1}} - 1 \right)^2 \right] \\
& \left. - 3 \left[\frac{(\varepsilon_{i-1} - 2\varepsilon_i + \varepsilon_{i+1})}{2} \left(\frac{c_i}{c_{i-1}} - 1 \right) + \frac{(3\varepsilon_{i-1} - 4\varepsilon_i + \varepsilon_{i+1})}{2} \left(\frac{c_i}{c_{i-1}} - 1 \right)^2 \right] \right\} + \tan \theta_{i-1} \\
= & \frac{\Delta l}{12c_{i-1}} \left\{ 12\varepsilon_{i-1} - 3(3\varepsilon_{i-1} - 4\varepsilon_i + \varepsilon_{i+1}) + 2(\varepsilon_{i-1} - 2\varepsilon_i + \varepsilon_{i+1}) \right. \\
& + \left(\frac{c_i}{c_{i-1}} - 1 \right) \left[-6\varepsilon_{i-1} + 2(3\varepsilon_{i-1} - 4\varepsilon_i + \varepsilon_{i+1}) - \frac{3}{2}(\varepsilon_{i-1} - 2\varepsilon_i + \varepsilon_{i+1}) \right] \\
& \left. + \left(\frac{c_i}{c_{i-1}} - 1 \right)^2 \left[4\varepsilon_{i-1} - \frac{3}{2}(3\varepsilon_{i-1} - 4\varepsilon_i + \varepsilon_{i+1}) \right] \right\} + \tan \theta_{i-1}
\end{aligned}$$

$$\begin{aligned}
&= \frac{\Delta l}{12c_{i-1}} \left[(5\varepsilon_{i-1} + 8\varepsilon_i - \varepsilon_{i+1}) + \left(\frac{c_i}{c_{i-1}} - 1 \right) \left(-\frac{3}{2}\varepsilon_{i-1} - 5\varepsilon_i + \frac{1}{2}\varepsilon_{i+1} \right) \right. \\
&\quad \left. + \left(\frac{c_i}{c_{i-1}} - 1 \right)^2 \left(-\frac{1}{2}\varepsilon_{i-1} + 6\varepsilon_i - \frac{3}{2}\varepsilon_{i+1} \right) \right] + \tan \theta_{i-1} \tag{G-13}
\end{aligned}$$

$(i = 1, 2, 3, \dots, n)$

After rearrangements, equation (G-13) becomes:

$$\begin{aligned}
\tan \theta_i &= \frac{\Delta l}{24c_{i-1}} \left[2(5\varepsilon_{i-1} + 8\varepsilon_i - \varepsilon_{i+1}) - \left(\frac{c_i}{c_{i-1}} - 1 \right) (3\varepsilon_{i-1} + 10\varepsilon_i - \varepsilon_{i+1}) \right. \\
&\quad \left. - \left(\frac{c_i}{c_{i-1}} - 1 \right)^2 (\varepsilon_{i-1} - 12\varepsilon_i + 3\varepsilon_{i+1}) \right] + \tan \theta_{i-1} \tag{G-14}
\end{aligned}$$

$(i = 1, 2, 3, \dots, n)$

which is equation (41) in the text, the Depth-expanded slope equation for the nonuniform beams.

Depth-Expanded Deflection Equations

The deflection, $y(x)$, of the uniform beam in the small domain, $x_{i-1} \leq x \leq x_i$, between the two adjacent strain-sensing stations, $\{x_{i-1}, x_i\}$, can be obtained by integrating the slope equation (G-12) with constant of integration determined by enforcing the continuity of deflection at the inboard adjacent strain-sensing station, x_{i-1} , as

$$y(x) = \int_{x_{i-1}}^x \underbrace{\tan \theta(x)}_{\text{Eq. (G-12)}} dx + \underbrace{y_{i-1}}_{\substack{\text{Deflection} \\ \text{at } x_{i-1}}} = \int_0^\xi \underbrace{\tan \theta(\xi)}_{\text{Eq. (G-12)}} d\xi + y_{i-1} \quad ; \quad (x_{i-1} \leq x \leq x_i) \tag{G-15}$$

Substituting equation (G-12) into equation (G-15), and carrying out integrations, one obtains (ref. 17):

$$\begin{aligned}
y(\xi) &= \frac{1}{c_{i-1}} \left\{ \varepsilon_{i-1} \frac{\xi^2}{2} - \left[\frac{(3\varepsilon_{i-1} - 4\varepsilon_i + \varepsilon_{i+1})}{2\Delta l} + \varepsilon_{i-1} \left(\frac{c_i}{c_{i-1}} - 1 \right) \frac{1}{\Delta l} \right] \frac{\xi^3}{6} \right. \\
&\quad + \left[\frac{(3\varepsilon_{i-1} - 4\varepsilon_i + \varepsilon_{i+1})}{2\Delta l} \left(\frac{c_i}{c_{i-1}} - 1 \right) \frac{1}{\Delta l} + \frac{(\varepsilon_{i-1} - 2\varepsilon_i + \varepsilon_{i+1})}{2(\Delta l)^2} + \varepsilon_{i-1} \left(\frac{c_i}{c_{i-1}} - 1 \right)^2 \frac{1}{(\Delta l)^2} \right] \frac{\xi^4}{12} \\
&\quad \left. - \left[\frac{(3\varepsilon_{i-1} - 4\varepsilon_i + \varepsilon_{i+1})}{2\Delta l} \left(\frac{c_i}{c_{i-1}} - 1 \right)^2 \frac{1}{(\Delta l)^2} + \frac{(\varepsilon_{i-1} - 2\varepsilon_i + \varepsilon_{i+1})}{2(\Delta l)^2} \left(\frac{c_i}{c_{i-1}} - 1 \right) \frac{1}{\Delta l} \right] \frac{\xi^5}{20} \right\} \\
&\quad + y_{i-1} + \xi \tan \theta_{i-1} \tag{G-16}
\end{aligned}$$

$(0 \leq \xi \leq \Delta l)$

At the strain-sensing station \mathbf{x}_i , one can write $\xi = \mathbf{x}_i - \mathbf{x}_{i-1} = \Delta l$, and equation (G-16) yields the deflection, $y_i[\equiv \mathbf{y}(\mathbf{x}_i)]$, at the strain-sensing station, \mathbf{x}_i , as follows:

$$\begin{aligned}
y_i &= \frac{(\Delta l)^2}{c_{i-1}} \left\{ \frac{1}{2} \varepsilon_{i-1} - \frac{1}{6} \left[\frac{(3\varepsilon_{i-1} - 4\varepsilon_i + \varepsilon_{i+1})}{2} + \varepsilon_{i-1} \left(\frac{c_i}{c_{i-1}} - 1 \right) \right] \right. \\
&\quad + \frac{1}{12} \left[\frac{(3\varepsilon_{i-1} - 4\varepsilon_i + \varepsilon_{i+1})}{2} \left(\frac{c_i}{c_{i-1}} - 1 \right) + \frac{(\varepsilon_{i-1} - 2\varepsilon_i + \varepsilon_{i+1})}{2} + \varepsilon_{i-1} \left(\frac{c_i}{c_{i-1}} - 1 \right)^2 \right] \\
&\quad \left. - \frac{1}{20} \left[\frac{(3\varepsilon_{i-1} - 4\varepsilon_i + \varepsilon_{i+1})}{2} \left(\frac{c_i}{c_{i-1}} - 1 \right)^2 + \frac{(\varepsilon_{i-1} - 2\varepsilon_i + \varepsilon_{i+1})}{2} \left(\frac{c_i}{c_{i-1}} - 1 \right) \right] \right\} + y_{i-1} + \Delta l \tan \theta_{i-1} \\
&= \frac{(\Delta l)^2}{60c_{i-1}} \left[30\varepsilon_{i-1} - 5(3\varepsilon_{i-1} - 4\varepsilon_i + \varepsilon_{i+1}) - 10 \left(\frac{c_i}{c_{i-1}} - 1 \right) \varepsilon_{i-1} \right. \\
&\quad + \frac{5}{2} (3\varepsilon_{i-1} - 4\varepsilon_i + \varepsilon_{i+1}) \left(\frac{c_i}{c_{i-1}} - 1 \right) + \frac{5}{2} (\varepsilon_{i-1} - 2\varepsilon_i + \varepsilon_{i+1}) + 5 \left(\frac{c_i}{c_{i-1}} - 1 \right)^2 \varepsilon_{i-1} \\
&\quad \left. - \frac{3}{2} (3\varepsilon_{i-1} - 4\varepsilon_i + \varepsilon_{i+1}) \left(\frac{c_i}{c_{i-1}} - 1 \right)^2 - \frac{3}{2} (\varepsilon_{i-1} - 2\varepsilon_i + \varepsilon_{i+1}) \left(\frac{c_i}{c_{i-1}} - 1 \right) \right] + y_{i-1} + \Delta l \tan \theta_{i-1} \\
&= \frac{(\Delta l)^2}{60c_{i-1}} \left\{ \left[30\varepsilon_{i-1} - 5(3\varepsilon_{i-1} - 4\varepsilon_i + \varepsilon_{i+1}) + \frac{5}{2} (\varepsilon_{i-1} - 2\varepsilon_i + \varepsilon_{i+1}) \right] \right. \\
&\quad + \left(\frac{c_i}{c_{i-1}} - 1 \right) \left[-10\varepsilon_{i-1} + \frac{5}{2} (3\varepsilon_{i-1} - 4\varepsilon_i + \varepsilon_{i+1}) - \frac{3}{2} (\varepsilon_{i-1} - 2\varepsilon_i + \varepsilon_{i+1}) \right] \\
&\quad \left. + \left(\frac{c_i}{c_{i-1}} - 1 \right)^2 \left[5\varepsilon_{i-1} - \frac{3}{2} (3\varepsilon_{i-1} - 4\varepsilon_i + \varepsilon_{i+1}) \right] \right\} + y_{i-1} + \Delta l \tan \theta_{i-1} \\
&= \frac{(\Delta l)^2}{60c_{i-1}} \left[\left(\frac{35}{2} \varepsilon_{i-1} + 15\varepsilon_i - \frac{5}{2} \varepsilon_{i+1} \right) - \left(\frac{c_i}{c_{i-1}} - 1 \right) (4\varepsilon_{i-1} + 7\varepsilon_i - \varepsilon_{i+1}) \right. \\
&\quad \left. + \left(\frac{c_i}{c_{i-1}} - 1 \right)^2 \left(\frac{1}{2} \varepsilon_{i-1} + 6\varepsilon_i - \frac{3}{2} \varepsilon_{i+1} \right) \right] + y_{i-1} + \Delta l \tan \theta_{i-1} \\
&= \frac{(\Delta l)^2}{120c_{i-1}} \left[(35\varepsilon_{i-1} + 30\varepsilon_i - 5\varepsilon_{i+1}) - 2 \left(\frac{c_i}{c_{i-1}} - 1 \right) (4\varepsilon_{i-1} + 7\varepsilon_i - \varepsilon_{i+1}) \right. \\
&\quad \left. + \left(\frac{c_i}{c_{i-1}} - 1 \right)^2 (\varepsilon_{i-1} + 12\varepsilon_i - 3\varepsilon_{i+1}) \right] + y_{i-1} + \Delta l \tan \theta_{i-1}
\end{aligned} \tag{G-17}$$

$$(i = 1, 2, 3, \dots, n)$$

After rearranging equation (G-17), there results:

$$y_i = \frac{(\Delta)^2}{24c_{i-1}} \left[(7\varepsilon_{i-1} + 6\varepsilon_i - \varepsilon_{i+1}) - \frac{2}{5} \left(\frac{c_i}{c_{i-1}} - 1 \right) (4\varepsilon_{i-1} + 7\varepsilon_i - \varepsilon_{i+1}) + \frac{1}{5} \left(\frac{c_i}{c_{i-1}} - 1 \right)^2 (\varepsilon_{i-1} + 12\varepsilon_i - 3\varepsilon_{i+1}) \right] + y_{i-1} + \Delta \tan \theta_{i-1} \quad (\text{G-18})$$

$(i = 1, 2, 3, \dots, n)$

which is equation (46) in the text, the Depth-expanded deflection equation for the nonuniform beams.

APPENDIX H

DERIVATIONS OF DEPTH-EXPANDED DISPLACEMENT TRANSFER FUNCTION FOR NONUNIFORM BEAMS

Appendix H presents the derivation of the final Depth-expanded Displacement Transfer Function written in dual summation form. The Depth-expanded slope equation (41) [or equation (G-14)] and Depth-expanded deflection equation (46) [or equation (G-18)] are duplicated below as equations (H-1) and (H-2) respectively:

$$\tan \theta_i = \frac{\Delta}{24c_{i-1}} \left[2(5\varepsilon_{i-1} + 8\varepsilon_i - \varepsilon_{i+1}) - \left(\frac{c_i}{c_{i-1}} - 1 \right) (3\varepsilon_{i-1} + 10\varepsilon_i - \varepsilon_{i+1}) - \left(\frac{c_i}{c_{i-1}} - 1 \right)^2 (\varepsilon_{i-1} - 12\varepsilon_i + 3\varepsilon_{i+1}) \right] + \tan \theta_{i-1} \quad (i=1,2,3,\dots,n) \quad (H-1)$$

$$y_i = \frac{(\Delta)^2}{24c_{i-1}} \left[(7\varepsilon_{i-1} + 6\varepsilon_i - \varepsilon_{i+1}) - \frac{2}{5} \left(\frac{c_i}{c_{i-1}} - 1 \right) (4\varepsilon_{i-1} + 7\varepsilon_i - \varepsilon_{i+1}) + \frac{1}{5} \left(\frac{c_i}{c_{i-1}} - 1 \right)^2 (\varepsilon_{i-1} + 12\varepsilon_i - 3\varepsilon_{i+1}) \right] + y_{i-1} + \Delta \tan \theta_{i-1} \quad (i=1,2,3,\dots,n) \quad (H-2)$$

In view of equation (H-1), equation (H-2) may be written out explicitly for different values of index, i , as follows:

For $i=1$:

$$y_1 = \frac{(\Delta)^2}{24c_0} \left[(7\varepsilon_0 + 6\varepsilon_1 - \varepsilon_2) - \frac{2}{5} \left(\frac{c_1}{c_0} - 1 \right) (4\varepsilon_0 + 7\varepsilon_1 - \varepsilon_2) + \frac{1}{5} \left(\frac{c_1}{c_0} - 1 \right)^2 (\varepsilon_0 + 12\varepsilon_1 - 3\varepsilon_2) \right] + y_0 + \Delta \tan \theta_0 \quad (H-3)$$

For $i=2$:

$$\begin{aligned} y_2 &= \frac{(\Delta)^2}{24c_1} \left[(7\varepsilon_1 + 6\varepsilon_2 - \varepsilon_3) - \frac{2}{5} \left(\frac{c_2}{c_1} - 1 \right) (4\varepsilon_1 + 7\varepsilon_2 - \varepsilon_3) + \frac{1}{5} \left(\frac{c_2}{c_1} - 1 \right)^2 (\varepsilon_1 + 12\varepsilon_2 - 3\varepsilon_3) \right] \\ &\quad + y_1 + \Delta \tan \theta_1 \\ &= \frac{(\Delta)^2}{24c_1} \left[(7\varepsilon_1 + 6\varepsilon_2 - \varepsilon_3) - \frac{2}{5} \left(\frac{c_2}{c_1} - 1 \right) (4\varepsilon_1 + 7\varepsilon_2 - \varepsilon_3) + \frac{1}{5} \left(\frac{c_1}{c_1} - 1 \right)^2 (\varepsilon_1 + 12\varepsilon_2 - 3\varepsilon_3) \right] \end{aligned}$$

$$\begin{aligned}
& + \underbrace{\left\{ \frac{(\Delta l)^2}{24c_0} \left[(7\varepsilon_0 + 6\varepsilon_1 - \varepsilon_2) - \frac{2}{5} \left(\frac{c_1}{c_0} - 1 \right) (4\varepsilon_0 + 7\varepsilon_1 - \varepsilon_2) + \frac{1}{5} \left(\frac{c_1}{c_0} - 1 \right)^2 (\varepsilon_0 + 12\varepsilon_1 - 3\varepsilon_2) \right] \right\}}_{y_1} \\
& + \underbrace{\frac{(\Delta l)^2}{24c_0} \left[2(5\varepsilon_0 + 8\varepsilon_1 - \varepsilon_2) - \left(\frac{c_1}{c_0} - 1 \right) (3\varepsilon_0 + 10\varepsilon_1 - \varepsilon_2) - \left(\frac{c_1}{c_0} - 1 \right)^2 (\varepsilon_0 - 12\varepsilon_1 + 3\varepsilon_2) \right]}_{\Delta l \tan \theta_0} + \Delta l \tan \theta_0
\end{aligned} \tag{H-4}$$

After grouping terms equation (H-4) becomes:

$$\begin{aligned}
y_2 &= \frac{(\Delta l)^2}{24c_1} \left[(7\varepsilon_1 + 6\varepsilon_2 - \varepsilon_3) - \frac{2}{5} \left(\frac{c_2}{c_1} - 1 \right) (4\varepsilon_1 + 7\varepsilon_2 - \varepsilon_3) + \frac{1}{5} \left(\frac{c_2}{c_1} - 1 \right)^2 (\varepsilon_1 + 12\varepsilon_2 - 3\varepsilon_3) \right] \\
& + \frac{(\Delta l)^2}{24c_0} \left[(7\varepsilon_0 + 6\varepsilon_1 - \varepsilon_2) - \frac{2}{5} \left(\frac{c_1}{c_0} - 1 \right) (4\varepsilon_0 + 7\varepsilon_1 - \varepsilon_2) + \frac{1}{5} \left(\frac{c_1}{c_0} - 1 \right)^2 (\varepsilon_0 + 12\varepsilon_1 - 3\varepsilon_2) \right] + y_0 \\
& + (2-1) \frac{(\Delta l)^2}{24c_0} \left[2(5\varepsilon_0 + 8\varepsilon_1 - \varepsilon_2) - \left(\frac{c_1}{c_0} - 1 \right) (3\varepsilon_0 + 10\varepsilon_1 - \varepsilon_2) - \left(\frac{c_1}{c_0} - 1 \right)^2 (\varepsilon_0 - 12\varepsilon_1 + 3\varepsilon_2) \right] \\
& + 2\Delta l \tan \theta_0
\end{aligned} \tag{H-5}$$

For $i=3$:

$$\begin{aligned}
y_3 &= \frac{(\Delta l)^2}{24c_2} \left[(7\varepsilon_2 + 6\varepsilon_3 - \varepsilon_4) - \frac{2}{5} \left(\frac{c_3}{c_2} - 1 \right) (4\varepsilon_2 + 7\varepsilon_3 - \varepsilon_4) + \frac{1}{5} \left(\frac{c_3}{c_2} - 1 \right)^2 (\varepsilon_2 + 12\varepsilon_3 - 3\varepsilon_4) \right] + y_2 + \Delta l \tan \theta_2 \\
& = \frac{(\Delta l)^2}{24c_2} \left[(7\varepsilon_2 + 6\varepsilon_3 - \varepsilon_4) - \frac{2}{5} \left(\frac{c_3}{c_2} - 1 \right) (4\varepsilon_2 + 7\varepsilon_3 - \varepsilon_4) + \frac{1}{5} \left(\frac{c_3}{c_2} - 1 \right)^2 (\varepsilon_2 + 12\varepsilon_3 - 3\varepsilon_4) \right] \\
& + \underbrace{\left\{ \frac{(\Delta l)^2}{24c_1} \left[(7\varepsilon_1 + 6\varepsilon_2 - \varepsilon_3) - \frac{2}{5} \left(\frac{c_2}{c_1} - 1 \right) (4\varepsilon_1 + 7\varepsilon_2 - \varepsilon_3) + \frac{1}{5} \left(\frac{c_2}{c_1} - 1 \right)^2 (\varepsilon_1 + 12\varepsilon_2 - 3\varepsilon_3) \right] \right\}}_{y_2} \\
& + \underbrace{\left\{ \frac{(\Delta l)^2}{24c_0} \left[(7\varepsilon_0 + 6\varepsilon_1 - \varepsilon_2) - \frac{2}{5} \left(\frac{c_1}{c_0} - 1 \right) (4\varepsilon_0 + 7\varepsilon_1 - \varepsilon_2) + \frac{1}{5} \left(\frac{c_1}{c_0} - 1 \right)^2 (\varepsilon_0 + 12\varepsilon_1 - 3\varepsilon_2) \right] + y_0 \right\}}_{y_2} \\
& + \underbrace{\left\{ \frac{(\Delta l)^2}{24c_0} \left[2(5\varepsilon_0 + 8\varepsilon_1 - \varepsilon_2) - \left(\frac{c_1}{c_0} - 1 \right) (3\varepsilon_0 + 10\varepsilon_1 - \varepsilon_2) - \left(\frac{c_1}{c_0} - 1 \right)^2 (\varepsilon_0 - 12\varepsilon_1 + 3\varepsilon_2) \right] + 2\Delta l \tan \theta_0 \right\}}_{y_2}
\end{aligned}$$

$$\left. \begin{aligned} & \left[\frac{\Delta}{24c_1} \left[2(5\varepsilon_1 + 8\varepsilon_2 - \varepsilon_3) - \left(\frac{c_2}{c_1} - 1 \right) (3\varepsilon_1 + 10\varepsilon_2 - \varepsilon_3) - \left(\frac{c_2}{c_1} - 1 \right)^2 (\varepsilon_1 - 12\varepsilon_2 + 3\varepsilon_3) \right] \right. \\ & \left. + \frac{\Delta}{24c_0} \left[2(5\varepsilon_0 + 8\varepsilon_1 - \varepsilon_2) - \left(\frac{c_1}{c_0} - 1 \right) (3\varepsilon_0 + 10\varepsilon_1 - \varepsilon_2) - \left(\frac{c_1}{c_0} - 1 \right)^2 (\varepsilon_0 - 12\varepsilon_1 + 3\varepsilon_2) \right] + \Delta \tan \theta_0 \right] \end{aligned} \right\} \Delta \tan \theta_2 \tag{H-6}$$

After grouping terms, equation (H-6) becomes:

$$\begin{aligned} y_3 = & \frac{(\Delta)^2}{24c_2} \left[(7\varepsilon_2 + 6\varepsilon_3 - \varepsilon_4) - \frac{2}{5} \left(\frac{c_3}{c_2} - 1 \right) (4\varepsilon_2 + 7\varepsilon_3 - \varepsilon_4) + \frac{1}{5} \left(\frac{c_3}{c_2} - 1 \right)^2 (\varepsilon_2 + 12\varepsilon_3 - 3\varepsilon_4) \right] \\ & + \frac{(\Delta)^2}{24c_1} \left[(7\varepsilon_1 + 6\varepsilon_2 - \varepsilon_3) - \frac{2}{5} \left(\frac{c_2}{c_1} - 1 \right) (4\varepsilon_1 + 7\varepsilon_2 - \varepsilon_3) + \frac{1}{5} \left(\frac{c_2}{c_1} - 1 \right)^2 (\varepsilon_1 + 12\varepsilon_2 - 3\varepsilon_3) \right] \\ & + \frac{(\Delta)^2}{24c_0} \left[(7\varepsilon_0 + 6\varepsilon_1 - \varepsilon_2) - \frac{2}{5} \left(\frac{c_1}{c_0} - 1 \right) (4\varepsilon_0 + 7\varepsilon_1 - \varepsilon_2) + \frac{1}{5} \left(\frac{c_1}{c_0} - 1 \right)^2 (\varepsilon_0 + 12\varepsilon_1 - 3\varepsilon_2) \right] + y_0 \\ & + (3-2) \frac{\Delta}{24c_1} \left[2(5\varepsilon_1 + 8\varepsilon_2 - \varepsilon_3) - \left(\frac{c_2}{c_1} - 1 \right) (3\varepsilon_1 + 10\varepsilon_2 - \varepsilon_3) - \left(\frac{c_2}{c_1} - 1 \right)^2 (\varepsilon_1 - 12\varepsilon_2 + 3\varepsilon_3) \right] \\ & + (3-1) \frac{(\Delta)^2}{24c_0} \left[2(5\varepsilon_0 + 8\varepsilon_1 - \varepsilon_2) - \left(\frac{c_1}{c_0} - 1 \right) (3\varepsilon_0 + 10\varepsilon_1 - \varepsilon_2) - \left(\frac{c_1}{c_0} - 1 \right)^2 (\varepsilon_0 - 12\varepsilon_1 + 3\varepsilon_2) \right] \\ & + 3 \tan \theta_0 \end{aligned} \tag{H-7}$$

.....

Observing the indicial behavior, equation (H-7) can be generalized for index i , and the deflection, y_i , can be expressed in dual summation form as:

$$y_i = \frac{(\Delta)^2}{24} \sum_{j=1}^i \frac{1}{c_{j-1}} \left[\begin{aligned} & (7\varepsilon_{j-1} + 6\varepsilon_j - \varepsilon_{j+1}) - \frac{2}{5} \left(\frac{c_j}{c_{j-1}} - 1 \right) (4\varepsilon_{j-1} + 7\varepsilon_j - \varepsilon_{j+1}) \\ & + \frac{1}{5} \left(\frac{c_j}{c_{j-1}} - 1 \right)^2 (\varepsilon_{j-1} + 12\varepsilon_j - 3\varepsilon_{j+1}) \end{aligned} \right] + y_0$$

Contributions from deflection terms

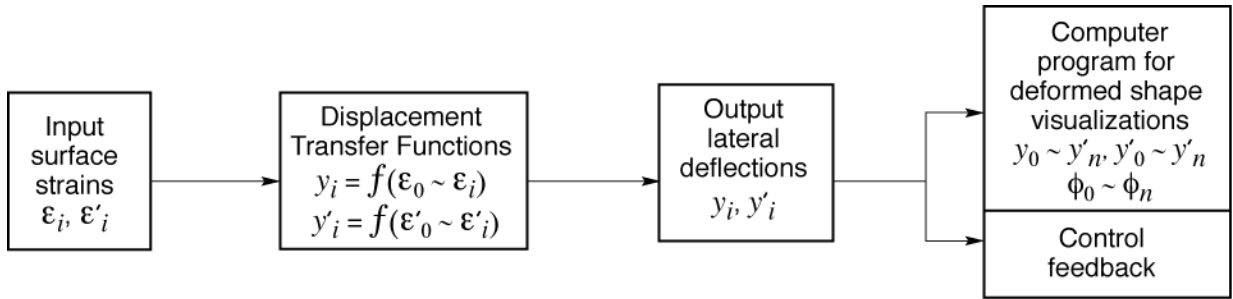
$$\begin{aligned}
& + \frac{(\Delta)^2}{24} \sum_{j=1}^{i-1} \frac{(i-j)}{c_{j-1}} \left[\begin{aligned} & 2(5\varepsilon_{j-1} + 8\varepsilon_j - \varepsilon_{j+1}) - \left(\frac{c_j}{c_{j-1}} - 1 \right) (3\varepsilon_{j-1} + 10\varepsilon_j - \varepsilon_{j+1}) \\ & - \left(\frac{c_j}{c_{j-1}} - 1 \right)^2 (\varepsilon_{j-1} - 12\varepsilon_j + 3\varepsilon_{j+1}) \end{aligned} \right] + (i)\Delta \tan \theta_0 \quad (\text{H-8}) \\
& \underbrace{\hspace{15em}}_{\text{Contributions from slope terms}} \quad (i=1, 2, 3, \dots, n)
\end{aligned}$$

which is equation (48) in the text, the Depth-expanded Displacement Transfer Function for the nonuniform beams.

APPENDIX I

FLOW CHART FOR STRUCTURE DEFORMED SHAPE VISUALIZATIONS

(cf., U.S. Patent No. 7,520,176, issued April, 2009)



120173

(Two-line strain-sensing system, refs. 1-3).

Displacement Transfer Functions (Depth-Expanded):

For the front strain-sensing line:

$$\begin{aligned}
 y_i = & \underbrace{\frac{(\Delta)^2}{24} \sum_{j=1}^i \frac{1}{c_{j-1}} \left[\begin{aligned} & \left(7\varepsilon_{j-1} + 6\varepsilon_j - \varepsilon_{j+1} \right) - \frac{2}{5} \left(\frac{c_j}{c_{j-1}} - 1 \right) \left(4\varepsilon_{j-1} + 7\varepsilon_j - \varepsilon_{j+1} \right) \\ & + \frac{1}{5} \left(\frac{c_j}{c_{j-1}} - 1 \right)^2 \left(\varepsilon_{j-1} + 12\varepsilon_j - 3\varepsilon_{j+1} \right) \end{aligned} \right]}_{\text{Contributions from deflection terms}} + y_0 \\
 & + \underbrace{\frac{(\Delta)^2}{24} \sum_{j=1}^i \frac{(i-j)}{c_{j-1}} \left[\begin{aligned} & 2(5\varepsilon_{j-1} + 8\varepsilon_j - \varepsilon_{j+1}) - \left(\frac{c_j}{c_{j-1}} - 1 \right) (3\varepsilon_{j-1} + 10\varepsilon_j - \varepsilon_{j+1}) \\ & - \left(\frac{c_j}{c_{j-1}} - 1 \right)^2 \left(\varepsilon_{j-1} - 12\varepsilon_j + 3\varepsilon_{j+1} \right) \end{aligned} \right]}_{\text{Contributions from slope terms}} + (i)\Delta/\tan \theta_0 \quad (I-1)
 \end{aligned}$$

$(i = 1, 2, 3, \dots, n)$

For the rear strain-sensing line:

$$\begin{aligned}
 y'_i = & \underbrace{\frac{(\Delta l)^2}{24} \sum_{j=1}^i \frac{1}{c'_{j-1}} \left[\begin{aligned} & \left(7\varepsilon'_{j-1} + 6\varepsilon'_j - \varepsilon'_{j+1} \right) - \frac{2}{5} \left(\frac{c'_j}{c'_{j-1}} - 1 \right) \left(4\varepsilon'_{j-1} + 7\varepsilon'_j - \varepsilon'_{j+1} \right) \\ & + \frac{1}{5} \left(\frac{c'_j}{c'_{j-1}} - 1 \right)^2 \left(\varepsilon'_{j-1} + 12\varepsilon'_j - 3\varepsilon'_{j+1} \right) \end{aligned} \right]}_{\text{Contributions from deflection terms}} + y'_0 \\
 & + \underbrace{\frac{(\Delta l)^2}{24} \sum_{j=1}^i \frac{(i-j)}{c'_{j-1}} \left[\begin{aligned} & 2(5\varepsilon'_{j-1} + 8\varepsilon'_j - \varepsilon'_{j+1}) - \left(\frac{c'_j}{c'_{j-1}} - 1 \right) (3\varepsilon'_{j-1} + 10\varepsilon'_j - \varepsilon'_{j+1}) \\ & - \left(\frac{c'_j}{c'_{j-1}} - 1 \right)^2 (\varepsilon'_{j-1} - 12\varepsilon'_j + 3\varepsilon'_{j+1}) \end{aligned} \right]}_{\text{Contributions from slope terms}} + (i)\Delta l \tan \theta'_0 \quad (I-2)
 \end{aligned}$$

$(i = 1, 2, 3, \dots, n)$

Cross-Sectional Twist Angle Equation:

$$\phi_i = \sin^{-1} \left(\frac{y_i - y'_i}{d_i} \right) ; \quad (i = 0, 1, 2, 3, \dots, n) \quad (I-3)$$

(d_i = strain-sensing lines separation distance, fig. I-1)

Tapered Wing Box

Figure I-1 shows the application of the two-line strain-sensing system to a tapered wing box structure (the neutral surface is located at half depth) to sense the surface bending strains induced by combined bending and torsion loadings.

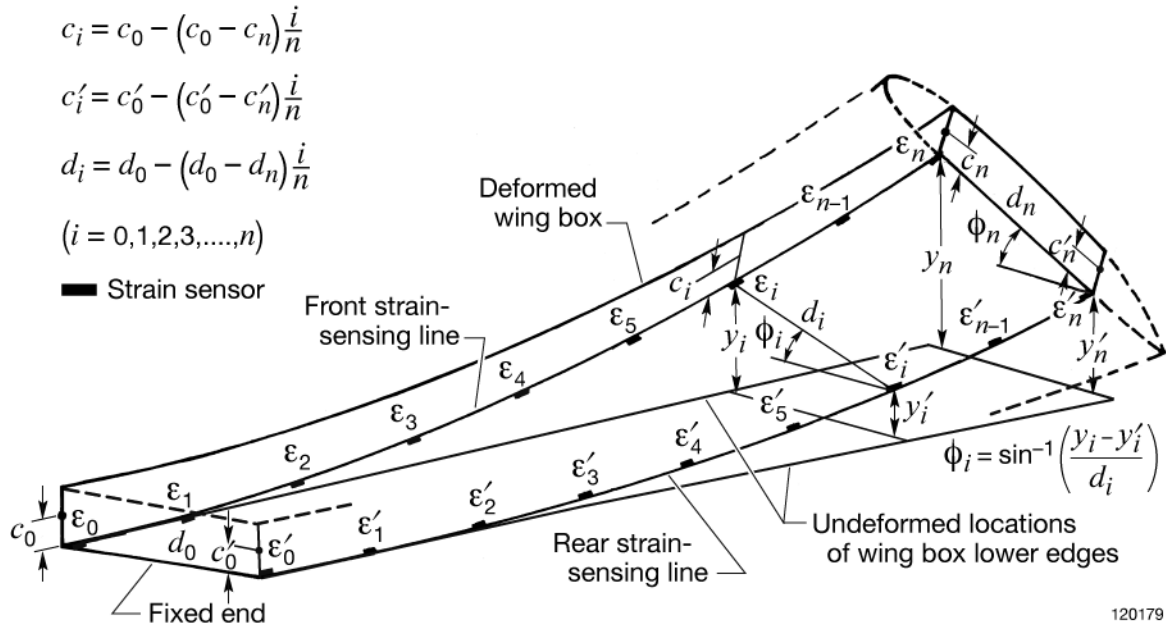


Figure I-1. Tapered cantilever wing box instrumented with two-line strain-sensing system for deformed shape predictions of structure under combined bending and torsion (ref. 2).

The two strain-sensing lines (front and rear) are located along the lower edges (front and rear) of the wing box with chord-wise separation distance, d_i , which decreases toward the wing box tip according to the wing box horizontal taper rate. The two strain-sensing lines may also be aligned parallel to each other (that is, $d_i = \text{constant}$) along the span of the wing box.

As shown in the flow chart, the surface strains, $\epsilon_i (i = 0, 1, 2, 3, \dots, n)$ are to be input to the left box of the chart, and the Displacement Transfer Functions {equation (I-1), equation (I-2)} (the second box from the left) are to convert the surface strains into out-of-plane deflections, $\{y_i, y'_i\}$ (the third box from the left), from which the cross-sectional twist angles, ϕ_i , can be calculated from the cross-sectional twist angle equation, equation (I-3). The resulting data could then be used to map the overall structural deformed shapes for visual display using the deformed-shape-visualization computer program (the fourth box from the left), and for control feedback.

If the neutral surface is not at the half depth, a second two-line strain-sensing system must be installed on the upper surface, right on top of the lower sensing lines. Using pairs of lower and upper strains, the depth factor, $c_i (i = 0, 1, 2, 3, \dots, n)$, needed for the deflection calculations, can be determined (see the Ikhana wing shape predictions, ref. 3).

Free-Free Beam Structure

A good example of the free-free (unsupported) beam structure is an aircraft fuselage during flight (fig. I-2).

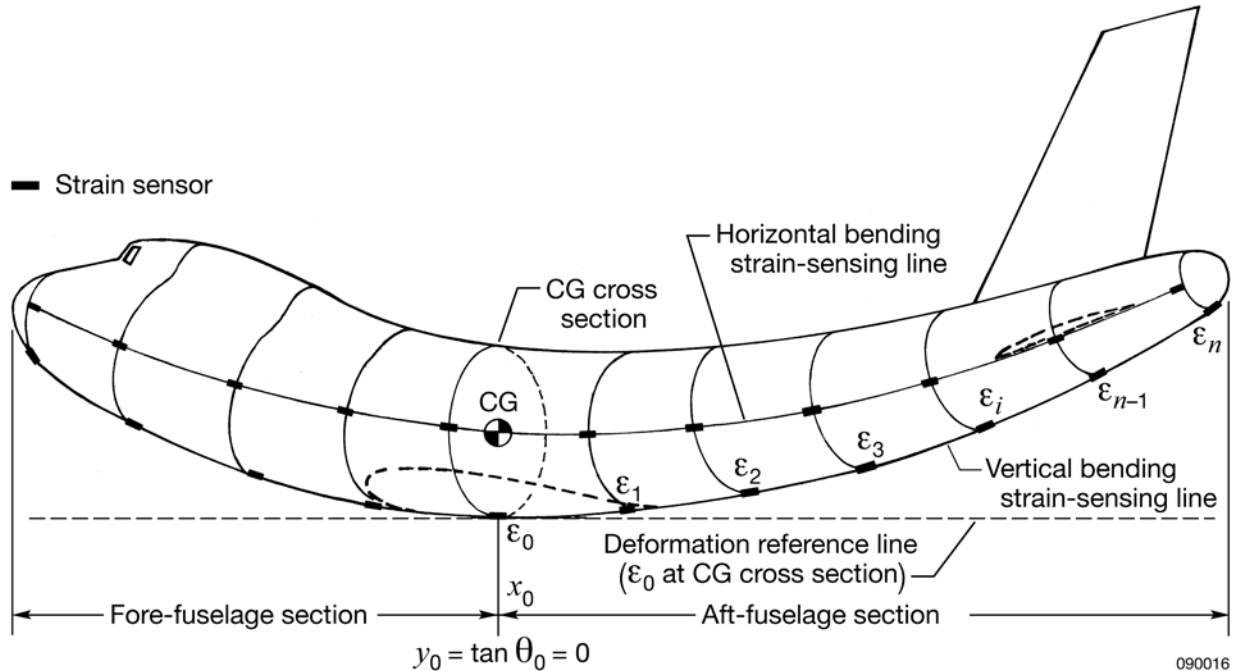


Figure I-2. Two-line strain-sensing system installed on an aircraft fuselage for horizontal and vertical bending strain sensing (ref. 2).

The fuselage may be considered as an union of two nonuniform cantilever tubular beams (that is, a fore- and an aft-fuselage section) that are joined together at the center-of-gravity (CG) cross section (fig. I-2). For monitoring the deflections of the airborne fuselage under vertical bending and horizontal bending, two strain-sensing lines can be installed axially on the bottom (belly) surface and on the side of the fuselage (fig. I-2). During the flight, the CG cross section has the least movement compared with the other fuselage cross sections. For practical purposes, it is best to choose the reference strain-sensing station, x_0 , at the CG cross section, and divide each strain-sensing line into two segments (fig. I-2). One segment is for the fore-fuselage section and the other for the aft-fuselage section. Thus, by imposing $y_0 = \tan \theta_0 = 0$ at the reference sensing station x_0 (considered as a moving built-in end), deflection equation (I-1) can be used for the bottom strain-sensing line to calculate the vertical deflections of the fore- and aft-fuselage sections. The vertical deflection, y_i , calculated from equation (I-1) will then be the relative deflection with respect to the tangent line passing through the reference sensing station, x_0 , which moves with the fuselage during flight (fig. I-2). The same arguments hold for the strain-sensing line for the horizontal bending.

REFERENCES

1. Ko, William L., W. L. Richards, and Van T. Tran, *Displacement Theories for In-Flight Deformed Shape Predictions of Aerospace Structures*, NASA/TP-2007-214612, October 2007.
2. Ko, William L., and Van Tran Fleischer, *Further Development of Ko Displacement Theory for Deformed Shape Predictions of Nonuniform Aerospace Structures*, NASA/TP-2009-214643, September 2009.
3. Ko, William L., W. L. Richards, and Van Tran Fleischer, *Applications of Ko Displacement Theory to the Deformed Shape Predictions of the Doubly-Tapered Ikhana Wing*, NASA/TP-2009-214652, November 2009.
4. Ko, William L., and Van Tran Fleischer, *Methods for In-Flight Wing Shape Predictions of Highly Flexible Aerospace Structures: Formulation of Ko Displacement Theory*, NASA/TP-2010-214656, August 2010.
5. Ko, William L., and Van Tran Fleischer, *First- and Second-Order Displacement Transfer Functions for Structural Shape Predictions Using Analytically Predicted Surface Strains*, NASA/TP-2012-215976, March 2012.
6. Bang, Hyung-Joon, Hyun-Kyu Kang, Chang-Sun Hong, and Chung-Gon Kim, "Optical Fiber Sensor Systems for Simultaneous Monitoring of Strain and Fractures in Composites," *Smart Materials and Structures*, Vol. 14, pp. N52-N58, 2005.
7. Wehrle, Gunther, Percy Nohama, Hypolito Jose Kalinowski, Pedro Ingacio Torres, and Luiz Carlos Guedes Valente, "A Fiber Optic Bragg Grating Strain Sensor for Monitoring Ventilatory Movements," *Measurement Science and Technology*, Vol. 12, pp. 805-809, 2001.
8. Baldwin, Chris S., Toni J. Salter, and Jason S. Kiddy, "Static Shape Measurements Using Multiplexed Fiber Bragg Grating Sensor System," *Smart Structures and Materials 2004: Smart Sensor Technology and Measurement Systems*, Vol. 5384, pp. 206-217, 2004.
9. Ko, William L., and W. Lance Richards, *Method for Real-Time Structure Shape-Sensing*, U.S. Patent No. 7,520,176, issued April 21, 2009.
10. Richards, W. Lance, and William L. Ko, *Process for Using Surface Strain Measurements to Obtain Operational Loads for Complex Structures*, U.S. Patent No. 7,715,994, issued, May 11, 2010.
11. Ko, William L., and Van Tran Fleischer, *Extension of Ko Straight-Beam Displacement Theory to Deformed Shape Predictions of Slender Curved Structures*, NASA/TP-2011-214657, April 2011.
12. Kopmaz, Osman, and Omer Gundogdu, "On the Curvature of an Euler-Bernoulli Beam," *International Journal of Mechanical Engineering Education*, Vol. 31, Issue 2, p. 132, 2004.
13. Hodges, Dewey H., "Proper Definition of Curvature in Nonlinear Beam Kinematics," *AIAA Journal*, Vol. 22, No. 12, pp. 1825-1827, December 1984.
14. Faupel, Joseph, H., *Engineering Design*, John Wiley and Sons, New York, 1964.

15. Roark, Raymond J., *Formulas for Stress and Strain*, McGraw-Hill Book Company, Inc., New York, 1954.
16. Whetstone, W. D., *SPAR Structural Analysis System Reference Manual, System Level 13A, Vol. 1, Program Execution*, NASA CR-158970-1, December 1978.
17. Hodgeman, Charles D., *Standard Mathematical Tables*, 7-th edition, Chemical Rubber Publishing Co. Cleveland, Ohio, 1957.
18. Jutte, Christine, William L. Ko, Craig Stephens, John A. Bakalyar, W. Lance Richards, and Allen R. Parker, *Deformed Shape Calculation of a Full-Scale Wing Using Fiber Optic Strain Data from a Ground Loads Test*, NASA/TP-2011-215975, December 2011.